Recent models for vision

AI602: Recent Advances in Deep Learning

Lecture 1

KAIST AI

Basic knowledge in **machine learning & classic model design** are assumed: (e.g., **AI501, AI502, AI601 course**)

Machine Learning

- Problems: classification, regression, etc.
- Optimization: stochastic gradient descent (SGD), regularizations, etc.
- Deep Neural Networks: basic structures, representation learning, etc.

Classic model designs

- Convolutional Neural Networks (CNNs)
 - Basic operations: convolution, spatial pooling, etc.
 - Design techniques: skip-connection, normalization, etc.
 - Some notable models: AlexNet, Inception, ResNet, etc.

• Transformers

• Transformer architecture: token data structure, self-attention, etc.

Convolutional neural networks have been tremendously successful in practical applications;

Classification and retrieval [Krizhevsky et al., 2012]



Segmentation [Farabet et al., 2013]



Detection [Ren et al., 2015]



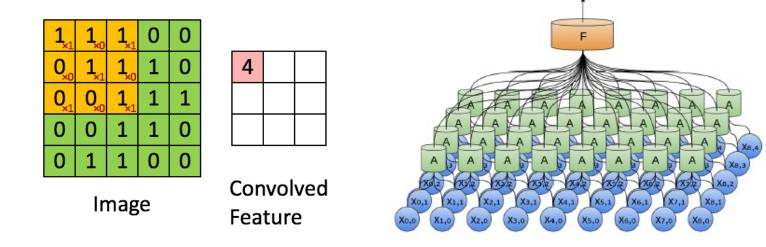


Neural networks that use convolution in place of general matrix multiplication

- Sharing parameters across multiple image locations
- Translation equivariant (invariant with **pooling**) operation

Specialized for processing data that has a known, grid-like topology

• e.g., time-series data (1D grid), image data (2D grid)



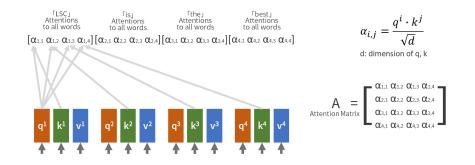
*sources :

- https://www.cc.gatech.edu/~san37/post/dlhc-cnn/
- http://colah.github.io/posts/2014-07-Conv-Nets-Modular/

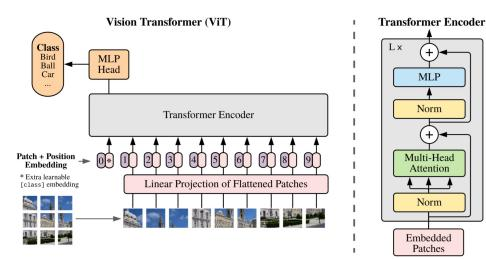
4

Vision transformers with self-attention for 2D spatial data also emerged recently

- Shares parameters across multiple image locations
 - However, self-attention adapts different weights per each location



Very small inductive-bias towards image data; everything is learned from data!



Part 1. Basics

- Evolution of CNN architectures
- Batch normalization and ResNet
- Attention module in CNNs
- Vision transformers

Part 2. Advanced Topics

- Toward automation of network design
- Flexible architectures
- Observational study on network architectures
- Deep spatial-temporal models

Part 3. Beyond CNNs and Vision Transformers

- Patch-based architectures for vision
- New design paradigms

Table of Contents

Part 1. Basics

- Evolution of CNN architectures
- Batch normalization and ResNet
- Attention module in CNNs
- Vision transformers

Part 2. Advanced Topics

- Toward automation of network design
- Flexible architectures
- Observational study on network architectures
- Deep spatial-temporal models

Part 3. Beyond CNNs and Vision Transformers

- Patch-based architectures for vision
- New design paradigms

Part 1. Basics

- Evolution of CNN architectures
- Batch normalization and ResNet
- Attention module in CNNs
- Vision transformers

Part 2. Advanced Topics

- Toward automation of network design
- Flexible architectures
- Observational study on network architectures
- Deep spatial-temporal models

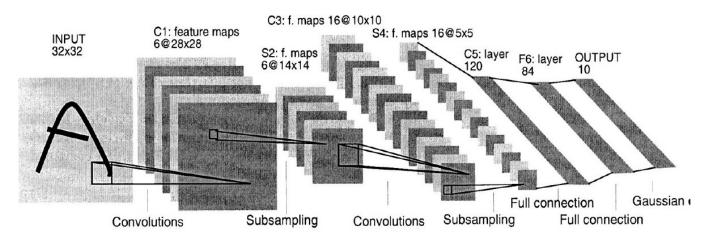
Part 3. Beyond CNNs and Vision Transformers

- Patch-based architectures for vision
- New design paradigms

Typically, designing a CNN model requires some effort

- There are a lot of **design choices**: # layers, # filters, sizes of kernel, pooling, ...
- It is **costly** to measure the performance of each model and choose the best one

Example: LeNet for handwritten digits recognition [LeCun et al., 1998]



- However, LeNet is not enough to solve real-world problems in AI domain
 - CNNs are typically applied to extremely complicated domains, e.g. raw RGB images
 - We need to design a larger model to solve them adequately

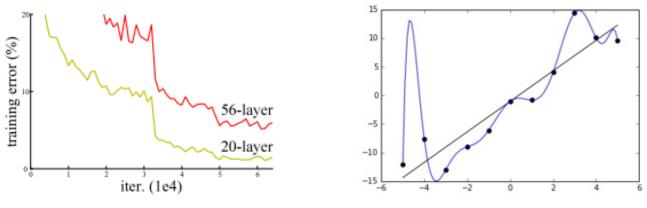
Problem: The larger the network, the more difficult it is to design

1. Optimization difficulty

- When the training loss is degraded
- Deeper networks are typically much harder to optimize
- Related to gradient vanishing and exploding

2. Generalization difficulty

- The training is done well, but the testing error is degraded
- Larger networks are more likely to over-fit, i.e., regularization is necessary
- Good architectures should be **scalable** that solves both of these problems



*sources :

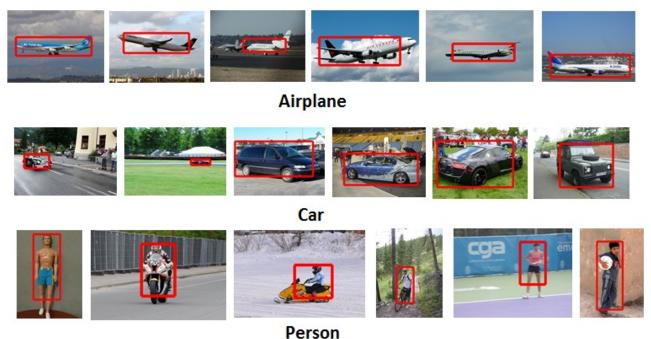
- He et al. "Deep residual learning for image recognition". CVPR 2016.

Algorithmic Intelligence Lab

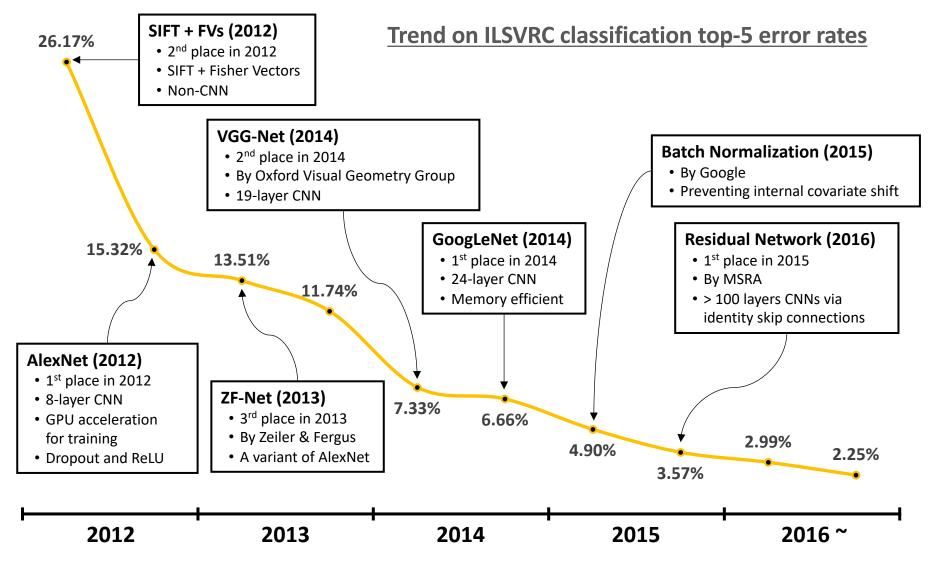
https://upload.wikimedia.org/wikipedia/commons/thumb/6/68/Overfitted_Data.png/300px-Overfitted_Data.png_10

ImageNet Large Scale Visual Recognition Challenge (ILSVRC)

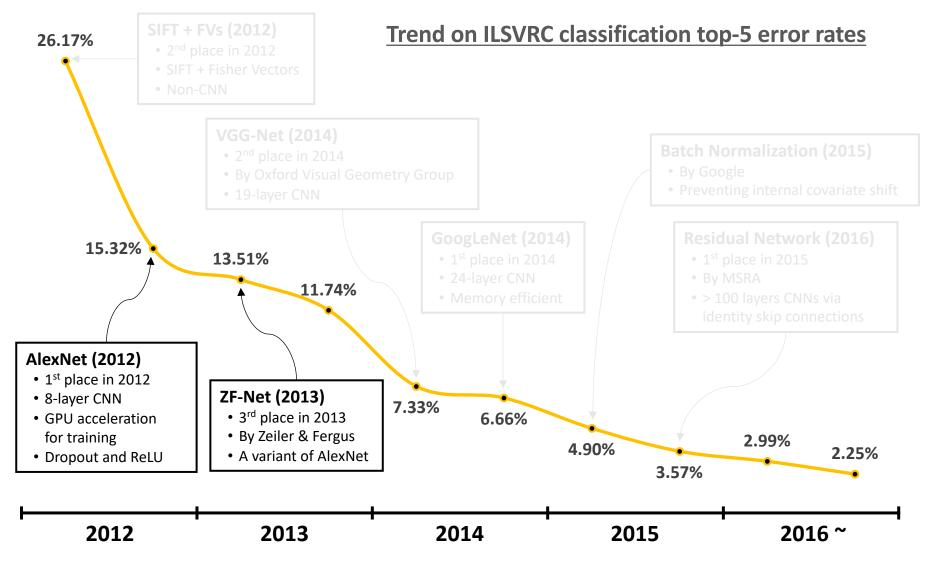
- ImageNet dataset: a large database of visual objects
 - ~14M labeled images, 20K classes
 - Human labels via Amazon MTurk
- Classification: 1,281,167 images for training / 1,000 categories
- Annually ran from 2010 to 2017, and now hosted by Kaggle
- For details, see [Russakovsky et al., 2015]



ILSVRC contributed greatly to development of CNN architectures

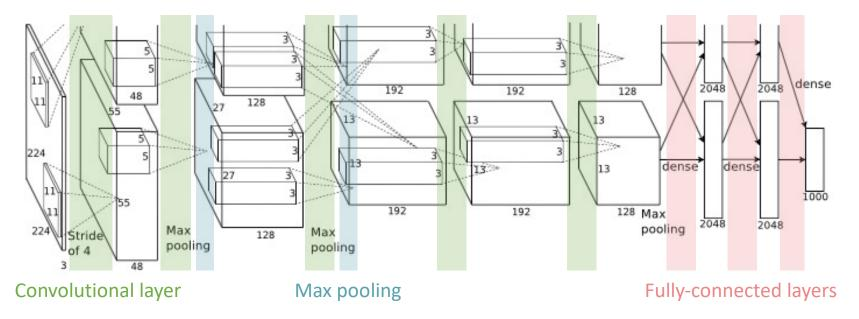


ILSVRC contributed greatly to development of CNN architectures



The first winner to use CNN in ILSVRC, with an astounding improvement

- Top-5 error is largely improved: $25.8\% \rightarrow 15.3\%$
- The 2nd best entry at that time was **26.2%**
- 8-layer CNN (5 Conv + 3 FC)
- Utilized 2 GPUs (GTX-580 \times 2) for training the network
 - Split a single network into 2 parts to distribute them into each GPU



Algorithmic Intelligence Lab

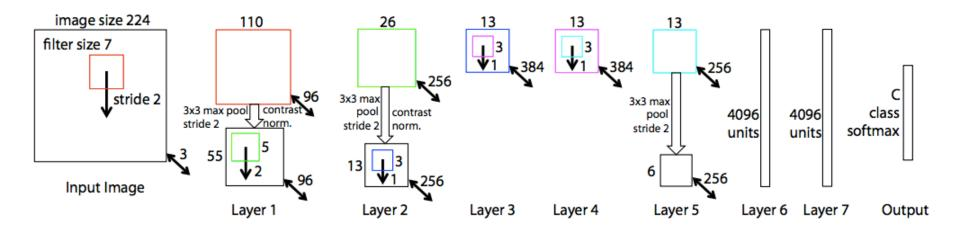
*source : Krizhevsky et al. "Imagenet classification with deep convolutional neural networks". NIPS 2012 14

A simple variant of AlexNet, placing the 3^{rd} in ILSVRC'13 (15.3% \rightarrow 13.5%)

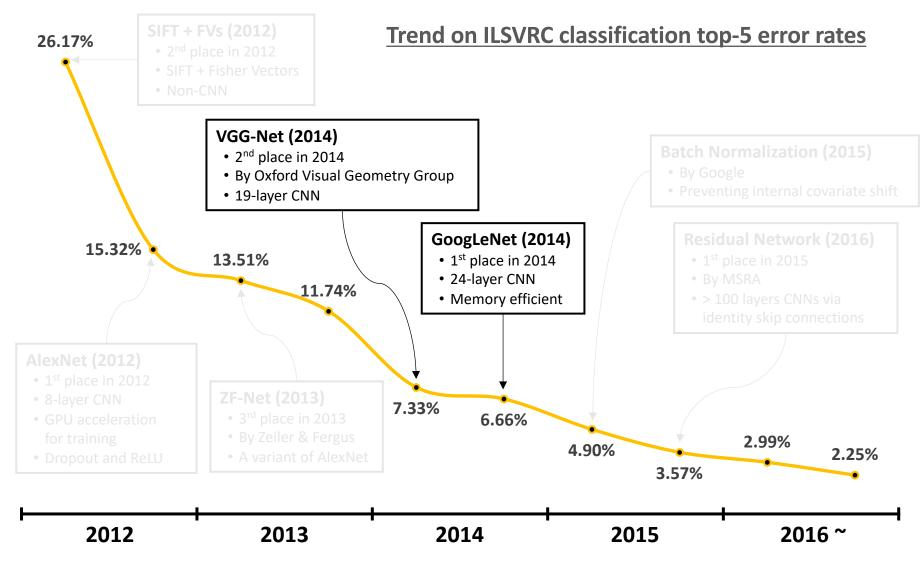
- Smaller kernel at input: $11 \times 11 \rightarrow 7 \times 7$
- Smaller stride at input: $4 \rightarrow 2$
- The # of hidden filters are doubled

Lessons

- 1. Design principle: Use smaller kernel, and smaller stride
- 2. CNN architectures can be very sensitive on hyperparameters



ILSVRC contributed greatly to development of CNN architectures

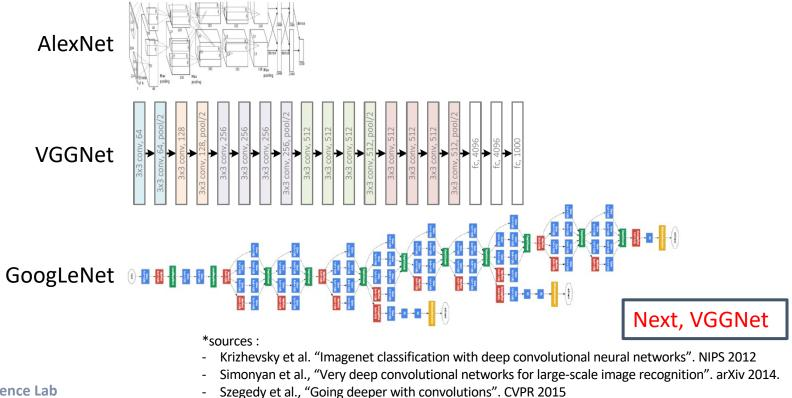


Networks were getting deeper

- AlexNet: 8 layers
- VGGNet: 19 layers
- GoogleNet: 24 layers

Both focused on parameter efficiency of each block

• Mainly to allow larger networks computable at that time



The 2nd place in ILSVRC'14 (11.7% \rightarrow 7.33%)

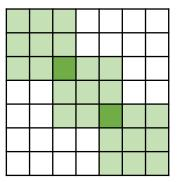
• Designed using only 3×3 kernels for convolutions

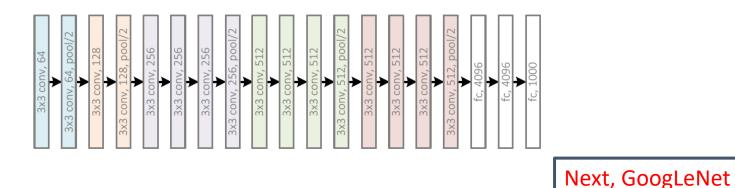
Lesson: Stacking multiple 3×3 is advantageous than using other kernels **Example**: $((3\times3)\times3)$ v.s. (7×7)

- Essentially, they get the same receptive field
- ((3×3)×3) have less # parameters

•
$$3 \times (C \times ((3 \times 3) \times C)) = 27C^2$$

- $C \times ((7 \times 7) \times C) = 49C^2$
- ((3×3)×3) gives more non-linearities



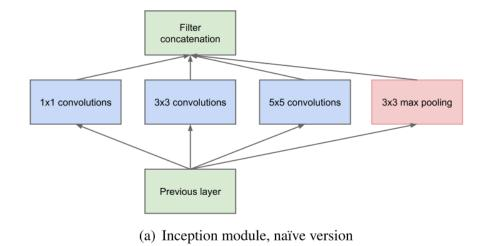


The winner of ILSVRC'14 (11.7% \rightarrow 6.66%)

Achieved 12× fewer parameters than AlexNet

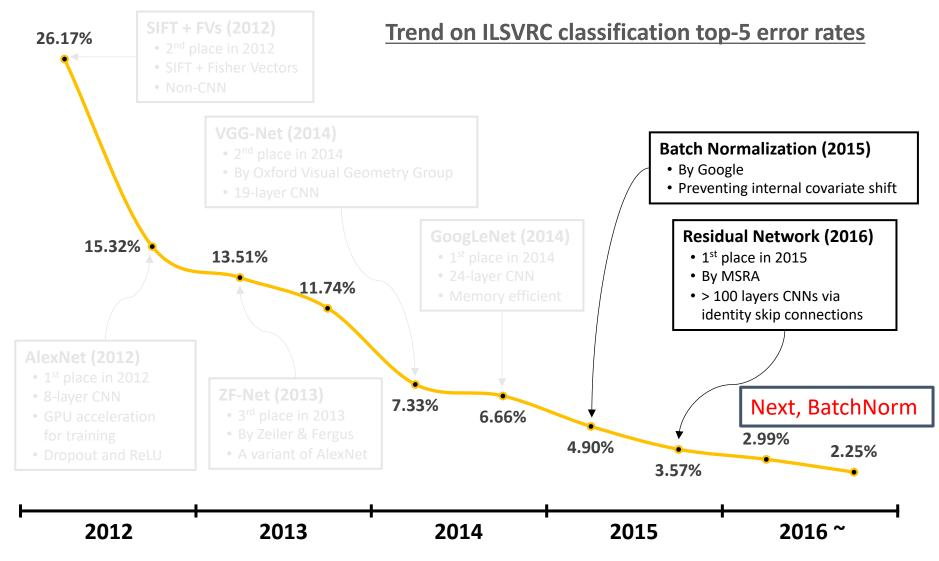
Inception module

- Multiple operation paths with different receptive fields
- Each of the outputs are **concatenated** in filter-wise
- Capturing sparse patterns in a stack of features





ILSVRC contributed greatly to development of CNN architectures



Part 1. Basics

- Evolution of CNN architectures
- Batch normalization and ResNet
- Attention module in CNNs
- Vision transformers

Part 2. Advanced Topics

- Toward automation of network design
- Flexible architectures
- Observational study on network architectures
- Deep spatial-temporal models

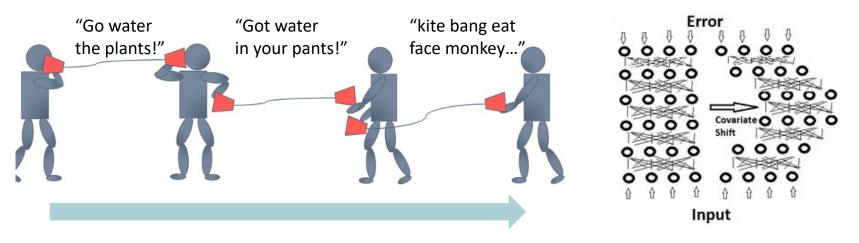
Part 3. Beyond CNNs and Vision Transformers

- Patch-based architectures for vision
- New design paradigms

Training a deep network well had been a delicate task

- It requires a careful initialization, with adequately low learning rate
- Gradient vanishing: networks containing saturating non-linearity

Ioffe et al. (2015): Such difficulties are come from **internal covariate shift Motivation**: "The cup game analogy"



- Similar problem happens during training of deep neural networks
- Updates in early layers may shift the inputs of later layers too much

*sources :

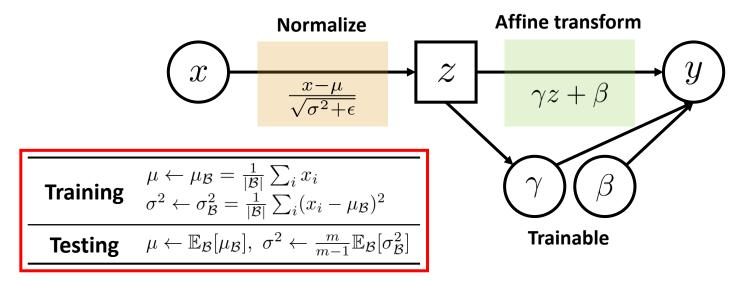
- Ioffe et al., "Batch Normalization: Accelerating Deep Network Training by Reducing Internal Covariate Shift". ICML 2015
 - http://pages.cs.wisc.edu/~shavlik/cs638/lectureNotes/Batch_Normalization.pptx

Algorithmic Intelligence Lab

https://www.quora.com/Why-does-batch-normalization-help

Batch normalization (BN) accelerates neural network training by eliminating internal covariate shift inside the network

Idea: A normalization layer that behaves differently in training and testing



- 1. During training, input distribution of y only depends on γ and β
 - Training mini-batches are always normalized into mean 0, variance 1
- 2. There is some gap between $\mu_{\mathcal{B}}$ and $\mathbb{E}[\mu_{\mathcal{B}}]$ ($\sigma_{\mathcal{B}}^2$, resp.)
 - Noise injection effect for each mini-batch ⇒ Regularization effect

Batch normalization (BN) accelerates neural network training by eliminating internal covariate shift inside the network

- BN allows much higher learning rates, i.e. faster training
- BN stabilizes gradient vanishing on saturating non-linearities
- BN also has its own **regularization effect**, so that it allows to reduce weight decay, and to remove dropout layers
- BN makes GoogLeNet much easier to train with great improvements

| Model | Resolution | Crops | Models | Top-1 error | Top-5 error |
|-------------------------------|------------|-------|--------|-------------|-------------|
| GoogLeNet ensemble | 224 | 144 | 7 | - | 6.67% |
| Deep Image low-res | 256 | - | 1 | - | 7.96% |
| Deep Image high-res | 512 | - | 1 | 24.88 | 7.42% |
| Deep Image ensemble | variable | - | - | - | 5.98% |
| BN-Inception single crop | 224 | 1 | 1 | 25.2% | 7.82% |
| BN-Inception multicrop | 224 | 144 | 1 | 21.99% | 5.82% |
| BN-Inception ensemble | 224 | 144 | 6 | 20.1% | 4.9%* |

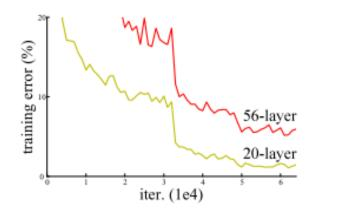
Next, ResNet

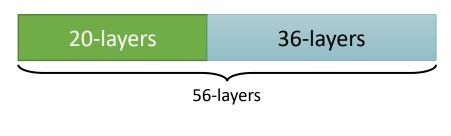
The winner of ILSVRC'15 (6.66% \rightarrow 3.57%)

- ResNet is the first architecture succeeded to train >100-layer networks
 - Prior works could until ~30 layers, but failed for the larger nets

What was the problem?

- 56-layer net gets higher training error than 20-layers network
- Deeper networks are much harder to optimize even if we use BNs
- It's not due to overfitting, but optimization difficulty
- Quiz: Why is that?



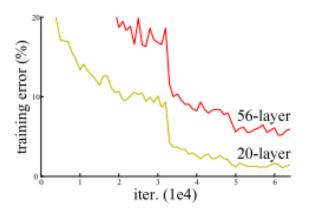


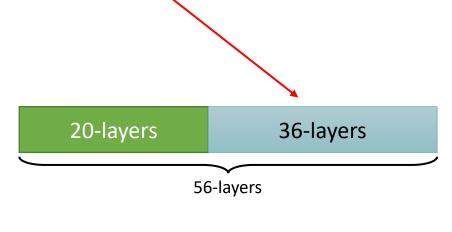
The winner of ILSVRC'15 (6.66% \rightarrow 3.57%)

- ResNet is the first architecture succeeded to train >100-layer networks
 - Prior works could until ~30 layers, but failed for the larger nets

What was the problem?

- It's not due to overfitting, but optimization difficulty
- Quiz: Why is that?
- If the 56-layer model optimized well, then it **must be better** than the 20-layer
 - There is a trivial solution for the 36-layer: identity





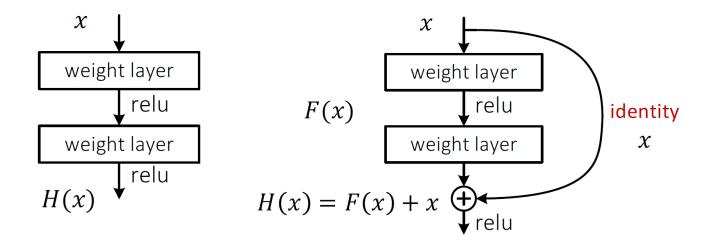
ResNet [He et al., 2016a]

Motivation: A non-linear layer may struggle to represent an identity function

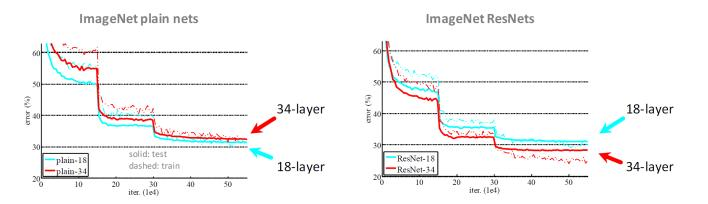
- Due to its internal non-linearities, e.g. ReLU
- This may cause the optimization difficulty on large networks

Idea: Reparametrize each layer to make them easy to represent an *identity*

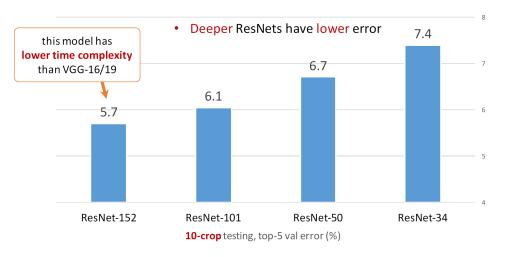
• When all the weights are set to zero, the layer represents an identity

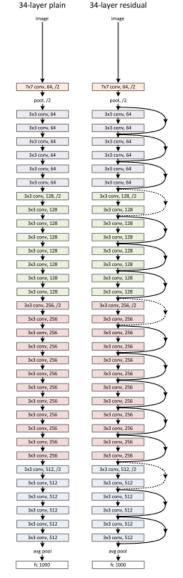


Plain nets v.s. ResNets



• Deeper ResNets can be trained without any difficulty





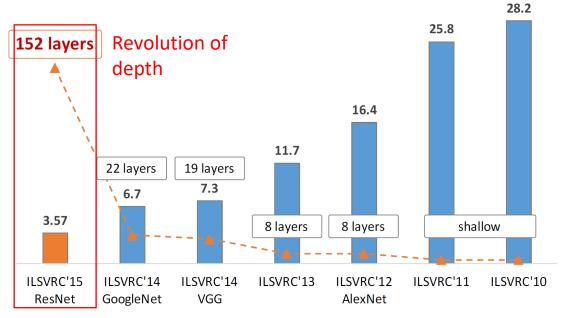
*sources :

- He et al., "Deep residual learning for image recognition". CVPR 2016
- He, Kaiming, "Deep Residual Networks: Deep Learning Gets Way Deeper." 2016. 28

Identity connection resolved a major difficulty on optimizing large networks

Revolution of depth: Training >100-layer network without difficulty

- Later, ResNet is revised to allow to train up to >1000 layers [He et al., 2016b]
- ResNet also shows good generalization ability as well



ImageNet Classification top-5 error (%)

*sources :

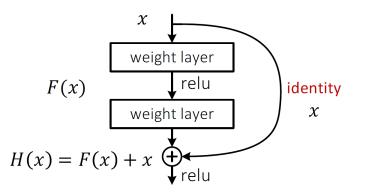
- He et al., "Deep residual learning for image recognition". CVPR 2016
- Kaiming He, "Deep Residual Networks: Deep Learning Gets Way Deeper." 2016.

Algorithmic Intelligence Lab

He et al. "Identity mappings in deep residual networks.", ECCV 2016

Various architectures now are based on ResNet

- ResNet with stochastic depth [Huang et al., 2016]
- Wide ResNet [Zagoruyko et al., 2016]
- ResNet in ResNet [Targ et al., 2016]
- ResNeXt [Xie et al., 2016]
- PyramidNet [Han et al., 2016]
- Inception-v4 [Szegedy et al., 2017]
- DenseNet [Huang et al., 2017]
- Dual Path Network [Chen et al., 2017]



Transition of design paradigm: Optimization ⇒ Generalization

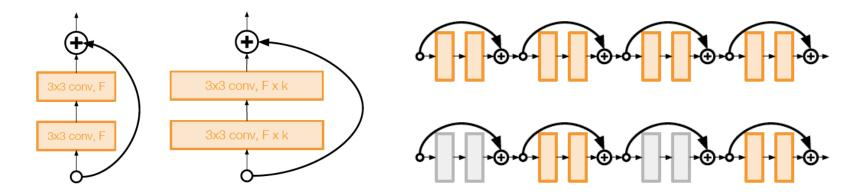
- People are now less concerned about optimization problems in a model
- Instead, they now focus more on its generalization ability
- "How well does an architecture generalize as its scale grows?"

Wide Residual Networks [Zagoruyko et al., 2016]

- Residuals can also work to enlarge the width, not only its depth
- Residual blocks with ×k wider filters
- Increasing width instead of depth can be more computationally efficient
 - GPUs are much better on handling "wide-but-shallow" than "thin-but-deep"
- WRN-50 outperforms ResNet-152

Deep Networks with Stochastic Depth [Huang et al., 2016]

- Randomly drop a subset of layers during training
- Bypassing via identity connections
- Reduces gradient vanishing, and training time as well

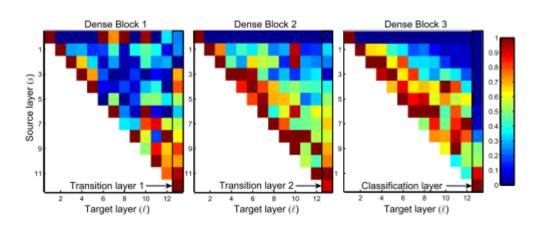


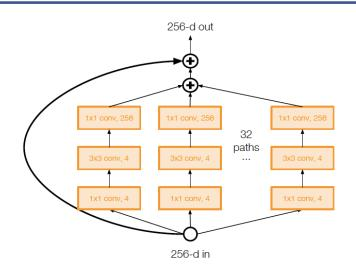
ResNeXt [Xie et al., 2016]

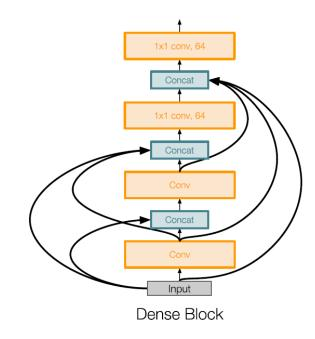
- Aggregating multiple parallel paths inside a residual block ("cardinality")
- Increasing cardinality is more effective than going deeper or wider

DenseNet [Huang et al. 2017]

- Passing all the previous representation directly via concatenation of features
- Strengthens feature propagation and feature reuse





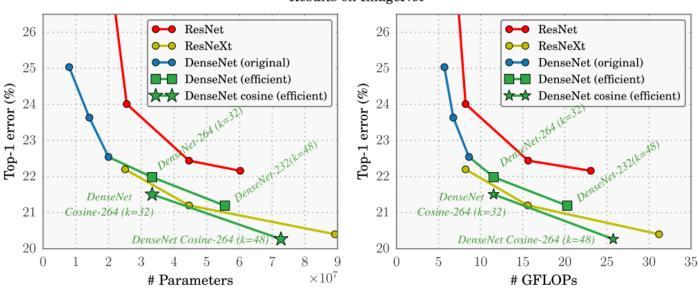


ResNeXt [Xie et al., 2016]

- Aggregating multiple parallel paths inside a residual block ("cardinality")
- Increasing cardinality is more effective than going deeper or wider

DenseNet [Huang et al. 2017]

- Passing all the previous representation directly via concatenation of features
- Strengthens feature propagation and feature reuse



Results on ImageNet

Part 1. Basics

- Evolution of CNN architectures
- Batch normalization and ResNet
- Attention module in CNNs
- Vision transformers

Part 2. Advanced Topics

- Toward automation of network design
- Flexible architectures
- Observational study on network architectures
- Deep spatial-temporal models

Part 3. Beyond CNNs and Vision Transformers

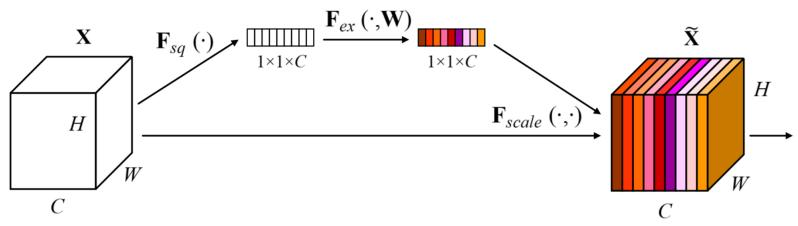
- Patch-based architectures for vision
- New design paradigms

Motivation: The deeper the model, the more feature maps are generated

- Many of them might be important for classification task
- Others might redundant or less important

Squeeze and Excitation Network [Hu et al., 2018]

- It selectively emphasizes informative feature maps and suppress less useful ones via global information in two steps
- **Squeeze** step: obtaining global information by shrinking feature maps
 - Global average pooling
- Excitation step: recalibrating weights of features by learning channel-wise weights
 - MLP of two fully-connected layers



Algorithmic Intelligence Lab

*source: Hu et al., "Squeeze-and-Excitation Networks", CVPR, 2018 35

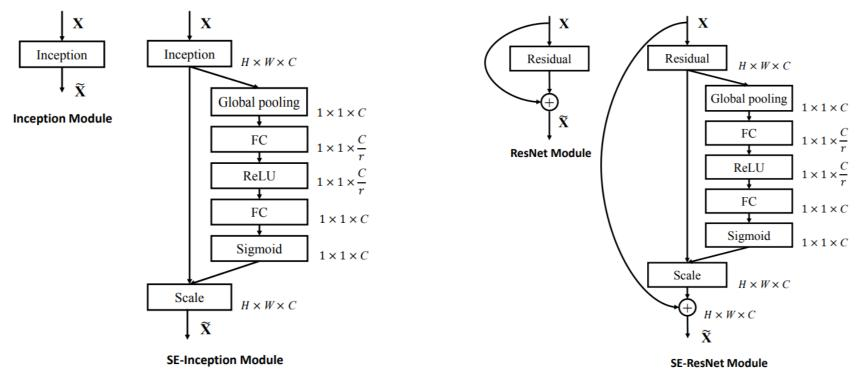
Squeeze and Excitation Module [Hu et al., 2018]

Motivation: The deeper the model, the more feature maps are generated

- Many of them might be important for classification task
- Others might redundant or less important

SE block integrates to Inception and ResNet module

• SENet ranked first in the ILSVRC'17 (2.99% \rightarrow 2.25%)



*source: Hu et al., "Squeeze-and-Excitation Networks", CVPR, 2018 36

Squeeze and Excitation Module [Hu et al., 2018]

Motivation: The deeper the model, the more feature maps are generated

- Many of them might be important for classification task
- Others might redundant or less important

SE block integrates to Inception and ResNet module

• SENet ranked first in the ILSVRC'17 (2.99% \rightarrow 2.25%)

| | orig | inal | re- | implementati | ion | SENet | | | |
|--------------------------|------------------|-----------------|------------|--------------|--------|------------------|-----------------|--------|--|
| | top-1 err. | top-5 err. | top-1 err. | top-5 err. | GFLOPs | top-1 err. | top-5 err. | GFLOPs | |
| ResNet-50 [13] | 24.7 | 7.8 | 24.80 | 7.48 | 3.86 | $23.29_{(1.51)}$ | $6.62_{(0.86)}$ | 3.87 | |
| ResNet-101 [13] | 23.6 | 7.1 | 23.17 | 6.52 | 7.58 | $22.38_{(0.79)}$ | $6.07_{(0.45)}$ | 7.60 | |
| ResNet-152 [13] | 23.0 | 6.7 | 22.42 | 6.34 | 11.30 | $21.57_{(0.85)}$ | $5.73_{(0.61)}$ | 11.32 | |
| ResNeXt-50 [19] | 22.2 | - | 22.11 | 5.90 | 4.24 | $21.10_{(1.01)}$ | $5.49_{(0.41)}$ | 4.25 | |
| ResNeXt-101 [19] | 21.2 | 5.6 | 21.18 | 5.57 | 7.99 | $20.70_{(0.48)}$ | $5.01_{(0.56)}$ | 8.00 | |
| VGG-16 [11] | - | - | 27.02 | 8.81 | 15.47 | $25.22_{(1.80)}$ | $7.70_{(1.11)}$ | 15.48 | |
| BN-Inception [6] | 25.2 | 7.82 | 25.38 | 7.89 | 2.03 | $24.23_{(1.15)}$ | $7.14_{(0.75)}$ | 2.04 | |
| Inception-ResNet-v2 [21] | 19.9^{\dagger} | 4.9^{\dagger} | 20.37 | 5.21 | 11.75 | $19.80_{(0.57)}$ | $4.79_{(0.42)}$ | 11.76 | |

Next, Convolutional Block Attention Module

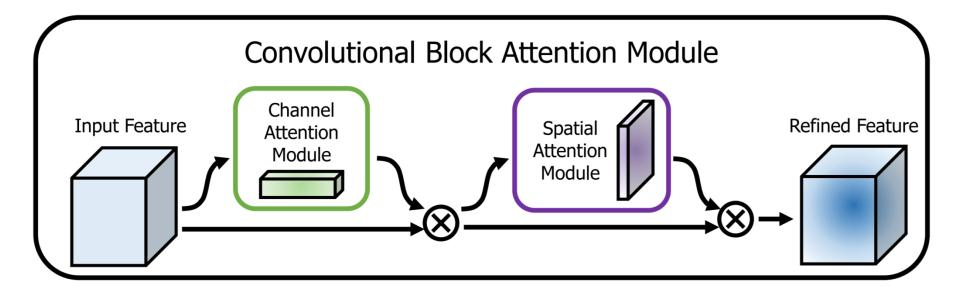
*source: Hu et al., "Squeeze-and-Excitation Networks", CVPR, 2018 37

Motivation: SENet only considers the contribution of feature maps

- It ignores the spatial locality of the object in image
- The spatial location of the object has a vital role in understanding image

Convolutional Block Attention Module (CBAM) [Woo et al., 2018]

- Learning 'what' and 'where' to attend in the channel and spatial axes respectively
- Channel and Spatial attention modules

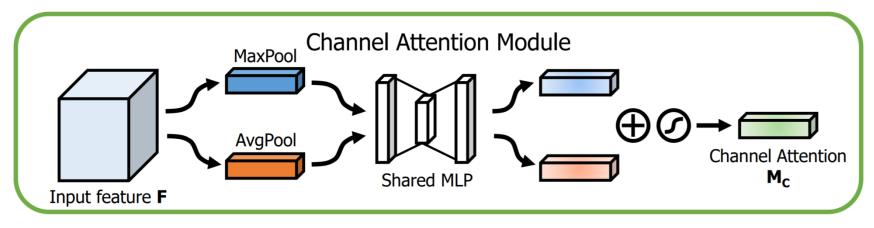


Motivation: SENet only considers the contribution of feature maps

- It ignores the spatial locality of the object in image
- The spatial location of the object has a vital role in understanding image

Channel attention module: It helps "what" to focus

- Both average-pooling and max-pooling are important
- **Max-pooling** provides the information of distinctive object features
- Both pooled features share a MLP with two fully-connected layers



 $\mathbf{M_c}(\mathbf{F}) = \sigma(MLP(AvgPool(\mathbf{F})) + MLP(MaxPool(\mathbf{F})))$

Algorithmic Intelligence Lab

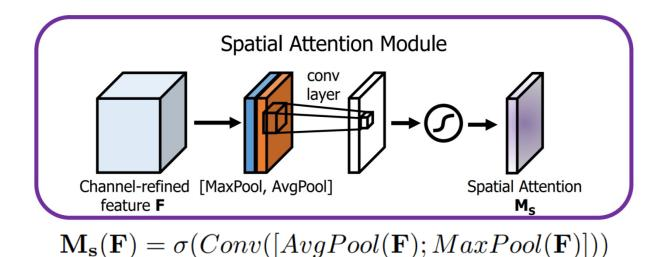
*source: Woo et al., "CBAM: Convolutional block attention module", ECCV, 2018 39

Motivation: SENet only considers the contribution of feature maps

- It ignores the spatial locality of the object in image
- The spatial location of the object has a vital role in understanding image

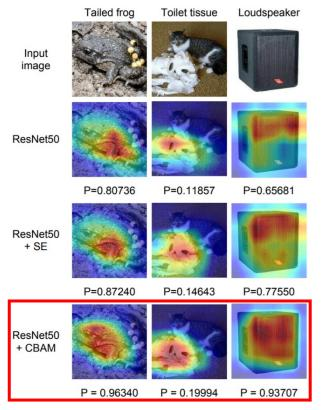
Spatial attention module: It helps "where" to focus

- Again, Both average-pooling and max-pooling are important
- It aggregates channel information of feature maps by using two pooling operations
- Capturing **spatial locality** via convolution



Motivation: SENet only considers the contribution of feature maps

- It ignores the spatial locality of the object in image
- The spatial location of the object has a vital role in understanding image
- **CBAM** module integrated with ResNet outperforms SE module



| Architecture | Param. | GFLOPs | Top-1 Error (%) | Top-5 Error (%) |
|-------------------------------------------------------------------------|--------|--------|-----------------|-----------------|
| ResNet18 [5] | 11.69M | 1.814 | 29.60 | 10.55 |
| ResNet18 $[5] + SE [28]$ | 11.78M | 1.814 | 29.41 | 10.22 |
| ResNet18 $[5] + CBAM$ | 11.78M | 1.815 | 29.27 | 10.09 |
| ResNet34 [5] | 21.80M | 3.664 | 26.69 | 8.60 |
| ResNet34 [5] + SE [28] | 21.96M | 3.664 | 26.13 | 8.35 |
| ResNet34[5] + CBAM | 21.96M | 3.665 | 25.99 | 8.24 |
| ResNet50 [5] | 25.56M | 3.858 | 24.56 | 7.50 |
| ResNet50 [5] + SE [28] | 28.09M | 3.860 | 23.14 | 6.70 |
| ResNet50[5] + CBAM | 28.09M | 3.864 | 22.66 | 6.31 |
| ResNet101 $[5]$ | 44.55M | 7.570 | 23.38 | 6.88 |
| ResNet101 [5] + SE [28] | 49.33M | 7.575 | 22.35 | 6.19 |
| $\operatorname{ResNet101}[5] + \operatorname{CBAM}$ | 49.33M | 7.581 | 21.51 | 5.69 |
| WideResNet18 [6] (widen= 1.5) | 25.88M | | 26.85 | 8.88 |
| WideResNet18 [6] (widen= 1.5) + SE [28] | 26.07M | 3.867 | 26.21 | 8.47 |
| WideResNet18 [6] (widen= 1.5) + CBAM | 26.08M | 3.868 | 26.10 | 8.43 |
| WideResNet18 [6] (widen= 2.0) | 45.62M | 6.696 | 25.63 | 8.20 |
| WideResNet18 [6] (widen= 2.0) + SE [28] | 45.97M | 6.696 | 24.93 | 7.65 |
| WideResNet18 [6] (widen= 2.0) + CBAM | 45.97M | 6.697 | 24.84 | 7.63 |
| ResNeXt50 [7] (32x4d) | 25.03M | 3.768 | 22.85 | 6.48 |
| ResNeXt50 [7] (32x4d) + SE [28] | 27.56M | 3.771 | 21.91 | 6.04 |
| $\operatorname{ResNeXt50}$ [7] (32x4d) + CBAM | 27.56M | 3.774 | 21.92 | 5.91 |
| ResNeXt101 [7] (32x4d) | 44.18M | 7.508 | 21.54 | 5.75 |
| ResNeXt101 [7] (32x4d) + SE [28] | 48.96M | | 21.17 | 5.66 |
| $\operatorname{ResNeXt101} [7] (32 \mathrm{x4d}) + \operatorname{CBAM}$ | 48.96M | 7.519 | 21.07 | 5.59 |

Grad-CAM visualization

*source: Woo et al., "CBAM: Convolutional block attention module", ECCV, 2018 41

Part 1. Basics

- Evolution of CNN architectures
- Batch normalization and ResNet
- Attention module in CNNs
- Vision transformers

Part 2. Advanced Topics

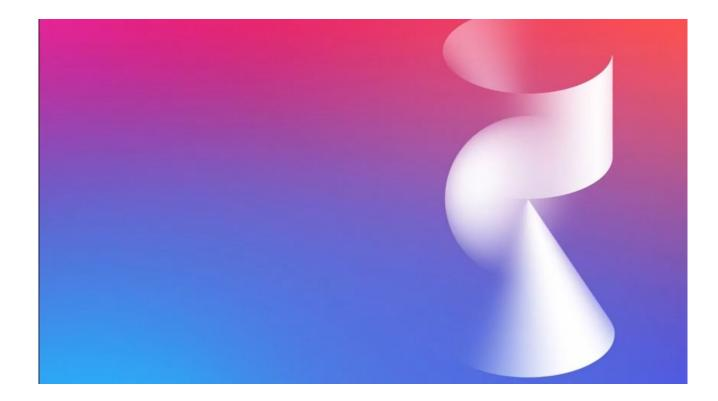
- Toward automation of network design
- Flexible architectures
- Observational study on network architectures
- Deep spatial-temporal models

Part 3. Beyond CNNs and Vision Transformers

- Patch-based architectures for vision
- New design paradigms

Success of Transformer in Language: GPT-3

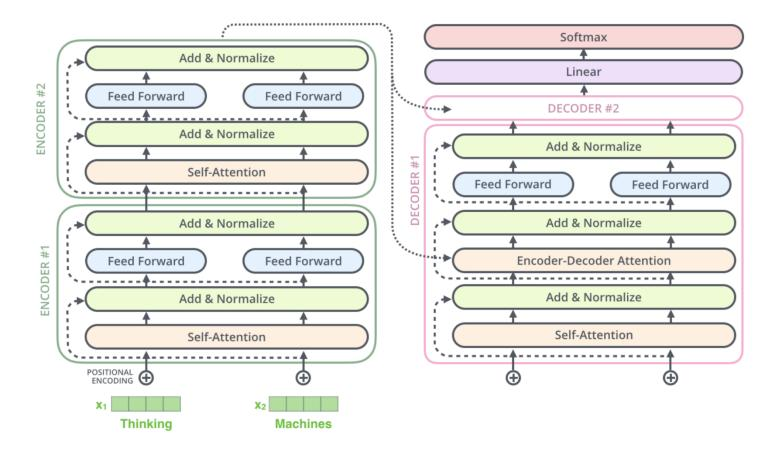
- In 2020, **GPT-3** achieved near-human results in various tasks
- OpenAI even trained a model with 175 billion parameters (350 GB of memory) and showed near-human performance on various few-shot tasks



*source : https://youtu.be/CSe3_u9P-RM

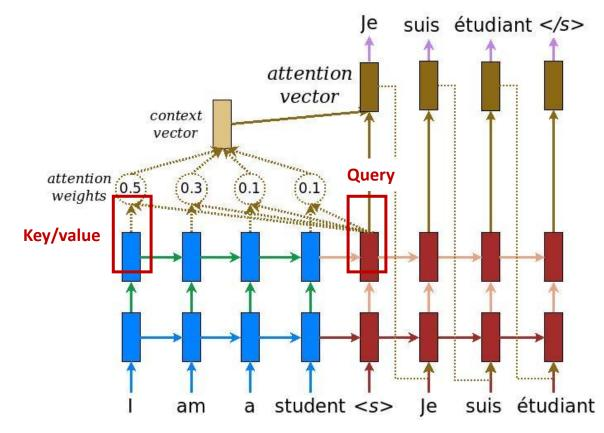
What is Transformer?

• Transformer [Vaswani et al., 2017] has an **encoder-decoder** structure and they are composed of multiple block with **self-attention** module



What is Transformer?

- Transformer [Vaswani et al., 2017] has an **encoder-decoder** structure and they are composed of multiple block with **self-attention** module
- The self-attention is a function of **query** (e.g., "Je") and **key/value** (e.g., "I")
 - It shows powerful performances in learning sequential input-output relations



Attention mechanism can be used for other type of input data, e.g. image

• Self-attention operation scales **quadratically** with the sequence length

| Layer Type | Complexity per Layer | Sequential Operations | Maximum Path Length |
|-----------------------------|--------------------------|-----------------------|---------------------|
| Self-Attention | $O(n^2 \cdot d)$ | O(1) | O(1) |
| Recurrent | $O(n \cdot d^2)$ | O(n) | O(n) |
| Convolutional | $O(k \cdot n \cdot d^2)$ | O(1) | $O(log_k(n))$ |
| Self-Attention (restricted) | $O(r \cdot n \cdot d)$ | O(1) | O(n/r) |

Question: How to transform an image to sequence data?

Dosovitskiy et al. (2021): splits an image into patches

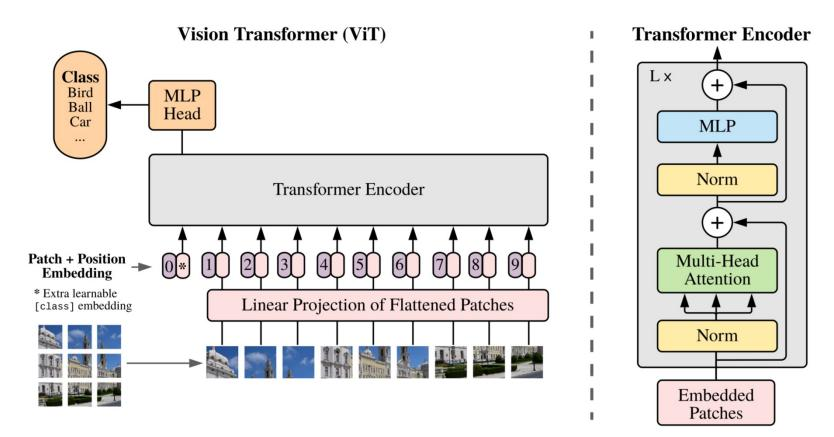


*source: [Chen et al. 2020] Generative Pretraining from Pixels, ICML 2020 [Dosovitskiy et al. 2021] An image is worth 16x16 words: Transformers for image recognition at scale, ICLR 2021

Vision Transformer [Dosovitskiy et al., 2021]

Vision Transformer [Dosovitskiy et al., 2021]

- Splitting an image into fixed-size patches (16x16)
 - Linearly embedding each of them
- Adding position embedding & [class] token



Vision Transformer [Dosovitskiy et al., 2021]

- Splitting an image into fixed-size patches (16x16)
 - Linearly embedding each of them ٠
- Adding position embedding & [class] token
- **Dosovitskiy et al.** (2021) pre-trains models on larger datasets (14M-300M images)
 - Vision Transformer achieves competitive performances compared to CNNs

| | Ours-JFT (ViT-H/14) | Ours-JFT (ViT-L/16) | Ours-I21k (ViT-L/16) | BiT-L (ResNet152x4) | Noisy Student (EfficientNet-L2) |
|-----------------------------------------------------------------------------------------------------------------|-------------------------------------------------------------------------------------------------------------------------------------------------------------------------------------------------------------------------------------------------------------|--------------------------------------------------------------------------------------------------------------------------------------------------------------------|-----------------------------------------------------------------------------------------------------------------------------------------------------------|--------------------------------------------------------------------------------------------------------------------------------------------------|-------------------------------------------------------------|
| ImageNet ImageNet ReaL CIFAR-10 CIFAR-100 Oxford-IIIT Pets Oxford Flowers-102 VTAB (19 tasks) | $\begin{array}{c} {\color{red} 88.55 \pm 0.04} \\ {\color{red} 90.72 \pm 0.05} \\ {\color{red} 99.50 \pm 0.06} \\ {\color{red} 94.55 \pm 0.04} \\ {\color{red} 97.56 \pm 0.03} \\ {\color{red} 99.68 \pm 0.02} \\ {\color{red} 77.63 \pm 0.23} \end{array}$ | $\begin{array}{c} 87.76 \pm 0.03 \\ 90.54 \pm 0.03 \\ 99.42 \pm 0.03 \\ 93.90 \pm 0.05 \\ 97.32 \pm 0.11 \\ \textbf{99.74} \pm 0.00 \\ 76.28 \pm 0.46 \end{array}$ | $\begin{array}{c} 85.30 \pm 0.02 \\ 88.62 \pm 0.05 \\ 99.15 \pm 0.03 \\ 93.25 \pm 0.05 \\ 94.67 \pm 0.15 \\ 99.61 \pm 0.02 \\ 72.72 \pm 0.21 \end{array}$ | $\begin{array}{c} 87.54 \pm 0.02 \\ 90.54 \\ 99.37 \pm 0.06 \\ 93.51 \pm 0.08 \\ 96.62 \pm 0.23 \\ 99.63 \pm 0.03 \\ 76.29 \pm 1.70 \end{array}$ | 88.4/88.5* 90.55 - - - - - - - - |
| TPUv3-core-days | 2.5k | 0.68k | 0.23k | 9.9k | 12.3k |
| | | | | | |

Vision Transformer

CNNs

Input Attention









Various architectures now are based on Vision Transformer

1. Modification for patch splitting

- Token-to-Token Vision Transformer [Li et al., 2021]
- Swin Transformer [Liu et al., 2021]

2. Modification for hierarchical structure

- Pooling-based Vision Transformer [Heo et al., 2021]
- Swin Transformer [Liu et al., 2021]

Question: What's a good way to split an image into a sequence of patches?

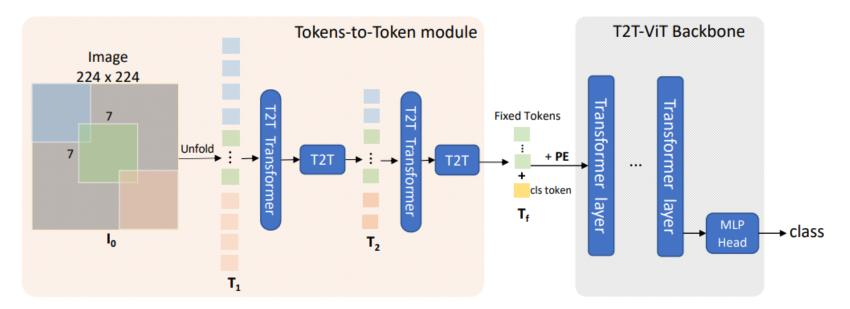
• Vision Transformer splits an image into a **fixed grid-shape** of **non-overlapping** patches



Token-to-Token Vision Transformer [Li et al., 2021]

Token-to-Token Vision Transformer [Li et al., 2021]

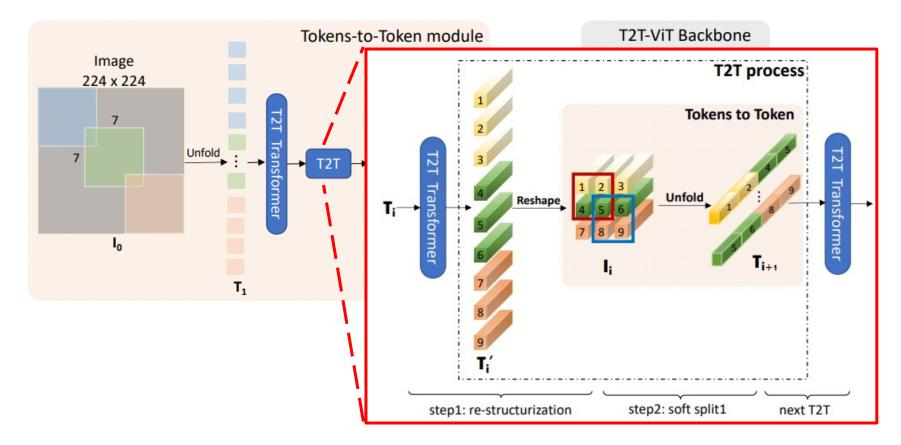
- (Soft-split) Splitting an image into overlapping patches
- (Re-structurization) Rearranging patch sequences into 2D image shape
- Iterating re-structurization and soft-split before Transformer backbone



Token-to-Token Vision Transformer [Li et al., 2021]

Token-to-Token Vision Transformer [Li et al., 2021]

- (Soft-split) Splitting an image into overlapping patches
- (Re-structurization) Rearranging patch sequences into 2D image shape
- Iterating re-structurization and soft-split before Transformer backbone



Pooling-based Vision Transformer [Heo et al., 2021]

Pooling-based Vision Transformer [Heo et al., 2021]

- Design of a hierarchical structure
 - Motivation: ResNet gradually downsamples the features from the input to the output

 $\frac{w}{2} \times \frac{h}{2} \times 2d$

Spatial tokens

 $\left(\frac{w}{2} \times \frac{h}{2}\right) \times 2d$

 $1 \times 2d$

Class token

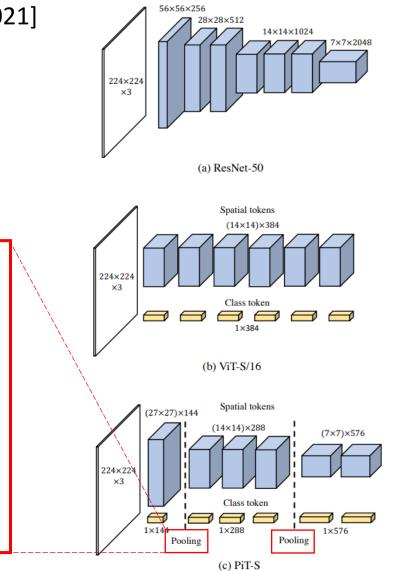
Reshape

- Downsampling via the pooling layer based on depth-wise convolution
- Spatial reduction with small parameters

Depth-wise

Convolution

Fully-connected layer



Algorithmic Intelligence Lab

 $1 \times d$

Class token

Spatial tokens

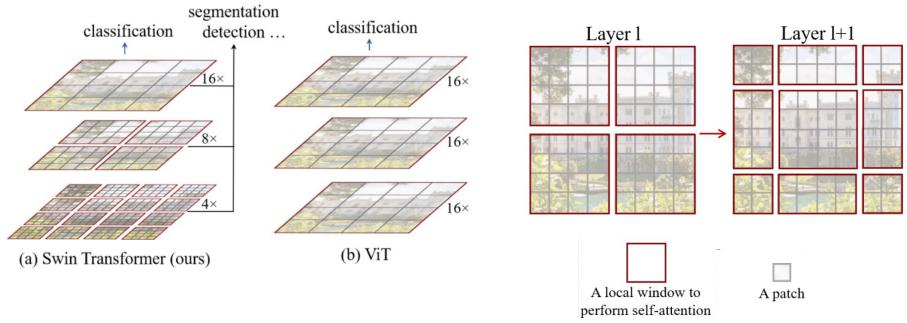
 $(w \times h) \times d$

Reshape

 $w \times h \times d$

Swin Transformer [Liu et al., 2021]

- Design of a hierarchical structure
- Various spatial resolutions (e.g., patch-shape) can be handled via shifted windows
- Efficient self-attention computation by using shifted windows scheme
- Concatenating 2 × 2 neighboring patches for downsampling operation
- Powerful performances in dense prediction tasks
 - e.g., object detection and semantic segmentation



Shifted window scheme

DeiT III [Touvron et al., 2022]

Question: Do vision transformers need some inductive bias under small data?

- Vision transformers achieved state-of-the-art performances but...
 - Required gigantic-scale training with JFT-300M data
 - Sub-optimal performance under the ImageNet-scale training
- Injecting some inductive bias (e.g., Swin, PiT) was needed for ImageNet-scale

| | Ours-JFT (ViT-H/14) | Ours-JFT (ViT-L/16) | Ours-I21k (ViT-L/16) | BiT-L (ResNet152x4) | Noisy Student (EfficientNet-L2) |
|--------------------|------------------------|------------------------|-------------------------|------------------------|------------------------------------|
| ImageNet | 88.55 ± 0.04 | 87.76 ± 0.03 | 85.30 ± 0.02 | 87.54 ± 0.02 | $88.4/88.5^{*}$ |
| ImageNet ReaL | 90.72 ± 0.05 | 90.54 ± 0.03 | 88.62 ± 0.05 | 90.54 | 90.55 |
| CIFAR-10 | 99.50 ± 0.06 | 99.42 ± 0.03 | 99.15 ± 0.03 | 99.37 ± 0.06 | _ |
| CIFAR-100 | 94.55 ± 0.04 | 93.90 ± 0.05 | 93.25 ± 0.05 | 93.51 ± 0.08 | _ |
| Oxford-IIIT Pets | 97.56 ± 0.03 | 97.32 ± 0.11 | 94.67 ± 0.15 | 96.62 ± 0.23 | _ |
| Oxford Flowers-102 | 99.68 ± 0.02 | 99.74 ± 0.00 | 99.61 ± 0.02 | 99.63 ± 0.03 | _ |
| VTAB (19 tasks) | 77.63 ± 0.23 | 76.28 ± 0.46 | 72.72 ± 0.21 | 76.29 ± 1.70 | _ |
| TPUv3-core-days | 2.5k | 0.68k | 0.23k | 9.9k | 12.3k |

DeiT III [Touvron et al., 2022]

Motivation: Do vision transformers need some inductive bias under small data?

- Vision transformers achieved state-of-the-art performances but...
 - Required gigantic-scale training with JFT-300M data
 - Sub-optimal performance under the ImageNet-scale training
- Injecting some inductive bias (e.g., Swin, PiT) was needed for ImageNet-scale

DeiT III [Touvron et al., 2022] finds that vanilla vision transformer can outperform CNNs in ImageNet-scale:

- The problem was in the **sub-optimal optimization designs**
 - LayerScale
 - Improved data augmentations could solve the optimization issues

Check the paper for details!

| | | Previous | approaches | Ours | | | |
|-------------------------------|-------------|----------------------------|-------------|-------------|-------------|-------------|-------------|
| Procedure \rightarrow | ViT | Steiner | DeiT | Wightman | ImNet-1k | et-21k | |
| Reference | [13] | et al. [<mark>42</mark>] | [48] | et al. [57] | | Pretrain. | Finetune. |
| Batch size | 4096 | 4096 | 1024 | 2048 | 2048 | 2048 | 2048 |
| Optimizer | AdamW | AdamW | AdamW | LAMB | LAMB | LAMB | LAMB |
| LR | 3.10^{-3} | 3.10^{-3} | 1.10^{-3} | 5.10^{-3} | 3.10^{-3} | 3.10^{-3} | 3.10^{-4} |
| LR decay | cosine | cosine | cosine | cosine | cosine | cosine | cosine |
| Weight decay | 0.1 | 0.3 | 0.05 | 0.02 | 0.02 | 0.02 | 0.02 |
| Warmup epochs | 3.4 | 3.4 | 5 | 5 | 5 | 5 | 5 |
| Label smoothing ε | 0.1 | 0.1 | 0.1 | X | X | 0.1 | 0.1 |
| Dropout | 1 | 1 | X | × | X | X | X |
| Stoch. Depth | X | 1 | 1 | 1 | 1 | 1 | 1 |
| Repeated Aug | X | X | 1 | 1 | 1 | X | X |
| Gradient Clip. | 1.0 | 1.0 | X | 1.0 | 1.0 | 1.0 | 1.0 |
| H. flip | 1 | 1 | 1 | 1 | 1 | 1 | 1 |
| RRC | 1 | 1 | 1 | 1 | 1 | X | × |
| Rand Augment | X | Adapt. | 9/0.5 | 7/0.5 | X | X | X |
| 3 Augment (ours) | X | X | X | X | 1 | 1 | 1 |
| LayerScale | X | X | X | X | 1 | 1 | 1 |
| Mixup alpha | X | Adapt. | 0.8 | 0.2 | 0.8 | X | X |
| Cutmix alpha | X | X | 1.0 | 1.0 | 1.0 | 1.0 | 1.0 |
| Erasing prob. | X | X | 0.25 | X | X | X | X |
| ColorJitter | X | X | X | × | 0.3 | 0.3 | 0.3 |
| Test crop ratio | 0.875 | 0.875 | 0.875 | 0.95 | 1.0 | 1.0 | 1.0 |
| Loss | CE | CE | CE | BCE | BCE | CE | CE |

Algorithmic Intelligence Lab

*source: Dai et al., "Deformable Convolutional Networks", ICCV, 2017 55

DeiT III [Touvron et al., 2022]

Motivation: Do vision transformers need some inductive bias under small data?

- Vision transformers achieved state-of-the-art performances but...
 - Required gigantic-scale training with JFT-300M data
 - Sub-optimal performance under the ImageNet-scale training
- Injecting some inductive bias (e.g., Swin, PiT) was needed for ImageNet-scale

DeiT III [Touvron et al., 2022] finds that vanilla vision transformer can outperform CNNs in ImageNet-scale:

| Architecture | | throughput | | | Top-1 | V2 | | Vision Trai | nsformers d | lerivative | | | |
|--------------------------------------|-------------------|--------------|-----------------|-------|-------|------|------------------------------|-------------|-------------|------------|-------|------|------|
| | $(\times 10^{6})$ | (im/s) | $(\times 10^9)$ | (MB) | Acc. | Acc. | Swin-B [31] | 87.8 | 532 | 15.4 | 4695 | 85.2 | 74.6 |
| | "Tradit | ional" Convl | Nets | | | | Swin-B†384 [31] | 87.9 | 160 | 47.0 | 19385 | 86.4 | 76.3 |
| R-101x3 ³ 84 [25] | 388 | | 204.6 | | 84.4 | | Swin-L [31] | 196.5 | 337 | 34.5 | 7350 | 86.3 | 76.3 |
| R-152x4 ⁴⁸⁰ [25] | 937 | - | 204.0 840.5 | | 85.4 | - | Swin-L↑384 [31] | 196.7 | 100 | 103.9 | 33456 | 87.3 | 77.0 |
| | | - | | | 1 | - | | Vanilla V | ision Trans | formers | | | |
| EfficientNetV2-S ³⁸⁴ [45] | 21.5 | 874 | 8.5 | | 84.9 | 74.5 | ViT-B/16 [42] | 86.6 | 831 | 17.6 | 2078 | 84.0 | |
| EfficientNetV2-M ⁴⁸⁰ [45] | 54.1 | 312 | 25.0 | | 86.2 | 75.9 | ViT-B/16 ³⁸⁴ [42] | 86.7 | 190 | 55.5 | 8956 | 85.5 | _ |
| EfficientNetV2-L↑480 [45] | 118.5 | 179 | 53.0 | 9540 | 86.8 | 76.9 | ViT-L/16 [42] | 304.4 | 277 | 61.6 | 3789 | 84.0 | _ |
| EfficientNetV2-XL ⁵¹² [45 |] 208.1 | - | 94.0 | - | 87.3 | 77.0 | ViT-L/16†384 [42] | 304.8 | 67 | 191.1 | 12866 | 85.5 | _ |
| | Patch- | based ConvN | lets | | | | | Our Vanilla | Vision Tra | nsformers | | | |
| ConvNeXt-B [32] | 88.6 | 563 | 15.4 | 3029 | 85.8 | 75.6 | ViT-S | 22.0 | 1891 | 4.6 | 987 | 83.1 | 73.8 |
| ConvNeXt-B ³⁸⁴ [32] | 88.6 | 190 | 45.1 | 7851 | 86.8 | 76.6 | ViT-B | 86.6 | 831 | 17.6 | 2078 | 85.7 | 76.5 |
| ConvNeXt-L [32] | 197.8 | 344 | 34.4 | 4865 | 86.6 | 76.6 | ViT-B↑384 | 86.9 | 190 | 55.5 | 8956 | 86.7 | 77.9 |
| ConvNeXt-L ³⁸⁴ [32] | 197.8 | 115 | 101 | 11938 | 87.5 | 77.7 | ViT-L | 304.4 | 277 | 61.6 | 3789 | 87.0 | 78.6 |
| ConvNeXt-XL [32] | 350.2 | 241 | 60.9 | 6951 | 87.0 | 77.0 | ViT-L↑384 | 304.8 | 67 | 191.2 | 12866 | 87.7 | 79.1 |
| ConvNeXt-XL ³⁸⁴ [32] | 350.2 | 80 | 179.0 | 16260 | 87.8 | 77.7 | ViT-H | 632.1 | 112 | 167.4 | 6984 | 87.2 | 79.2 |

Table of Contents

Part 1. Basics

- Evolution of CNN architectures
- Batch normalization and ResNet
- Attention module in CNNs
- Vision transformers

Part 2. Advanced Topics

- Toward automation of network design
- Flexible architectures
- Observational study on network architectures
- Deep spatial-temporal models

Part 3. Beyond CNNs and Vision Transformers

- Patch-based architectures for vision
- New design paradigms

Table of Contents

Part 1. Basics

- Evolution of CNN architectures
- Batch normalization and ResNet
- Attention module in CNNs
- Vision transformers

Part 2. Advanced Topics

- Toward automation of network design
- Flexible architectures
- Observational study on network architectures
- Deep spatial-temporal models

Part 3. Beyond CNNs and Vision Transformers

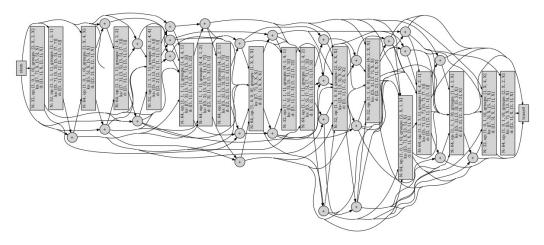
- Patch-based architectures for vision
- New design paradigms

Although the CNN architecture has evolved greatly, our **design principles are still relying on heuristics**

• Smaller kernel and smaller stride, increase cardinality instead of width ...

Recently, there have been works on automatically finding a structure which can outperform existing human-crafted architectures

- 1. Search space: Naïvely searching every model is nearly impossible
- 2. Searching algorithm: Evaluating each model is very costly, and black-boxed



A sample architecture found in [Brock et al., 2018]

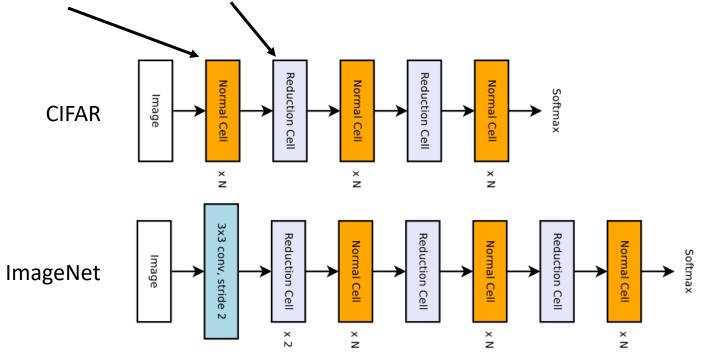
Toward Automation of Network Design: NASNet [Zoph et al., 2018]

Designing a good search space is important in architecture searching

NASNet reduces the search space by incorporating our design principles

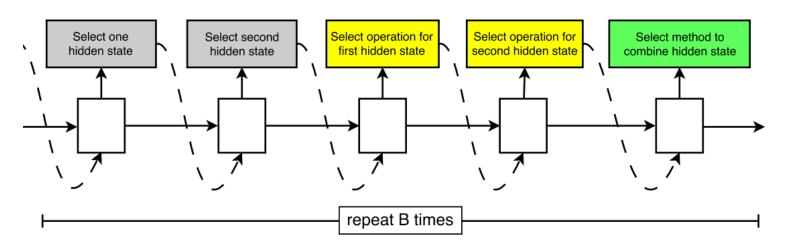
Motivation: modern architectures are built simply: a repeated modules

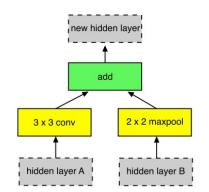
- Try not to search the whole model, but only cells modules
- Normal cell and Reduction cell (cell w/ stride 2)



Designing a good search space is important in architecture searching

- NASNet reduces the search space by incorporating our design principles
- Each cell consists of *B* blocks
- Each block is determined by selecting methods
 - 1. Select two hidden states from h_i , h_{i-1} or of existing block
 - 2. Select methods to process for each of the selected states
 - 3. Select a method to combine the two states
 - (1) element-wise addition or (2) concatenation





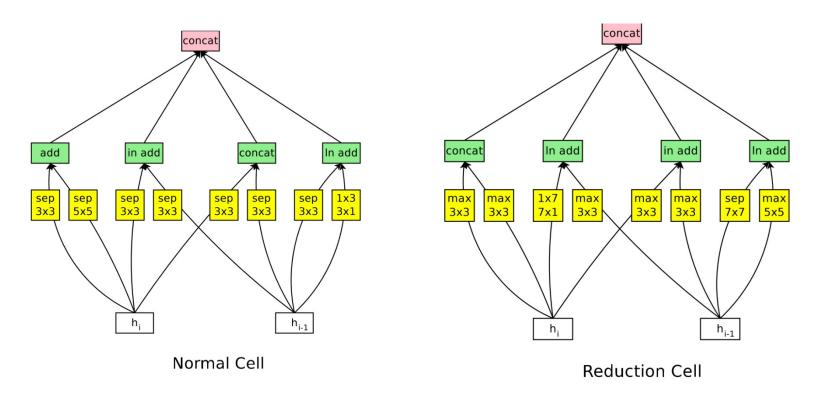
Algorithmic Intelligence Lab

*source : Zoph et al., "Learning Transferable Architectures for Scalable Image Recognition", CVPR 2018 61

Toward Automation of Network Design: NASNet [Zoph et al., 2018]

Designing a good search space is important in architecture searching

- NASNet reduces the search space by incorporating our design principles
- Each cell consists of *B* blocks
 - Example: B = 4



Designing a good search space is important in architecture searching

- NASNet reduces the search space by incorporating our design principles
- Set of methods to be selected based on their prevalence in the CNN literature
 - identity
 - 1x7 then 7x1 convolution
 - 3x3 average pooling
 - 5x5 max pooling
 - 1x1 convolution
 - 3x3 depthwise-separable conv
 - 7x7 depthwise-separable conv

- 1x3 then 3x1 convolution
- 3x3 dilated convolution
- 3x3 max pooling
- 7x7 max pooling
- 3x3 convolution
- 5x5 depthwise-seperable conv

- Any searching methods can be used
 - Random search [Bergstra et al., 2012] could also work
 - RL-based search [Zoph et al., 2016] is mainly used in this paper

- The pool of workers consisted of 500 GPUs, processing over 4 days
- All architecture searches are performed on CIFAR-10
 - NASNet-A: State-of-the-art error rates could be achieved
 - NASNet-B/C: Extremely parameter-efficient models were also found

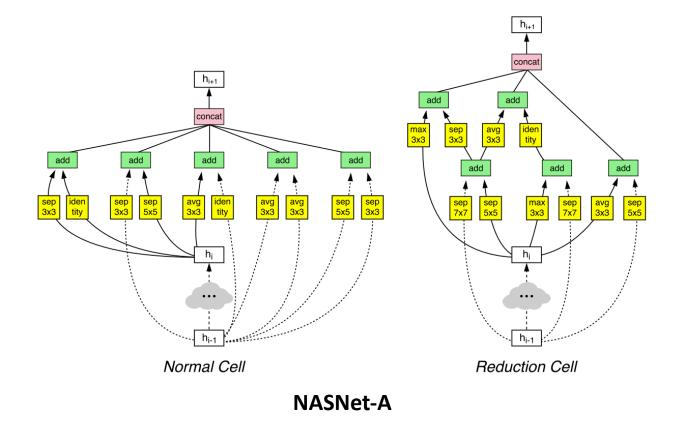
| model | depth | # params | error rate (%) |
|--------------------------------------|-------|----------|----------------|
| DenseNet $(L = 40, k = 12)$ [26] | 40 | 1.0M | 5.24 |
| DenseNet $(L = 100, k = 12)$ [26] | 100 | 7.0M | 4.10 |
| DenseNet $(L = 100, k = 24)$ [26] | 100 | 27.2M | 3.74 |
| DenseNet-BC $(L = 100, k = 40)$ [26] | 190 | 25.6M | 3.46 |
| Shake-Shake 26 2x32d [18] | 26 | 2.9M | 3.55 |
| Shake-Shake 26 2x96d [18] | 26 | 26.2M | 2.86 |
| Shake-Shake 26 2x96d + cutout [12] | 26 | 26.2M | 2.56 |
| NAS v3 [70] | 39 | 7.1M | 4.47 |
| NAS v3 [70] | 39 | 37.4M | 3.65 |
| NASNet-A (6 @ 768) | - | 3.3M | 3.41 |
| NASNet-A (6 @ 768) + cutout | - | 3.3M | 2.65 |
| NASNet-A (7 @ 2304) | - | 27.6M | 2.97 |
| NASNet-A (7 @ 2304) + cutout | - | 27.6M | 2.40 |
| NASNet-B (4 @ 1152) | - | 2.6M | 3.73 |
| NASNet-C (4 @ 640) | - | 3.1M | 3.59 |

Toward Automation of Network Design: NASNet [Zoph et al., 2018]

• The pool of workers consisted of **500 GPUs**, processing over **4 days**

All architecture searches are performed on CIFAR-10

- NASNet-A: State-of-the-art error rates could be achieved
- NASNet-B/C: Extremely parameter-efficient models were also found



• The pool of workers consisted of **500 GPUs**, processing **over 4 days** All architecture searches are performed on **CIFAR-10**

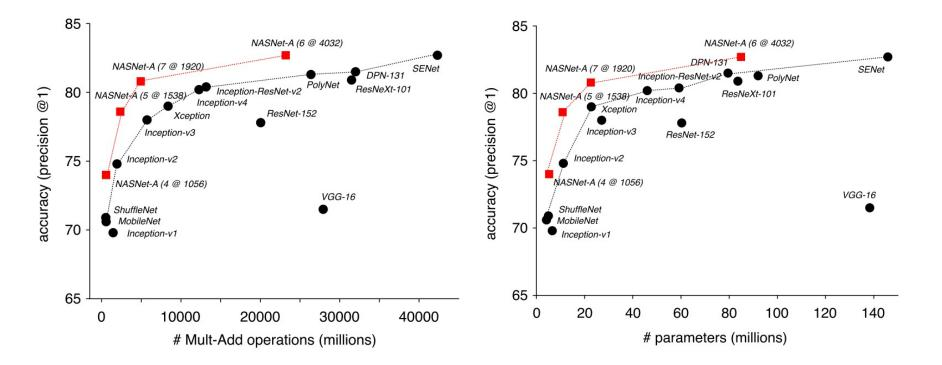
Cells found in CIFAR-10 could also transferred well into ImageNet

| Model | image size | # parameters | Mult-Adds | Top 1 Acc. (%) | Top 5 Acc. (%) |
|----------------------------|------------|---------------|---------------|----------------|-----------------------|
| Inception V2 [29] | 224×224 | 11.2 M | 1.94 B | 74.8 | 92.2 |
| NASNet-A (5 @ 1538) | 299×299 | 10.9 M | 2.35 B | 78.6 | 94.2 |
| Inception V3 [59] | 299×299 | 23.8 M | 5.72 B | 78.0 | 93.9 |
| Xception [9] | 299×299 | 22.8 M | 8.38 B | 79.0 | 94.5 |
| Inception ResNet V2 [57] | 299×299 | 55.8 M | 13.2 B | 80.4 | 95.3 |
| NASNet-A (7 @ 1920) | 299×299 | 22.6 M | 4.93 B | 80.8 | 95.3 |
| ResNeXt-101 (64 x 4d) [67] | 320×320 | 83.6 M | 31.5 B | 80.9 | 95.6 |
| PolyNet [68] | 331×331 | 92 M | 34.7 B | 81.3 | 95.8 |
| DPN-131 [8] | 320×320 | 79.5 M | 32.0 B | 81.5 | 95.8 |
| SENet [25] | 320×320 | 145.8 M | 42.3 B | 82.7 | 96.2 |
| NASNet-A (6 @ 4032) | 331×331 | 88.9 M | 23.8 B | 82.7 | 96.2 |

Toward Automation of Network Design: NASNet [Zoph et al., 2018]

• The pool of workers consisted of **500 GPUs**, processing **over 4 days** All architecture searches are performed on **CIFAR-10**

Cells found in CIFAR-10 could also transferred well into ImageNet

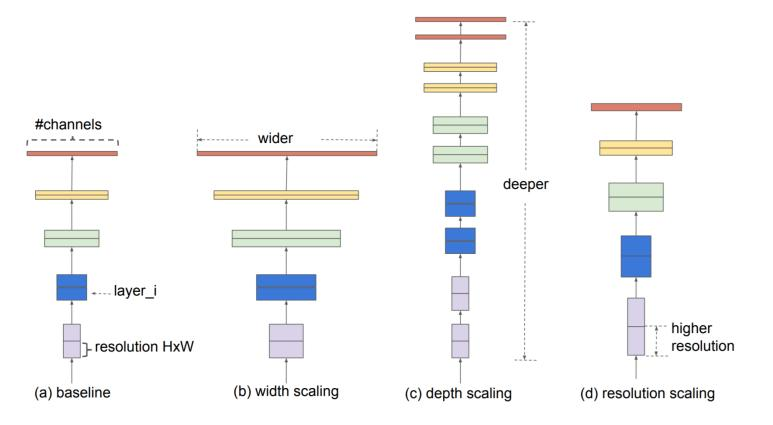


Toward Automation of Network Design: Principle of Network Scaling

Although **Scaling up** CNNs is widely used to achieve better generalization, the process of scaling has never been understood

• The common way is scaling model depth, width, and image resolution

Question: Is there a principled scaling method for better accuracy and efficiency?

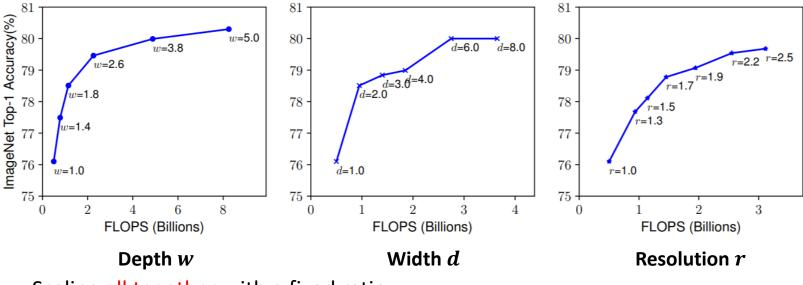


The state-of-the-art ILSVRC classification in 2019 (top-5 error rate 2.9%)

• EfficientNet uniformly scales network width, depth, and resolution with a set of fixed scaling coefficients (called "compound scaling")

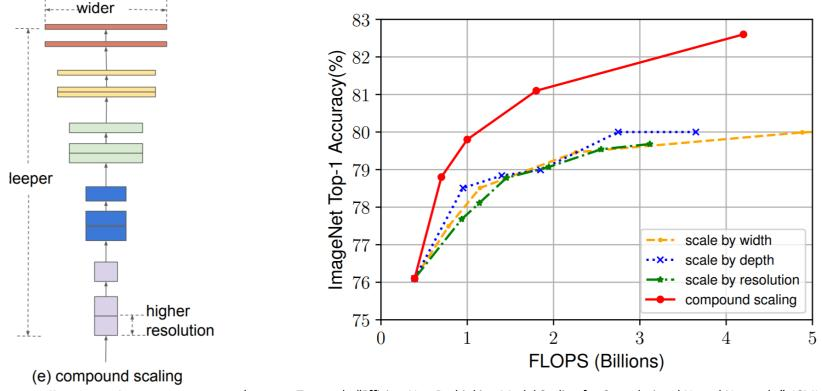
Motivation: There exists certain relationship between network width, depth and image resolution

- Scaling single dimension has a limitation
 - Gain diminishes for bigger models.



• Scaling all together with a fixed ratio

- Compound scaling: Scaling all together with a fixed ratio ϕ in a principled way
 - Depth $d = \alpha^{\phi}$, $\alpha \ge 1$
 - Width $w = \beta^{\phi}$, $\beta \ge 1$
 - Resolution $r = \gamma^{\phi}, \gamma \ge 1$
 - Finding α , β , γ under compound constraint $\alpha \cdot \beta^2 \cdot \gamma^2 \approx 2$
 - Why? Such scaling approximately increases total FLOPS by $(\alpha \cdot \beta^2 \cdot \gamma^2)^{\phi} \approx 2^{\phi}$

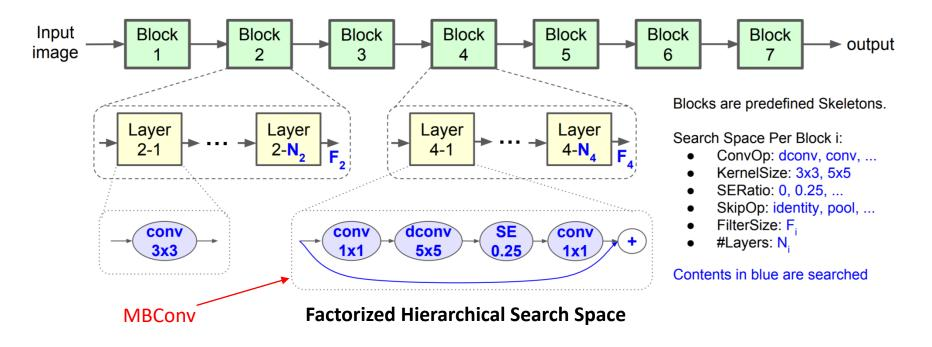


Algorithmic Intelligence Lab

*source : Tan et al., "EfficientNet: Rethinking Model Scaling for Convolutional Neural Networks", ICML 2019 70

Having a good baseline network is also critical!

- Multi-objective neural architecture search
 - Optimizing both accuracy and FLOPS
 - Search space is the same as MnasNet [Tan et al., 2019]
- Mobile-size baseline, called EfficientNet-B0
 - Main building block is mobile inverted bottleneck, MBConv
 - Adding squeeze-and-excitation (SE) optimization [Hu et al., 2018]

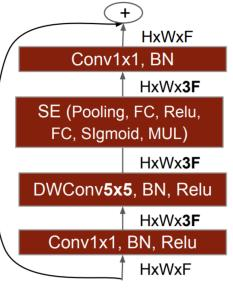


Having a good baseline network is also critical!

- Multi-objective neural architecture search
 - Optimizing both accuracy and FLOPS
 - Search space is the same as MnasNet [Tan et al., 2019]
- Mobile-size baseline, called EfficientNet-B0
 - Main building block is mobile inverted bottleneck, MBConv
 - Adding squeeze-and-excitation (SE) optimization [Hu et al., 2018]
 - DWConv denotes depthwise convolution [Howard et al ., 2017]

| Stage <i>i</i> | Operator $\hat{\mathcal{F}}_i$ | Resolution $\hat{H}_i \times \hat{W}_i$ | #Channels \hat{C}_i | #Layers \hat{L}_i |
|----------------|--------------------------------|-----------------------------------------|-----------------------|---------------------|
| 1 | Conv3x3 | 224×224 | 32 | 1 |
| 2 | MBConv1, k3x3 | 112×112 | 16 | 1 |
| 3 | MBConv6, k3x3 | 112×112 | 24 | 2 |
| 4 | MBConv6, k5x5 | 56×56 | 40 | 2 |
| 5 | MBConv6, k3x3 | 28×28 | 80 | 3 |
| 6 | MBConv6, k5x5 | 14×14 | 112 | 3 |
| 7 | MBConv6, k5x5 | 14×14 | 192 | 4 |
| 8 | MBConv6, k3x3 | 7	imes 7 | 320 | 1 |
| 9 | Conv1x1 & Pooling & FC | 7 	imes 7 | 1280 | 1 |

Architecture of EfficientNet-B0



MBConv

*source : Tan et al., "EfficientNet: Rethinking Model Scaling for Convolutional Neural Networks", ICML 2019 Tan et al., "Mnasnet: Platform-aware neural architecture search for mobile", CVPR 2019

From EfficientNet-B0 to B7

- EfficientNet-BO: Baseline model with $\alpha = 1.2, \beta = 1.1, \gamma = 1.15$
- EfficientNet-B1 to B7: Scaling up EfficientNet-B0 with different ϕ

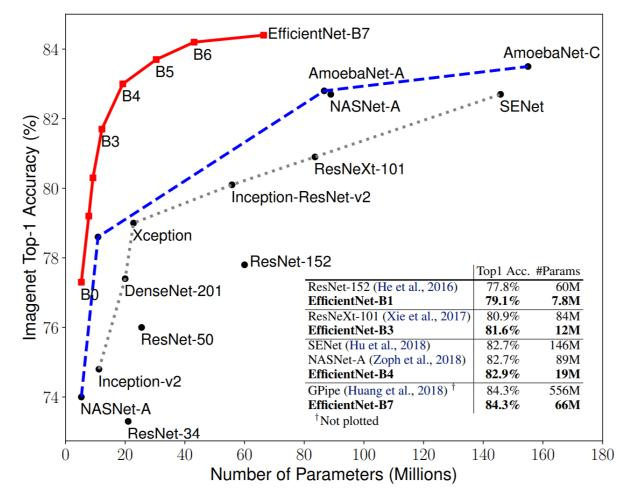
| Model | Top-1 Acc. | Top-5 Acc. | #Params | Ratio-to-EfficientNet | #FLOPs | Ratio-to-EfficientNet |
|--------------------------------------------|------------|------------|---------|-----------------------|--------|-----------------------|
| EfficientNet-B0 | 77.1% | 93.3% | 5.3M | 1x | 0.39B | 1x |
| ResNet-50 (He et al., 2016) | 76.0% | 93.0% | 26M | 4.9x | 4.1B | 11x |
| DenseNet-169 (Huang et al., 2017) | 76.2% | 93.2% | 14M | 2.6x | 3.5B | 8.9x |
| EfficientNet-B1 | 79.1% | 94.4% | 7.8M | 1x | 0.70B | 1x |
| ResNet-152 (He et al., 2016) | 77.8% | 93.8% | 60M | 7.6x | 11B | 16x |
| DenseNet-264 (Huang et al., 2017) | 77.9% | 93.9% | 34M | 4.3x | 6.0B | 8.6x |
| Inception-v3 (Szegedy et al., 2016) | 78.8% | 94.4% | 24M | 3.0x | 5.7B | 8.1x |
| Xception (Chollet, 2017) | 79.0% | 94.5% | 23M | 3.0x | 8.4B | 12x |
| EfficientNet-B2 | 80.1% | 94.9% | 9.2M | 1x | 1.0B | 1x |
| Inception-v4 (Szegedy et al., 2017) | 80.0% | 95.0% | 48M | 5.2x | 13B | 13x |
| Inception-resnet-v2 (Szegedy et al., 2017) | 80.1% | 95.1% | 56M | 6.1x | 13B | 13x |
| EfficientNet-B3 | 81.6% | 95.7% | 12M | 1x | 1.8B | 1x |
| ResNeXt-101 (Xie et al., 2017) | 80.9% | 95.6% | 84M | 7.0x | 32B | 18x |
| PolyNet (Zhang et al., 2017) | 81.3% | 95.8% | 92M | 7.7x | 35B | 19x |
| EfficientNet-B4 | 82.9% | 96.4% | 19M | 1x | 4.2B | 1x |
| SENet (Hu et al., 2018) | 82.7% | 96.2% | 146M | 7.7x | 42B | 10x |
| NASNet-A (Zoph et al., 2018) | 82.7% | 96.2% | 89M | 4.7x | 24B | 5.7x |
| AmoebaNet-A (Real et al., 2019) | 82.8% | 96.1% | 87M | 4.6x | 23B | 5.5x |
| PNASNet (Liu et al., 2018) | 82.9% | 96.2% | 86M | 4.5x | 23B | 6.0x |
| EfficientNet-B5 | 83.6% | 96.7% | 30M | 1x | 9.9B | 1x |
| AmoebaNet-C (Cubuk et al., 2019) | 83.5% | 96.5% | 155M | 5.2x | 41B | 4.1x |
| EfficientNet-B6 | 84.0% | 96.8% | 43M | 1x | 19B | 1x |
| EfficientNet-B7 | 84.3% | 97.0% | 66M | 1x | 37B | 1x |
| GPipe (Huang et al., 2018) | 84.3% | 97.0% | 557M | 8.4x | - | - |

Algorithmic Intelligence Lab

*source : Tan et al., "EfficientNet: Rethinking Model Scaling for Convolutional Neural Networks", ICML 2019 73

From EfficientNet-B0 to B7

- EfficientNet-BO: Baseline model with $\alpha = 1.2$, $\beta = 1.1$, $\gamma = 1.15$
- EfficientNet-B1 to B7: Scaling up EfficientNet-B0 with different ϕ



EfficientNet-B7 achieves new state-of-the-art 84.3% top-1 accuracy but being 1.3x smaller than NASNet-A.

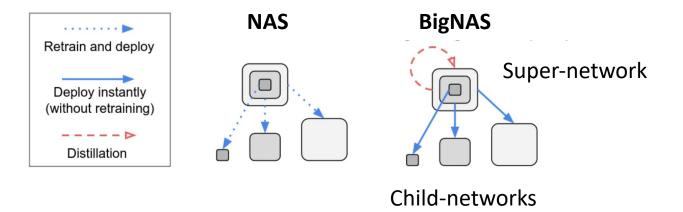
EfficientNet-B1 is 7.6x smaller and 5.7x faster than ResNet-152

Algorithmic Intelligence Lab

Automation of networks at different scales: BigNAS [Yu et al., 2020]

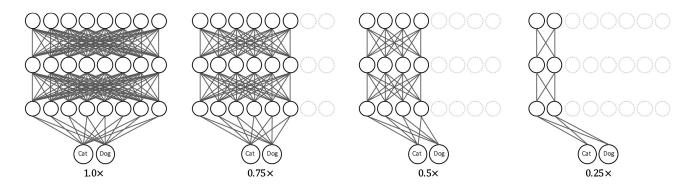
A searched architecture at each scale requires re-training from scratch

- Can we share weights between architecture instances?
- BigNAS trains a single set of parameters (super-network), then sample its subset (childnetwork)
 - A child-network can be evaluated and deployed without re-training!
 - How to train such a super-network?



A searched architecture at each scale requires re-training from scratch

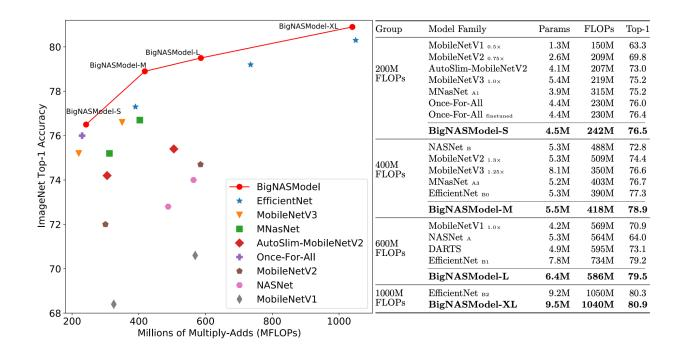
- Can we share weights between architecture instances?
- BigNAS trains a single set of parameters (super-network), then sample its subset (childnetwork)
 - Sandwich Training Rule (each iteration)
 - Sample the **biggest, smallest, and N random-sized children**
 - Gradients are averaged between all children
 - Inplace Distillation
 - Soft labels predicted by the biggest child model supervises all other child models



Automation of networks at different scales: BigNAS [Yu et al., 2020]

A searched architecture at each scale requires re-training from scratch

- Can we share weights between architecture instances?
- BigNAS trains a single set of parameters (super-network), then sample its subset (childnetwork)
 - BigNAS sampled at different scale outperforms existing models without re-training
 - Training & evaluating BigNAS takes only 1300 TPU-hours (c.f., 60000 GPU-hours in original NAS)



Architecture searching is still an active research area

- AmoebaNet [Real et al., 2018]
- NAONet [Luo et al., 2018]
- BigNAS [Yu et al., 2020]
- NASViT [Gong et al., 2022]
- Specifically, NAS for vision transformers is emerging
 - Careful NAS design is required due to architectural differences
 - e.g., Vision transformers are instable during the early training stage due to the lack of inductive bias for images

| Group | Method | M FLOPs | Top-1 accuracy (%) |
|----------------|----------------------------------|---------|--------------------|
| 200-300 (M) | AlphaNet-A0 | 203 | 77.9 |
| 200-500 (101) | NASViT-A0 (ours) | 208 | 78.2 |
| | LeViT (Graham et al., 2021) | 300 | 76.6 |
| 300-400 (M) | NASViT-A1 (ours) | 309 | 79.7 |
| | AlphaNet-A2 | 317 | 79.4 |
| | FBNetV3 (Dai et al., 2020) | 357 | 79.6 |
| 400-500 (M) | LeViT | 406 | 78.6 |
| | NASViT-A2 (ours) | 421 | 80.5 |
| | AlphaNet-A4 | 444 | 80.4 |
| 500-600 (M) | NASViT-A3 (ours) | 528 | 81.0 |
| | FBNetV3 | 557 | 80.8 |
| | NASViT-A4 (ours) | 591 | 81.4 |
| | AlphaNet | 596 | 81.1 |
| 600 - 1000 (M) | LeViT | 658 | 80.0 |
| | NASViT-A5 (ours) | 757 | 81.8 |
| | FBNetV3 | 762 | 81.5 |
| > 1000 (M) | AutoFormer* (Chen et al., 2021a) | 1,300 | 74.7 |
| | PiT-XS (Heo et al., 2021) | 1,400 | 79.1 |
| | ViTAS-D* (Su et al., 2021) | 1,600 | 76.2 |
| | NASViT (supernet) (ours) | 1,881 | 82.9 |
| | CVT-13-NAS* (Wu et al., 2021) | 4,100 | 82.2 |
| | Swin-Tiny* (Liu et al., 2021) | 4,500 | 81.3 |
| | CVT-13* (Wu et al., 2021) | 4,500 | 81.6 |
| | T2T-ViT-14* (Yuan et al., 2021a) | 5,200 | 81.5 |
| | DeepViT (Zhou et al., 2021) | 6,200 | 82.3 |

Table of Contents

Part 1. Basics

- Evolution of CNN architectures
- Batch normalization and ResNet
- Attention module in CNNs
- Vision transformers

Part 2. Advanced Topics

- Toward automation of network design
- Flexible architectures
- Observational study on network architectures
- Deep spatial-temporal models

Part 3. Beyond CNNs and Vision Transformers

- Patch-based architectures for vision
- New design paradigms

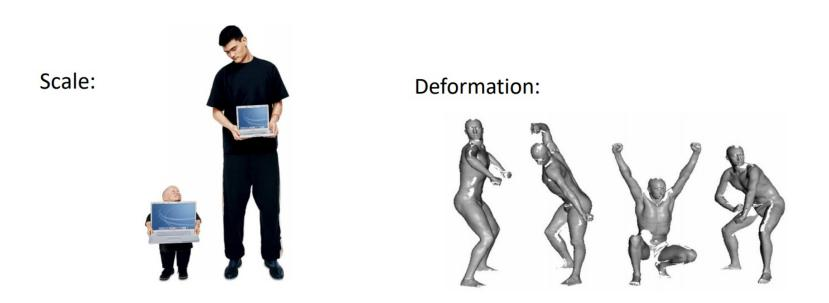
Algorithmic Intelligence Lab

Objects in real-world often contain sophisticated spatial information

- Multiple scales
- Irregular shapes

Drawbacks: geometric transformations are assumed fixed and known

- Different size and shape of kernels may be required
- But, regular kernels have fixed-size and shape

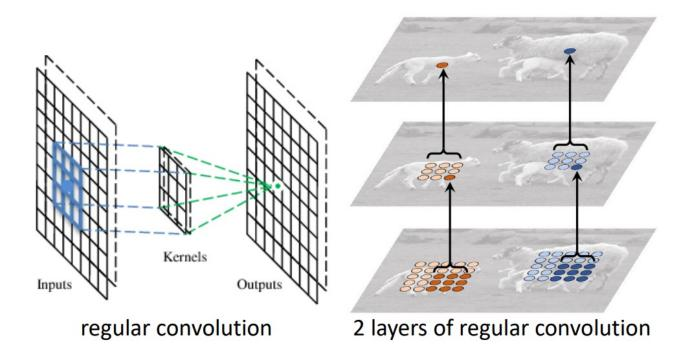


Objects in real-world often contain sophisticated spatial information

- Multiple scales
- Irregular shapes

Drawbacks: geometric transformations are assumed fixed and known

- Different size and shape of kernels may be required
- But, regular kernels have fixed-size and shape

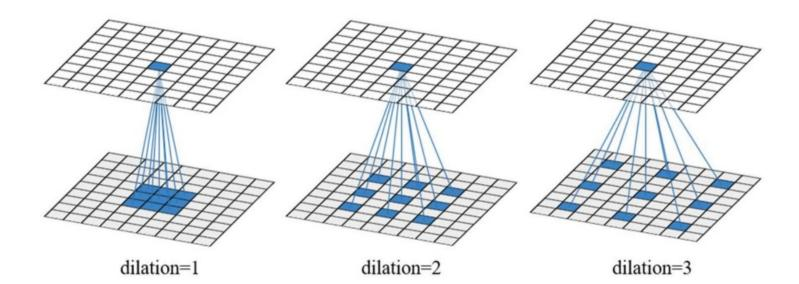


Motivation: Images in real-world usually contain multi-scale objects

- Regular convolution has a fixed-size of field of view
- Different size of kernels are required for multi-scale objects
- But, large-size of kernels may increase computational costs

Dilated convolution: Filling with **zero values** inside of large-size of kernels for efficient computation

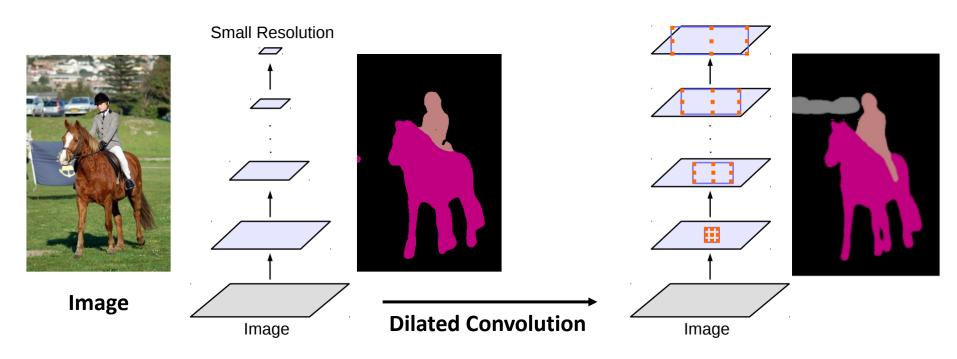
• It can enlarge field-of-view to incorporate multi-scale context



Dilated Convolution [Chen et al., 2017]

Motivation: Images in real-world usually contain multi-scale objects

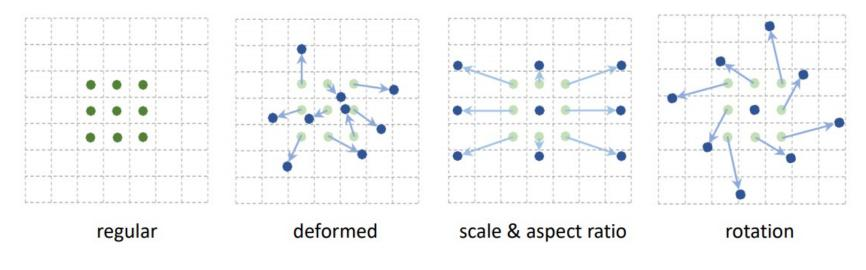
- Regular convolution has a fixed-size of field of view
- Different size of kernels are required for multi-scale objects
- But, large-size of kernels may increase computational costs
- Example: Dilated convolution in semantic segmentation



- Different shape of kernels are required for irregular objects
- Regular convolution has a fixed-shape of kernel

Deformable convolution: Learning sampling location of kernels to capture irregular shape of objects

• Adding offset field to generate irregular sampling locations

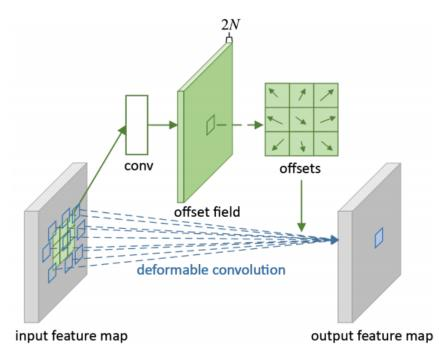


Different types of sampling locations

- Different shape of kernels are required for irregular objects
- Regular convolution has a fixed-shape of kernel

Deformable convolution: Learning sampling location of kernels to capture irregular shape of objects

Adding offset field to generate irregular sampling locations



Regular convolution

$$\mathbf{y}(\mathbf{p}_0) = \sum_{\mathbf{p}_n \in \mathcal{R}} \mathbf{w}(\mathbf{p}_n) \cdot \mathbf{x}(\mathbf{p}_0 + \mathbf{p}_n)$$

Deformable convolution

$$\mathbf{y}(\mathbf{p}_0) = \sum_{\mathbf{p}_n \in \mathcal{R}} \mathbf{w}(\mathbf{p}_n) \cdot \mathbf{x}(\mathbf{p}_0 + \mathbf{p}_n + \Delta \mathbf{p}_n)$$

where Δp_n is generated by a sibling branch of regular convolution (offset field)

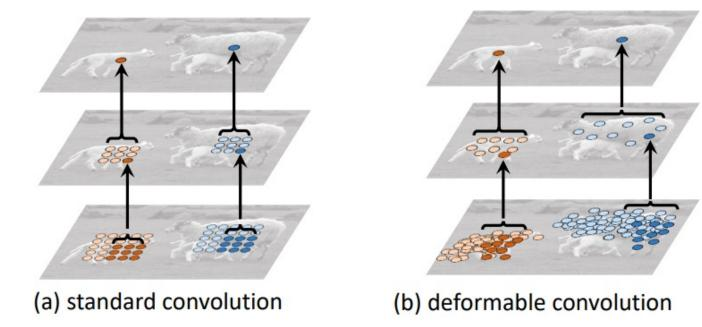
Algorithmic Intelligence Lab

*source : https://jifengdai.org/slides/Deformable_Convolutional_Networks_Oral.pdf 85

- Different shape of kernels are required for irregular objects
- Regular convolution has a fixed-shape of kernel

Deformable convolution: Learning sampling location of kernels to capture irregular shape of objects

• Adding offset field to generate irregular sampling locations



Algorithmic Intelligence Lab

*source : https://jifengdai.org/slides/Deformable_Convolutional_Networks_Oral.pdf 86

- Different shape of kernels are required for irregular objects
- Regular convolution has a fixed-shape of kernel

Learned offsets in the **deformable convolution** layers are highly adaptive to the image content

• Different size and shape of kernels for multiple objects



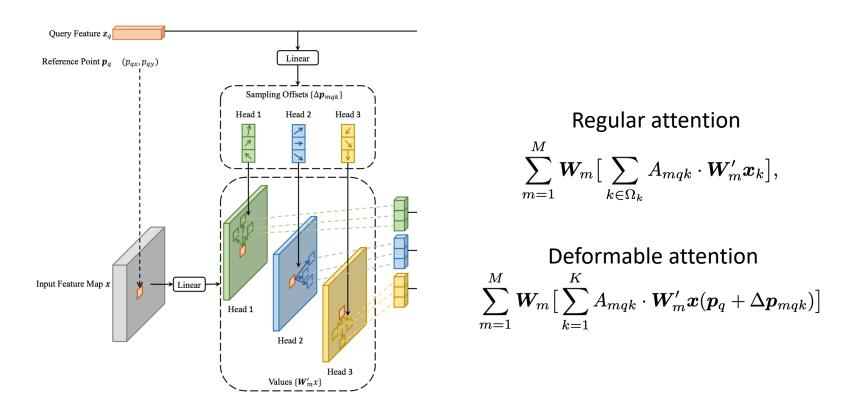
Visualizations of sampling locations

*source: Dai et al., "Deformable Convolutional Networks", ICCV, 2017 87

Motivation: Make image patches in vision transformers deformable!

Square patches in the vision transformers could be too restrictive for localization (e.g., object detection, segmentation)

• Deformable DETR [Zhu et al., 2020] additionally learns the offset of pixels in a patch

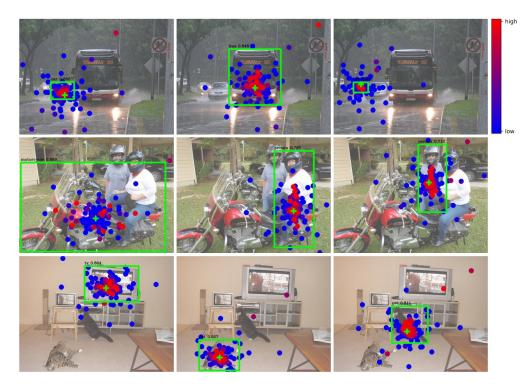


Algorithmic Intelligence Lab

Motivation: Make image patches in vision transformers deformable!

Square patches in the vision transformers could be too restrictive for localization (e.g., object detection, segmentation)

- Deformable DETR [Zhu et al., 2021] additionally learns the offset of pixels in a patch
- Self-attention is regularized around the localization of objects



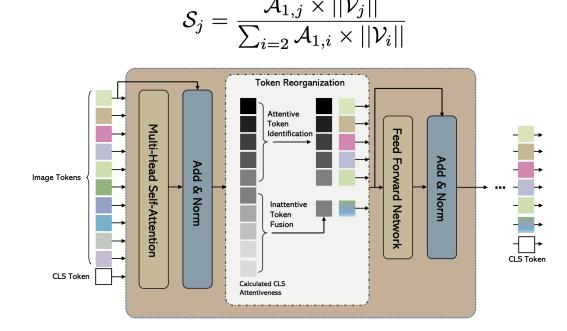
Algorithmic Intelligence Lab

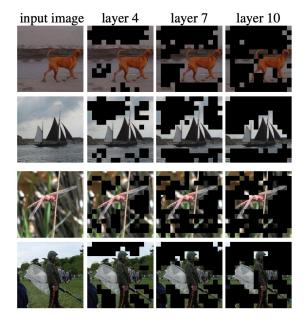
*source: Dai et al., "Deformable Convolutional Networks", ICCV, 2017 89

Motivation: Not all patches are equivalently important

Some **image patches** could contain **redundant** and less important information

- EViT [Liang et al., 2022], ATS [Fayyaz et al., 2022] merges these patches
- Less important patches (e.g., background) are identified at each attention layer
 - Attention & value-norms are used as importance scores



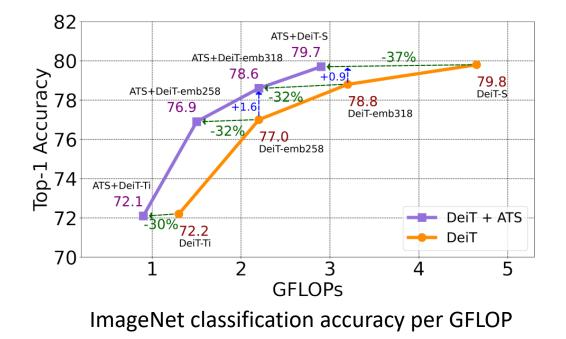


Algorithmic Intelligence Lab

Motivation: Not all patches are equivalently important

Some image patches could contain redundant and less important information

- EViT [Liang et al., 2022], ATS [Fayyaz et al., 2022] merges these patches
- ATS [Fayyaz et al., 2022] achieves the comparable accuracy at 37% reduced computations (GFLOPs) than DeiT



Algorithmic Intelligence Lab

*source: Dai et al., "Deformable Convolutional Networks", ICCV, 2017 91

Table of Contents

Part 1. Basics

- Evolution of CNN architectures
- Batch normalization and ResNet
- Attention module in CNNs
- Vision transformers

Part 2. Advanced Topics

- Toward automation of network design
- Flexible architectures
- Observational study on network architectures
- Deep spatial-temporal models

Part 3. Beyond CNNs and Vision Transformers

- Patch-based architectures for vision
- New design paradigms

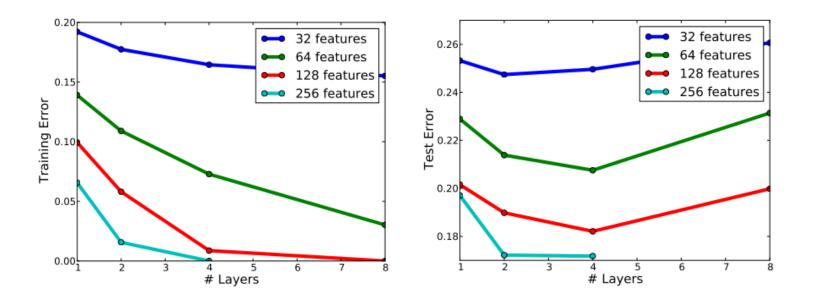
Algorithmic Intelligence Lab

ResNet improved generalization by revolution of depth

Quiz: But, does it fully explain why deep ResNets generalize well?

Increasing depth **does not always mean** better generalization

• Naïve CNNs are very easy to overfit on deeper networks [Eigen et al., 2014]

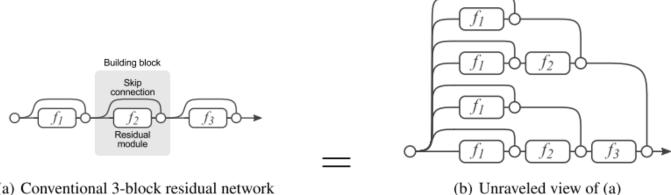


Veit et al. (2016): ResNet can be viewed as a collection of many paths, instead of a single ultra-deep network

• Each module in a ResNet receives a **mixture of** 2^{n-1} different distributions

$$y_{3} = y_{2} + f_{3}(y_{2})$$

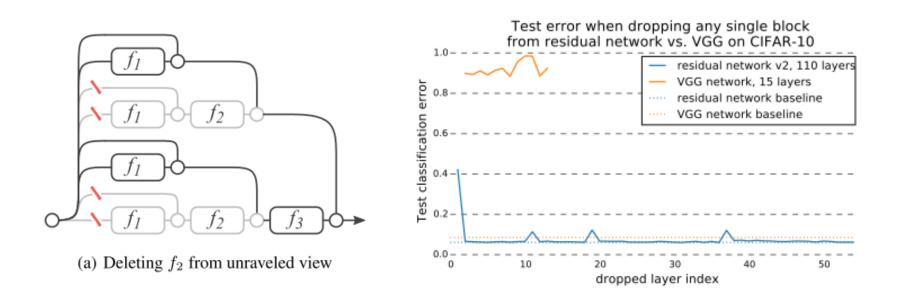
= $y_{1} + f_{2}(y_{1})$] + $f_{3}(y_{1} + f_{2}(y_{1}))$
= $y_{0} + f_{1}(y_{0}) + f_{2}(y_{0} + f_{1}(y_{0}))$] + $f_{3}(y_{0} + f_{1}(y_{0}) + f_{2}(y_{0} + f_{1}(y_{0})))$



(a) Conventional 3-block residual network

Veit et al. (2016): ResNet can be viewed as a collection of many paths, instead of a single ultra-deep network

- Deleting a module in ResNet has a minimal effect on performance
- Similar effect as removing 2ⁿ⁻¹ paths out of 2ⁿ: still 2ⁿ⁻¹ paths alive!



Next, visualizing loss functions in CNN

Visualizing the loss landscape of neural nets [Li et al., 2018]

Trainability of neural nets is highly dependent on network architecture

- However, the effect of each choice on the underlying loss surface is unclear
 - Why are we able to minimize highly non-convex neural loss?
 - Why do the resulting minima generalize?

Li et al. (2018) analyzes random-direction 2D plot of loss around local minima

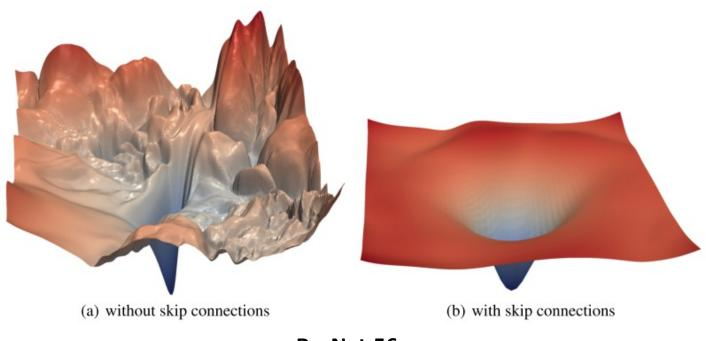
$$f(\alpha,\beta) = L(\theta^* + \alpha\delta + \beta\eta)$$

Local minima Random directions

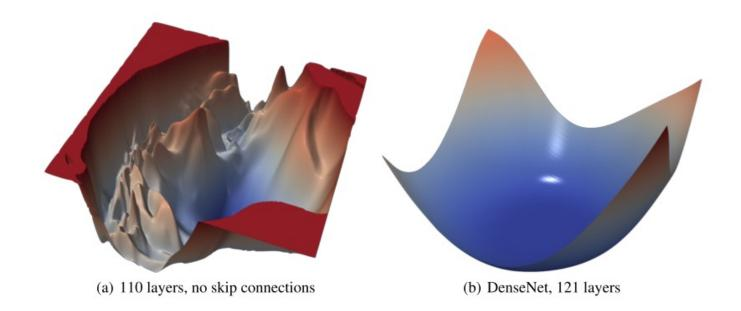
- δ and η are sampled from a random Gaussian distribution
- To remove some scaling effect, δ and η are normalized filter-wise

$$\delta_{i,j} \leftarrow \frac{\delta_{i,j}}{||\delta_{i,j}||} ||\theta_{i,j}|| \qquad i^{\text{th}} \text{ laver, } i^{\text{th}} \text{ filter}$$

Modern architectures prevent the loss to be chaotic as depth increases

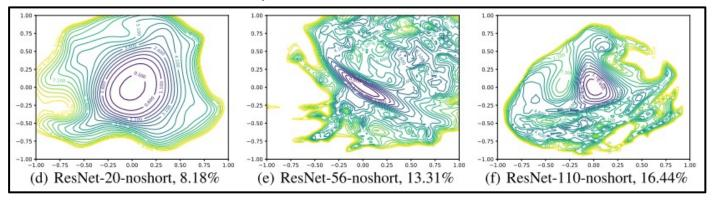


Modern architectures prevent the loss to be chaotic as depth increases

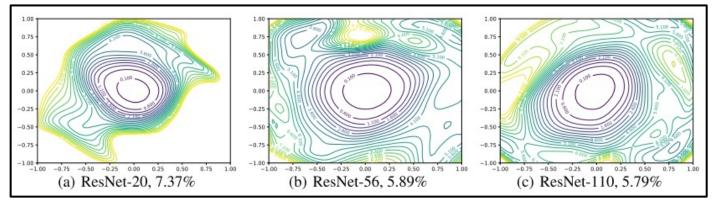


Modern architectures prevent the loss to be chaotic as depth increases

ResNet, **no shortcuts** ⇒ sharp minima



$ResNet \Rightarrow flat minima$

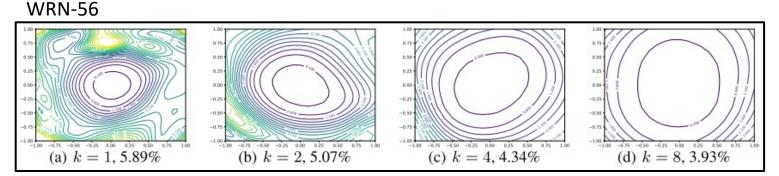


Algorithmic Intelligence Lab

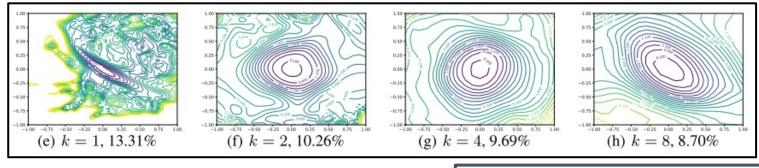
*source : Li et al., "Visualizing the loss landscape of neural nets", ICLR Workshop 2018 99

Wide-ResNet lead the network toward more flat minimizer

- WideResNet-56 with width-multiplier k = 1, 2, 4, 8
- Increased width flatten the minimizer in ResNet



WRN-56, no shortcuts



Next, minimum energy paths in CNNs

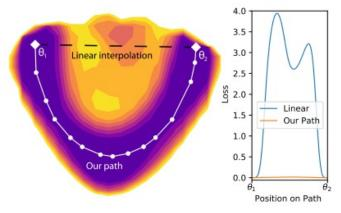
Algorithmic Intelligence Lab

*source : Li et al., "Visualizing the loss landscape of neural nets", ICLR Workshop 2018 100

Draxler et al. (2018) analyzes **minimum energy paths** [Jónsson et al., 1998] between two local minima θ_1 and θ_2 of a given model:

$$p(\theta_i, \theta_2)^* = \operatorname*{argmin}_{\text{path } p: \ \theta_1 \to \theta_2} \left(\max_{\theta \in p} L(\theta) \right)$$

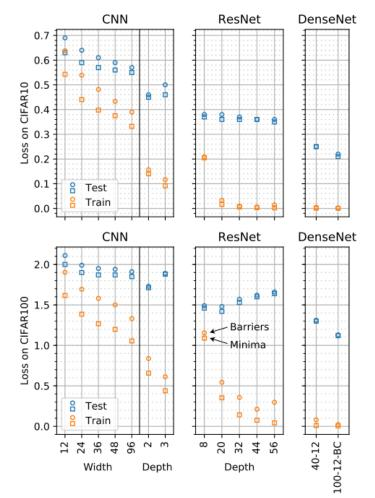
- They found a path $\theta_1 \rightarrow \theta_2$ with almost zero barrier
 - A path that keeps low loss constantly both in training and test
- The gap vanishes as the model grows, especially on modern architectures
 - e.g. ResNet, DenseNet
- Minima of a loss of deep neural networks are perhaps on a single connected manifold



DenseNet-40-12

For a given model with two local minima θ_1 and θ_2 , they applied **AutoNEB** [Kolsbjerg et al., 2016] to find a minimum energy path

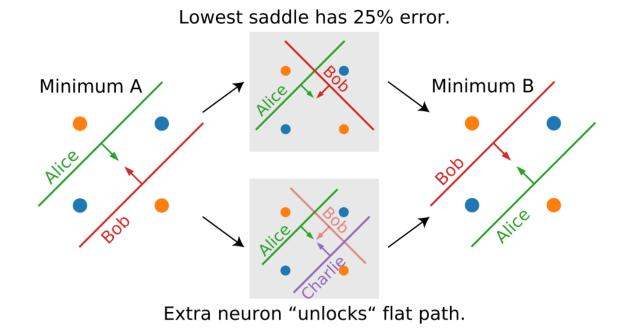
- A state-of the-art for connecting minima from molecular statistical mechanics
- The deeper and wider an architecture, the lower are the saddles between minima
- They essentially vanish for current-day deep architectures
- The test accuracy is also preserved
 - **CIFAR-10**: < +0.5%
 - CIFAR-100: < +2.2%



- The deeper and wider an architecture, the lower are the barriers
- They essentially vanish for current-day deep architectures

Why do this phenomenon happen?

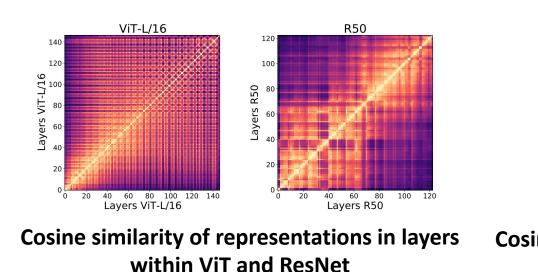
Parameter redundancy may help to flatten the neural loss

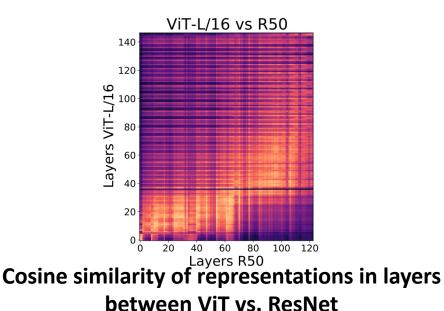


Do Vision Transformers See Like Convolutional Neural Networks? [Raghu et al., 2021]

Raghu et al. (2021) analyzes representation similarity in transformer layers:

- ViT tends to have uniform representation over different layers
 - All layers in ViT show much greater similarity than ResNet
 - In ResNet, similarity is divided into different (lower/higher) stages
- ViT and ResNet features are similar in lower stages, but significantly different in higher stages



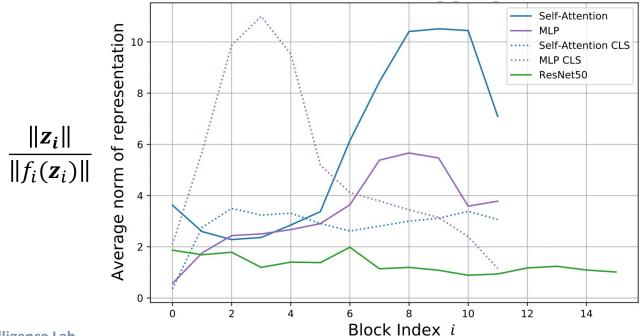


Algorithmic Intelligence Lab

*source : Draxler et al., "Essentially no barriers in neural network energy landscape", ICML 2018 104

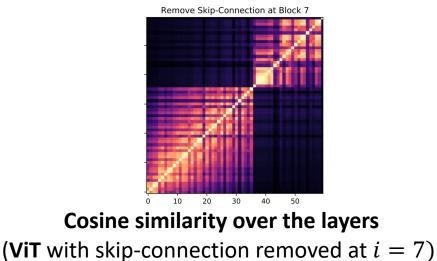
Raghu et al. (2021) analyzes representation similarity in transformer layers:

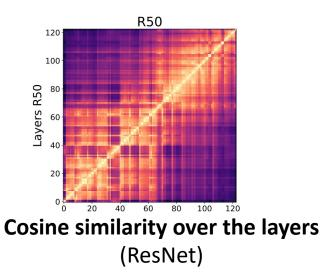
- ViT tends to have uniform representation over different layers
 - All layers in ViT show much greater similarity than ResNet
 - In ResNet, similarity is divided into different (lower/higher) stages
- This is mainly due to stronger skip-connection in ViT
 - $\frac{\|z_i\|}{\|f_i(z_i)\|}$: norm ratio of z_i (skip-connection) and f_i (MLP or Self-Attention)
 - The skip-connection in ViT is even stronger in deeper layers



Raghu et al. (2021) analyzes representation similarity in transformer layers:

- ViT tends to have uniform representation over different layers
 - All layers in ViT show much greater similarity than ResNet
 - In ResNet, similarity is divided into different (lower/higher) stages
- This is mainly due to stronger skip-connection in ViT
 - $\frac{\|z_i\|}{\|f_i(z_i)\|}$: norm ratio of z_i (skip-connection) and f_i (MLP or Self-Attention)
 - The skip-connection in ViT is even stronger in deeper layers
- When skip-connection removed at a middle-block (e.g., i = 7) the cosine similarity of ViT becomes similar to that of ResNets

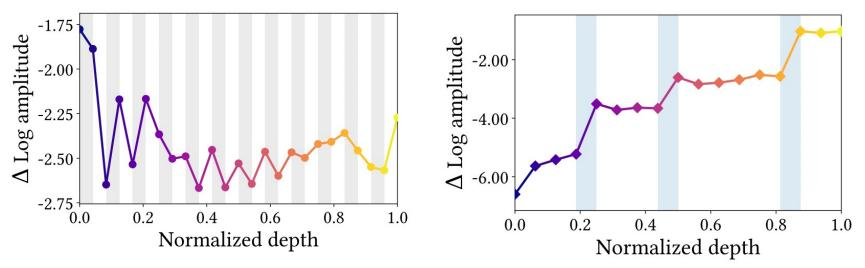




How do vision transformers work? [Park et al., 2022]

Park et al. (2022) analyzes frequency domain of vision transformer layers:

- Self-attention layer keeps high-frequency information
 - MLPs variants (e.g., CNNs, MLP in transformers) act as high-pass filters
 - However, self-attention tend to act as low-pass filters
 - ViT deals with both high- and low-frequency information (while CNNs simply pass high-frequency information)

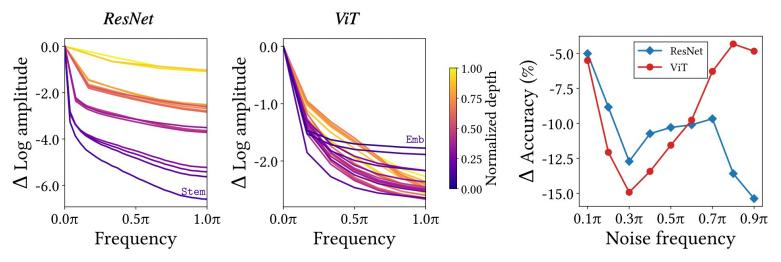


Amplitude of high-frequency signals in Fourier space of feature maps

Park et al. (2022) analyzes frequency domain of vision transformer layers:

- Self-attention layer keeps high-frequency information
 - MLPs variants (e.g., CNNs, MLP in transformers) act as high-pass filters
 - However, self-attention tend to act as low-pass filters
- Processing both low- and high-frequency information contributes to robustness against high-frequency noises in ViT vs. ResNet
 - Frequency-specific noise with Gaussian noise ${oldsymbol \delta}$ and Fourier transform ${\mathcal F}$

$$m{x}_{ ext{noise}} = m{x}_0 + \mathcal{F}^{-1}\left(\mathcal{F}(\delta)\odot\mathbf{M}_f
ight)$$
 frequency mask



Algorithmic (a) Relative log amplitudes of Fourier transformed feature maps.

(b) Robustness for noise frequency

Table of Contents

Part 1. Basics

- Evolution of CNN architectures
- Batch normalization and ResNet
- Attention module in CNNs
- Vision transformers

Part 2. Advanced Topics

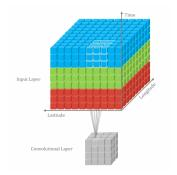
- Toward automation of network design
- Flexible architectures
- Observational study on network architectures
- Deep spatial-temporal models

Part 3. Beyond CNNs and Vision Transformers

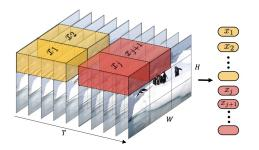
- Patch-based architectures for vision
- New design paradigms

Deep **spatial-temporal model** as an extension of spatial models

• 3D convolutional neural networks and video vision transformers



3D Convolutional Neural Networks



Video Vision Transformers

Video Action Recognition [Karpathy et al., 2014]



source: https://towardsdatascience.com/downloading-the-kinetics-dataset-for-human-action-recognition-in-deep-learning-500c3d50f776

Deep Object Tracking [Wang et al., 2020]



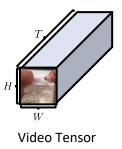
*source: https://github.com/Zhongdao/Towards-Realtime-MOT

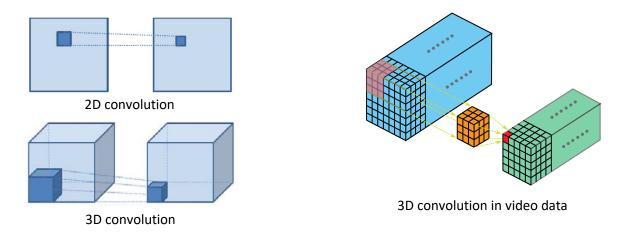
Problem: The curse of dimensionality

- Spatial-temporal data is high-dimensional (e.g., channels × height × width × time)
- Brute-force extension of spatial models is often intractable
- Data sub-sampling & approximated network architectures are typically employed:
 - How to fuse information from spatial cue (appearance) and temporal cue (motion)
 - Long-range modeling

Good models should be **computationally scalable** (e.g., linear complexity to temporal dimension) and should deal with **information fusion** & **long-range modeling** problems

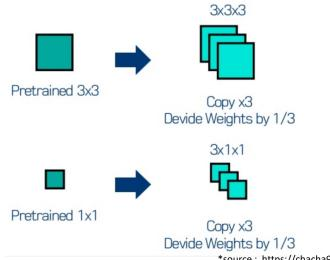
- Raw video data structure
 - Video is a **3D tensor** with 2 spatial and 1 time axes
 - How to learn good representation for video?
 - **3D CNN** directly extends convolution with cuboid (3D) kernel





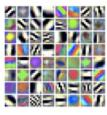
- Some early works employed 3D CNNs for video, however:
 - 3D-Conv [Ji et al., 2012] and C3D [Tran et al., 2015]
 - Their performances were **unsatisfactory** due to **optimization difficulty of 3D CNNs**
 - Can we leverage pre-trained representation for images? i.e., transfer learning

- Inflated 3D (I3D) [Carreira and Zisserman, 2017]
 - Adapting a pre-trained 2D CNN model for 3D CNN
 - I3D utilizes the Inception architecture
 - Instead of training from scratch, I3D leverages ImageNet-pretraining
 - Weight inflating technique for initializing 3D kernels with 2D kernels
 - 1. Extend a dimension by stacking existing 2D kernel
 - 2. Divide weights by the stack length to ensure the same output scale

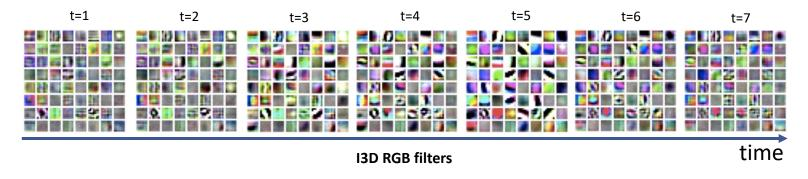


*source : https://chacha95.github.io/2019-07-04-VideoUnderstanding3/

- Inflated 3D (I3D) [Carreira and Zisserman, 2017]
 - 3D Convolutional feature map learned by I3D
 - Top row: the 3D filter trained with I3D networks
 - Bottom row: the original 2D filter from Inception
 - 3D kernel sliced at each time resembles geometric patterns of the 2D filter
 - Representation of 2D CNN is **effectively transferred to 3D**



Original 2D filters from Inception



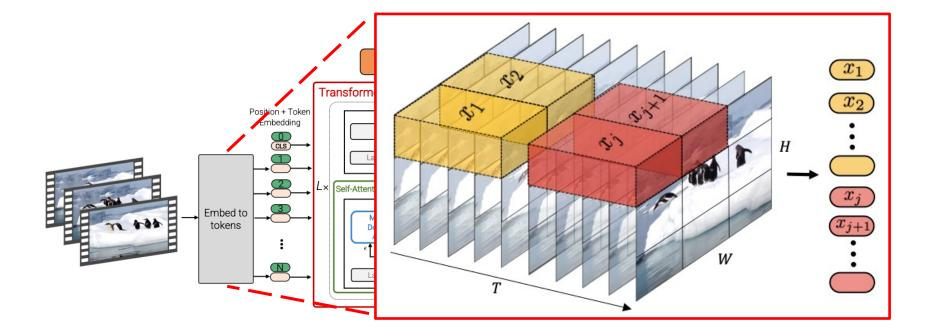
- Inflated 3D (I3D) [Carreira and Zisserman, 2017]
 - I3D beats hand-craft video representations (e.g., optical flow) by a large margin
 - Transferring the architecture of 2D CNN models is the key idea
 - **ResNet3D** [Hara et al., 2018]
 - Residual connections for 3D CNN
 - Transfers ResNet [He et al., 2016] architecture to 3D CNN
 - ResNeXt for 3D [Chen et al., 2018]
 - Multi-Fiber Networks for Video Recognition
 - Translates the multiple parallel path to 3D CNN
 - **STCNet** [Diba et al., 2018]
 - Spatio-Temporal Channel correlation networks
 - Translates the Sequeeze-and-Excitation mechanism to 3D CNN

- Executing **3D CNNs** is computationally expensive
 - I3D [Carreira and Zisserman, 2017] demands computation burden comparable to the state-of-the-art transformer models (100+ GFLOPs)
 - A line of research pursuing efficient 3D CNN architectures
- Factorization of 3D kernel
 - A **3D** CNN kernel of size ($P \times M \times N$) can be factorized to two convolutions;
 - A spatial 2D kernel $(1 \times M \times N)$ and a temporal 1D kernel $(P \times 1 \times 1)$
 - **R2+1D** [Tran et al., 2018] and **P3D** [Qiu et al., 2017] directly adopts this idea to largely save FLOPs
- Application of **channel-wise separated convolutions**
 - **CSN** [Tran et al., 2019] shows the efficacy of separating channel interactions and spatiotemporal interactions
 - State-of-the-art performance is achieved with ×3 less computations than I3D [Carreira and Zisserman, 2017]

Transformers for spatial-temporal data : Extension of ViT - ViViT

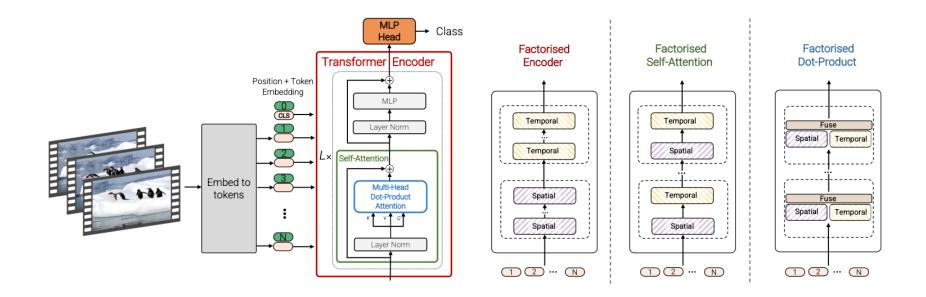
Video Vision Transformer (ViViT) [Arnab & Dehghani et al., 2021]

- ViViT is a pure **transformer** framework for video classification
- Tubelet embedding (3D extension of ViT)
 - Extract non-overlapping, spatial-temporal tubes from input volume
 - Linearly project them into \mathbb{R}^d



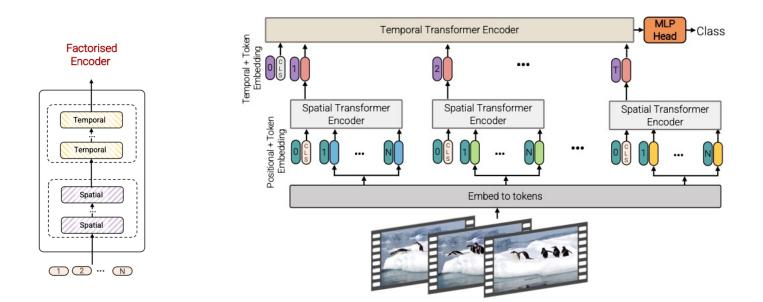
Video Vision Transformer (ViViT) [Arnab & Dehghani et al., 2021]

- Suggests different designs of spatial & temporal attention
 - 1. Joint Spatio-temporal attention
 - Simply forwards all pairwise interactions between all spatio-temporal tokens through transformer encoder
 - Unlike CNN, it can model long-range interactions across the video from the 1st layer
 - Requires quadratic complexity, $\mathcal{O}((n_h \cdot n_w \cdot n_t)^2)$, with number of tokens



Video Vision Transformer (ViViT) [Arnab & Dehghani et al., 2021]

- Suggests different designs of spatial & temporal attention
 - 2. Factorized encoder
 - **Spatial encoder** models interactions between tokens from the same temporal index
 - **Temporal encoder** models interactions between tokens from different temporal indices
 - Requires more transformer layers (i.e., more parameters) than the joint design
 - But less complexity, $\mathcal{O}((n_h \cdot n_w)^2 + n_t^2)$



Video Vision Transformer (ViViT) [Arnab & Dehghani et al., 2021]

- The factorized encoder design shows the best accuracy-to-FLOPs ratio
- However, the joint-design performs better and requires smaller number of parameters.
- Instead of factorizing the model, can we design approximate attention for both performance and FLOPs efficiency?

| | K400 | EK | FLOPs $(\times 10^9)$ | Params $(\times 10^6)$ | Runtime (ms) |
|-------------------------------|------|------|-----------------------|------------------------|-----------------|
| Model 1: Spatio-temporal | 80.0 | 43.1 | 455.2 | 88.9 | 58.9 |
| Model 2: Fact. encoder | 78.8 | 43.7 | 284.4 | 115.1 | 17.4 |
| Model 3: Fact. self-attention | 77.4 | 39.1 | 372.3 | 117.3 | 31.7 |
| Model 4: Fact. dot product | 76.3 | 39.5 | 277.1 | 88.9 | 22.9 |
| Model 2: Ave. pool baseline | 75.8 | 38.8 | 283.9 | 86.7 | 17.3 |

Comparison between model variants

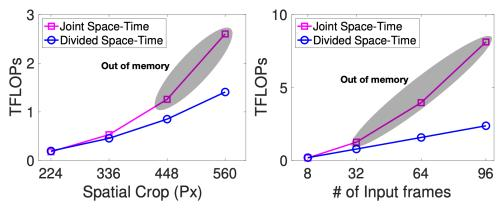
| Method | Top 1 | Top 5 | Views | TFLOPs |
|-----------------------|-------|-------|---------------|--------|
| blVNet [19] | 73.5 | 91.2 | _ | _ |
| STM [33] | 73.7 | 91.6 | - | - |
| TEA [42] | 76.1 | 92.5 | 10×3 | 2.10 |
| TSM-ResNeXt-101 [43] | 76.3 | _ | _ | - |
| I3D NL [75] | 77.7 | 93.3 | 10×3 | 10.77 |
| CorrNet-101 [70] | 79.2 | - | 10×3 | 6.72 |
| ip-CSN-152 [66] | 79.2 | 93.8 | 10×3 | 3.27 |
| LGD-3D R101 [51] | 79.4 | 94.4 | - | - |
| SlowFast R101-NL [21] | 79.8 | 93.9 | 10×3 | 7.02 |
| X3D-XXL [20] | 80.4 | 94.6 | 10×3 | 5.82 |
| TimeSformer-L [4] | 80.7 | 94.7 | 1×3 | 7.14 |
| ViViT-L/16x2 FE | 80.6 | 92.7 | 1×1 | 3.98 |
| ViViT-L/16x2 FE | 81.7 | 93.8 | 1×3 | 11.94 |

Kinetics-400 dataset benchmark

Transformers for spatial-temporal data : Approximated Attentions

Brute-force joint spatial-temporal attention is intractable for transformers

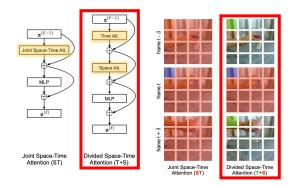
- Due to the quadratic complexity with respect to inputs
- This motivates the development of more efficient attention scheme
 - Time-Space Transformer (TimeSformer) [Bertasius et al., 2021]
 - Video Swin Transformer [Liu et al., 2021]



Video classification cost in TFLOPs

Time-Space Transformer (TimeSformer) [Bertasius et al., 2021]

- Proposes divided space-time attention
 - Instead of exhaustively comparing all pairs of patches (i.e., joint space-time attention), it separately applies temporal attention and spatial attention one after the other
- Temporal attention
 - Each patch (blue) is compared only with the patches at the same spatial location in other frames (green)
 - Initialized to zero (so that function as identity mapping in early training stages)
- Spatial attention
 - Each patch (blue) is compared only with the patches within the same frame (red)
- Designs may look similar to ViViT (model 3) in a big picture, however, implementation details differ including 1) time- then-space att., 2) zero initializations for temporal layers



Time-Space Transformer (TimeSformer) [Bertasius et al., 2021]

- Divided space-time attention leads to dramatic computational savings with respect to spatial resolution/video length
- Outperforms SOTA models while requiring less computational complexity
 - $O(S^2T) + O(ST^2)$ instead of $O(S^2T^2)$

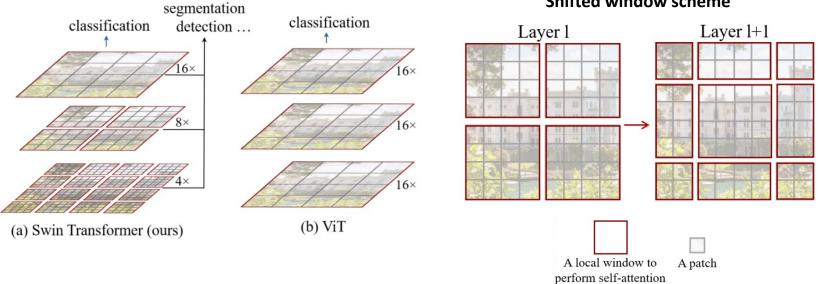
| | Method | Top-1 | Top-5 | TFLOPs | |
|-------------------------------------------|----------------------------------------|-------------|-------------|--------|-------------|
| | R(2+1)D (Tran et al., 2018) | 72.0 | 90.0 | 17.5 | |
| | bLVNet (Fan et al., 2019) | 73.5 | 91.2 | 0.84 | |
| 3 - Joint Space-Time | TSM (Lin et al., 2019) | 74.7 | N/A | N/A | |
| Divided Space-Time Divided Space-Time | S3D-G (Xie et al., 2018) | 74.7 | 93.4 | N/A | |
| Out of memory O 5 Out of memory | Oct-I3D+NL (Chen et al., 2019) | 75.7 | N/A | 0.84 | |
| | D3D (Stroud et al., 2020) | 75.9 | N/A | N/A | 3D CNNs |
| | I3D+NL (Wang et al., 2018b) | 77.7 | 93.3 | 10.8 | |
| 8 8 | ip-CSN-152 (Tran et al., 2019) | 77.8 | 92.8 | 3.2 | |
| 0 224 336 448 560 8 32 64 96 | CorrNet (Wang et al., 2020a) | 79.2 | N/A | 6.7 | |
| Spatial Crop (Px) # of Input frames | LGD-3D-101 (Qiu et al., 2019) | 79.4 | 94.4 | N/A | |
| | SlowFast (Feichtenhofer et al., 2019b) | 79.8 | 93.9 | 7.0 | |
| | X3D-XXL (Feichtenhofer, 2020) | 80.4 | 94.6 | 5.8 | |
| | TimeSformer | 78.0 | 93.7 | 0.59 | _ |
| | TimeSformer-HR | 79.7 | 94.4 | 5.11 | TimeSformer |
| | TimeSformer-L | 80.7 | 94.7 | 7.14 | |

Kinetics-400 dataset benchmark

Video Swin Transformer [Liu et al., 2021]

- Recall: Swin Transformer [Liu et al., 2021] ٠
 - Design of a hierarchical structure ٠
 - Various spatial resolutions (e.g., patch-shape) can be handled via shifted windows ٠
 - Efficient self-attention computation by using shifted windows scheme ٠
 - Concatenating 2×2 neighboring patches for downsampling operation ٠
 - Powerful performances in dense prediction tasks ٠

e.g., object detection and semantic segmentation



Shifted window scheme

Algorithmic Intelligence Lab

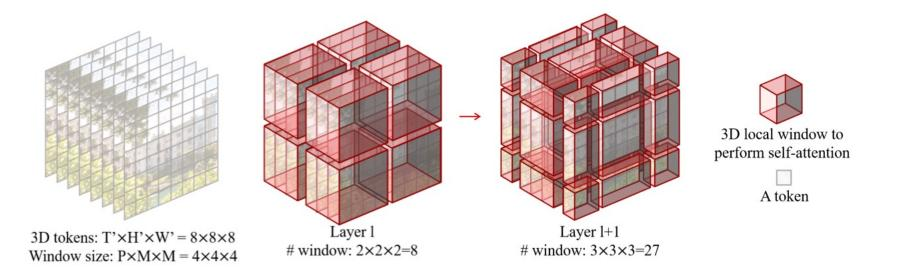
*source: [Liu et al. 2021] Swin Transformer: Hierarchical Vision Transformer using Shifted Windows, ICCV 2021 124

Transformers for spatial-temporal data : Approximated Attentions - Video Swin Transformer

Video Swin Transformer [Liu et al., 2021]

- In videos, pixels that are closer to each other in spatiotemporal distance are more likely to be correlated (i.e., spatiotemporal locality)
- Thus, **local** attention computation well approximates spatiotemporal self-attention
- Video Swin Transformer is a spatial-temporal adaptation of Swin Transformer

i.e., extension from spatial locality to spatial-temporal locality



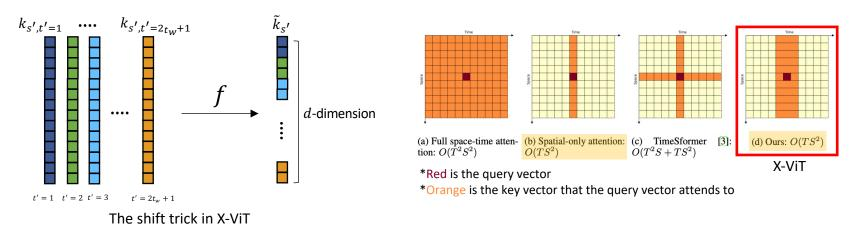
Video Swin Transformer [Liu et al., 2021]

- Outperforms SOTA 3D CNN models while requiring smaller computation costs for inference
- Also outperforms SOTA transformer-based models while requiring half less computational costs

| Method | Pretrain | Top-1 | Top-5 | Views | FLOPs | Param | |
|-------------------------|--------------|-------|-------|---------------|-------|-------|--------------|
| R(2+1)D [37] | - | 72.0 | 90.0 | 10 × 1 | 75 | 61.8 | |
| I3D [6] | ImageNet-1K | 72.1 | 90.3 | - | 108 | 25.0 | |
| NL I3D-101 [40] | ImageNet-1K | 77.7 | 93.3 | 10×3 | 359 | 61.8 | 3D CNNs |
| ip-CSN-152 [36] | - | 77.8 | 92.8 | 10×3 | 109 | 32.8 | SD CIVINS |
| CorrNet-101 [39] | - | 79.2 | - | 10 × 3 | 224 | - | |
| SlowFast R101+NL [13] | - | 79.8 | 93.9 | 10×3 | 234 | 59.9 | |
| X3D-XXL [12] | - | 80.4 | 94.6 | 10×3 | 144 | 20.3 | |
| MViT-B, 32×3 [10] | - | 80.2 | 94.4 | 1 × 5 | 170 | 36.6 | |
| MViT-B, 64×3 [10] | - | 81.2 | 95.1 | 3 × 3 | 455 | 36.6 | |
| TimeSformer-L [3] | ImageNet-21K | 80.7 | 94.7 | 1 × 3 | 2380 | 121.4 | |
| ViT-B-VTN [29] | ImageNet-21K | 78.6 | 93.7 | 1×1 | 4218 | 11.04 | Transformer- |
| ViViT-L/16x2 [1] | ImageNet-21K | 80.6 | 94.7 | 4 × 3 | 1446 | 310.8 | based models |
| ViViT-L/16x2 320 [1] | ImageNet-21K | 81.3 | 94.7 | 4 × 3 | 3992 | 310.8 | buscu mouchs |
| ip-CSN-152 [<u>36]</u> | IG-65M | 82.5 | 95.3 | 10×3 | 109 | 32.8 | |
| ViViT-L/16x2 [1] | JFT-300M | 82.8 | 95.5 | 4×3 | 1446 | 310.8 | |
| ViViT-L/16x2 320 [1] | JFT-300M | 83.5 | 95.5 | 4 × 3 | 3992 | 310.8 | |
| ViViT-H/16x2 [1] | JFT-300M | 84.8 | 95.8 | 4 × 3 | 8316 | 647.5 | |
| Swin-T | ImageNet-1K | 78.8 | 93.6 | 4 × 3 | 88 | 28.2 | |
| Swin-S | ImageNet-1K | 80.6 | 94.5 | 4 × 3 | 166 | 49.8 | |
| Swin-B | ImageNet-1K | 80.6 | 94.6 | 4 × 3 | 282 | 88.1 | - |
| Swin-B | ImageNet-21K | 82.7 | 95.5 | 4 × 3 | 282 | 88.1 | Ours |
| Swin-L | ImageNet-21K | 83.1 | 95.9 | 4 × 3 | 604 | 197.0 | |
| Swin-L (384↑) | ImageNet-21K | 84.6 | 96.5 | 4×3 | 2107 | 200.0 | |
| Swin-L (384↑) | ImageNet-21K | 84.9 | 96.7 | 10×5 | 2107 | 200.0 | |

X-ViT [Bulat et al., 2021]

- Space-time mixing attention $-O(TS^2)$ complexity
 - The following architectural changes in X-ViT reduce the full quadratic complexity $O(T^2S^2)$ to the proposed $O(TS^2)$
 - 1. Restricting attentions within a temporal window of $[t t_w, t + t_w]$ for each $q_{s,t}$ \rightarrow The complexity becomes $O(T(2t_w + 1)^2S^2)$
 - 2. Instead of individual space-time keys, the **time compression** f is applied such that a single attention is considered over time with $\tilde{k}_{s'} \triangleq f([k_{s',t-t_w}; ...; k_{s',t+t_w}])$
 - 3. Instead of general affine transforms, **"shift trick"** is employed as the implementatio n of *f* to further save computations:
 - Given a key $k_{s',t'} \in \mathbb{R}^d$, split its channels into $(2t_w + 1)$ segments, then pick t he $t' \in [1, 2t_w + 1]$ th index to form the final $\tilde{k}_{s'} \rightarrow$ The complexity becomes $O(T(2t_w + 1)s^2)$ can be disregarded as 2t + 1 is a small constant



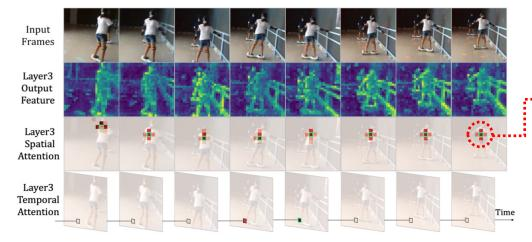
X-ViT [Bulat et al., 2021]

- Achieves comparable performance to SOTA models while requiring significantly lower computational complexity
 - X-ViT (16-frames, 850 GFLOPs) achieves performance comparable to heavy-weight variants of TimeSformer (96-frames, 7140 GFLOPs) and ViViT (32 frames, 4340 GFLOPs)
- Allows for an efficient approximation of local space-time attention at no extra cost

| Method | Top-1 | Top-5 | # Frames | Views | Params | FLOPs ($\times 10^9$) |
|----------------------------|-------|-------------|---------------|---------------|--------|-------------------------|
| bLVNet [14] | 73.5 | 91.2 | 24×2 | 3×3 | 25M | 840 |
| STM [19] | 73.7 | 91.6 | 16 | - | 24M | - |
| TEA [25] | 76.1 | 92.5 | 16 | 10×3 | 25.6M | 2,100 |
| TSM R50 [26] | 74.7 | - | 16 | 10×3 | 25.6M | 650 |
| I3D NL [44] | 77.7 | 93.3 | 128 | 10×3 | - | 10,800 |
| CorrNet-101 [40] | 79.2 | - | 32 | 10×3 | - | 6,700 |
| ip-CSN-152 [38] | 79.2 | 93.8 | 8 | 10×3 | - | 3,270 |
| LGD-3D R101 [31] | 79.4 | 94.4 | 16 | - | - | - |
| SlowFast 8×8 R101+NL [16] | 78.7 | 93.5 | 8 | 10×3 | - | 3,480 |
| SlowFast 16×8 R101+NL [16] | 79.8 | 93.9 | 16 | 10×3 | - | 7,020 |
| X3D-XXL [15] | 80.4 | 94.6 | - | 10×3 | 20.3M | 5,823 |
| TimeSformer-L [3] | 80.7 | 94.7 | 96 | 1×3 | 121M | 7,140 |
| ViViT-L/16x2 [1] | 80.6 | 94.7 | 32 | 4×3 | 312M | 17,352 |
| X-ViT (Ours) | 78.5 | 93.7 | 8 | 1×3 | 92M | 425 |
| X-ViT (Ours) | 79.4 | 93.9 | 8 | 2×3 | 92M | 850 |
| X-ViT (Ours) | 80.2 | 94.7 | 16 | 1×3 | 92M | 850 |
| X-ViT (Ours) | 80.7 | 94.7 | 16 | 2×3 | 92M | 1700 |

3D convolutions vs. Vision Transformers

- 3D convolutions
 - Pro: Can capture detailed local spatiotemporal features to suppress local redundancy
 - Con: Inefficient to capture global (long-range) dependency due to limited receptive field
- Vision Transformers
 - Pro: Can capture global (long-range) dependency by self-attention mechanism
 - Con: Inefficient to encode spatiotemporal feature in shallow layers (local redundancy) and requires explicit position embedding (which could be sub-optimal for videos)



Integrating merits of both, a <u>unified model</u> has been proposed

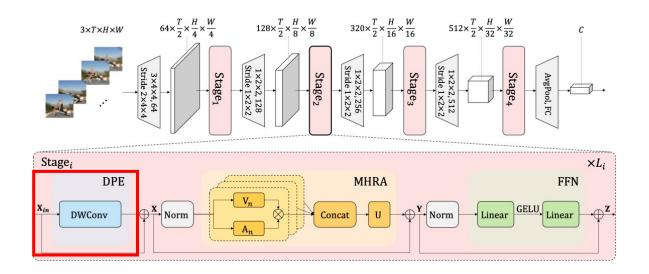
- Vision transformer learns local repre sentations with redundant global at tention
- This wastes large computation to en code only very local spatiotemporal representations

Visualizations of TimeSformer [Bertasius et al., 2021]

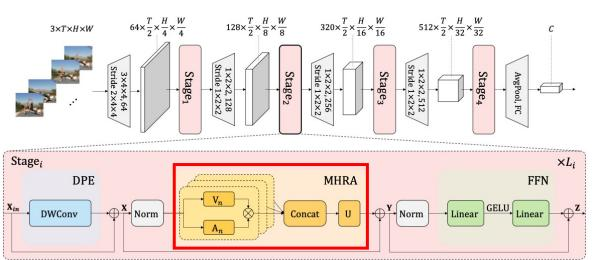
- Dynamic Position Embedding (DPE)
 - Instead of explicit position embedding, dynamic position embedding (DPE) is used:

$$DPE(\mathbf{X}_{in}) = DWConv(\mathbf{X}_{in})$$

- DPE dynamically integrates 3D position information into all tokens
- **DWConv** is a simple 3D depth-wise convolution with zero paddings
 - Shared parameters & locality of convolution tackles permutation-invariance
 - In CPE, zero paddings help tokens on the borders be aware of their absolute positions
 - That is, all tokens progressively encode their position information via querying their neighbor



- Multi-Head Relation Aggregator (MHRA)
 - 1) Local MHRA (for shallow layers)
 - Aim for shallow layers is to learn detailed video representation from local spatiotemporal context to reduce redundancy
 - Design token affinity to be local learnable parameter matrix, which depends only on relative 3D position between tokens
 - RA learns local spatiotemporal affinity between one anchor token X_i and other tokens in the small tube $\Omega_i^{t \times h \times w}$

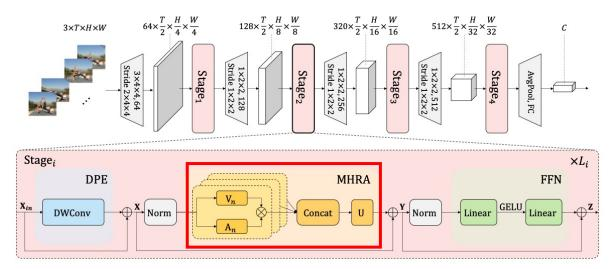


 $\mathbf{A}_n^{local}(\mathbf{X}_i, \mathbf{X}_j) = a_n^{i-j}, \ where \ j \in \Omega_i^{t imes h imes w}$

- Multi-Head Relation Aggregator (MHRA)
 - 2) Global MHRA (for deep layers)
 - Aim for deep layers is to capture long-term token dependency in global video clip
 - Design token affinity via comparing content similarity among all tokens in global view

$$\mathbf{A}_{n}^{global}(\mathbf{X}_{i}, \mathbf{X}_{j}) = \frac{e^{Q_{n}(\mathbf{X}_{i})^{T}K_{n}(\mathbf{X}_{j})}}{\sum_{j' \in \Omega_{T \times H \times W}} e^{Q_{n}(\mathbf{X}_{i})^{T}K_{n}(\mathbf{X}_{j'})}}$$

- X_j can be any token in global 3D tube $\Omega_{T \times H \times W}$
- $Q_n(\cdot)$ and $K_n(\cdot)$ are two different linear transformations



- Uniformer outperforms existing models with much fewer computational cost
- Achieves a preferable balance between computation and accuracy

| Method | Pretrain | #Frame | GFLOPs | SSV1 | | SSV2 | |
|----------------------------------------|----------|------------------------|--------|-------|-------|-------|-------|
| Method | Pretrain | #Frame | GFLOPS | Top-1 | Top-5 | Top-1 | Top-5 |
| TSN(Wang et al., 2016) | IN-1K | 16×1×1 | 66 | 19.9 | 47.3 | 30.0 | 60.5 |
| TSM(Lin et al., 2019) | IN-1K | 16×1×1 | 66 | 47.2 | 77.1 | - | - |
| GST(Luo & Yuille, 2019) | IN-1K | 16×1×1 | 59 | 48.6 | 77.9 | 62.6 | 87.9 |
| MSNet(Kwon et al., 2020) | IN-1K | 16×1×1 | 101 | 52.1 | 82.3 | 64.7 | 89.4 |
| CT-Net(Li et al., 2021a) | IN-1K | 16×1×1 | 75 | 52.5 | 80.9 | 64.5 | 89.3 |
| $CT-Net_{EN}$ (Li et al., 2021a) | IN-1K | 8+12+16+24 | 280 | 56.6 | 83.9 | 67.8 | 91.1 |
| TDN(Wang et al., 2020b) | IN-1K | $16 \times 1 \times 1$ | 72 | 53.9 | 82.1 | 65.3 | 89.5 |
| TDN_{EN} (Wang et al., 2020b) | IN-1K | 8+16 | 198 | 56.8 | 84.1 | 68.2 | 91.6 |
| TimeSformer-HR(Bertasius et al., 2021) | IN-21K | 16×3×1 | 5109 | - | - | 62.5 | - |
| X-ViT(Bulat et al., 2021) | IN-21K | $32 \times 3 \times 1$ | 1270 | - | - | 65.4 | 90.7 |
| Mformer-L(Patrick et al., 2021) | K400 | $32 \times 3 \times 1$ | 3555 | - | - | 68.1 | 91.2 |
| ViViT-L(Arnab et al., 2021) | K400 | $16 \times 3 \times 4$ | 11892 | - | - | 65.4 | 89.8 |
| MViT-B,64×3(Fan et al., 2021) | K400 | $64 \times 1 \times 3$ | 1365 | - | - | 67.7 | 90.9 |
| MViT-B-24,32×3(Fan et al., 2021) | K600 | $32 \times 1 \times 3$ | 708 | - | - | 68.7 | 91.5 |
| Swin-B(Liu et al., 2021b) | K400 | $32 \times 3 \times 1$ | 963 | - | - | 69.6 | 92.7 |
| Our UniFormer-S | K400 | 16×1×1 | 42 | 53.8 | 81.9 | 63.5 | 88.5 |
| Our UniFormer-S | K600 | 16×1×1 | 42 | 54.4 | 81.8 | 65.0 | 89.3 |
| Our UniFormer-S | K400 | $16 \times 3 \times 1$ | 125 | 57.2 | 84.9 | 67.7 | 91.4 |
| Our UniFormer-S | K600 | 16×3×1 | 125 | 57.6 | 84.9 | 69.4 | 92.1 |
| Our UniFormer-B | K400 | 16×3×1 | 290 | 59.1 | 86.2 | 70.4 | 92.8 |
| Our UniFormer-B | K600 | $16 \times 3 \times 1$ | 290 | 58.8 | 86.5 | 70.2 | 93.0 |
| Our UniFormer-B | K400 | $32 \times 3 \times 1$ | 777 | 60.9 | 87.3 | 71.2 | 92.8 |
| Our UniFormer-B | K600 | 32×3×1 | 777 | 61.0 | 87.6 | 71.2 | 92.8 |

Table of Contents

Part 1. Basics

- Evolution of CNN architectures
- Batch normalization and ResNet
- Attention module in CNNs
- Vision transformers

Part 2. Advanced Topics

- Toward automation of network design
- Flexible architectures
- Observational study on network architectures
- Deep spatial-temporal models

Part 3. Beyond CNNs and Vision Transformers

- Patch-based architectures for vision
- New design paradigms

Table of Contents

Part 1. Basics

- Evolution of CNN architectures
- Batch normalization and ResNet
- Attention module in CNNs
- Vision transformers

Part 2. Advanced Topics

- Toward automation of network design
- Flexible architectures
- Observational study on network architectures
- Deep spatial-temporal models

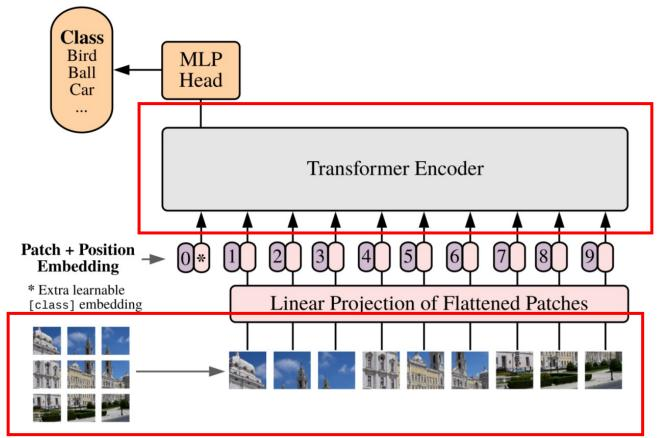
Part 3. Beyond CNNs and Vision Transformers

- Patch-based architectures for vision
- New design paradigms

General Patch-based Architectures: MLP architectures

Question: Is the success of Vision Transformers due to

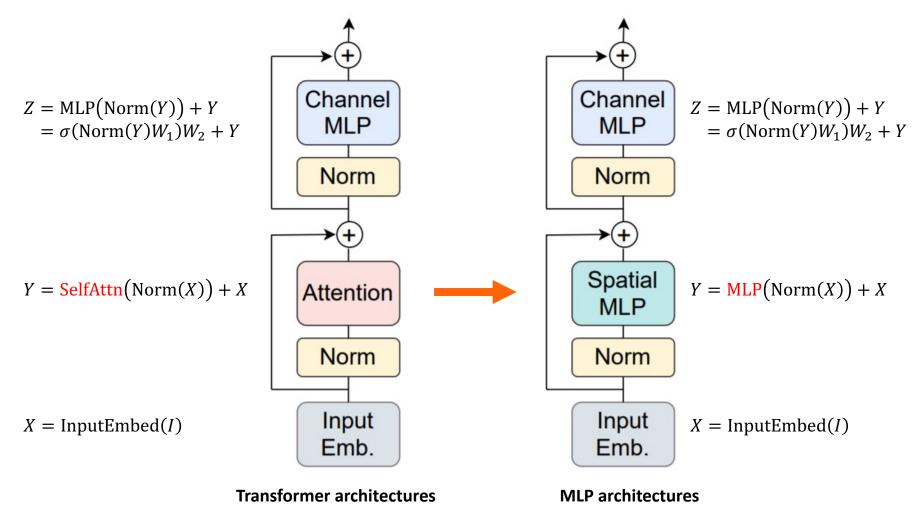
- 1. the powerful Transformer architecture?
- 2. using patches as the input representation?



Vision Transformer (ViT)

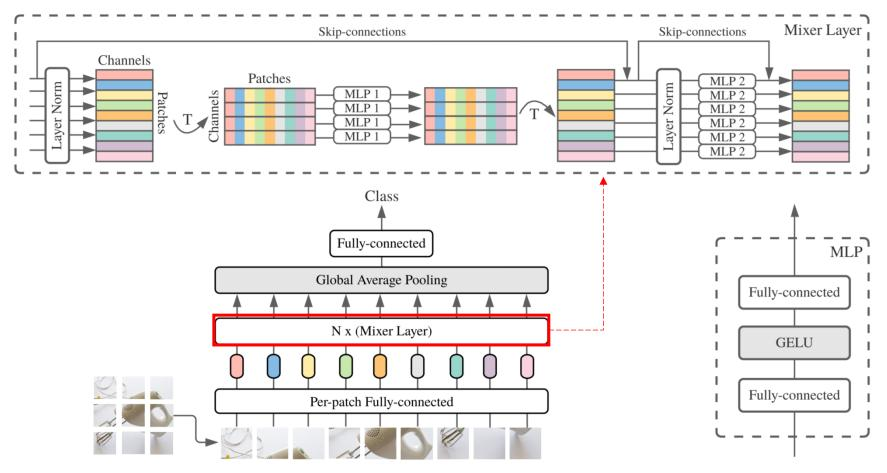
Algorithmic Intelligence Lab *source: [Dosovitskiy et al. 2021] An image is worth 16x16 words: Transformers for image recognition at scale, ICLR 2021 136

- Tolstikhin et al. (2021) suggests MLP module as an alternative of self-attention module
 - For a given Image *I*,



MLP-Mixer [Tolstikhin et al., 2021]

- Replacing the self-attention into MLP layers
- Removing position embedding & [class] token
- Mixing spatial & channel dimension separately

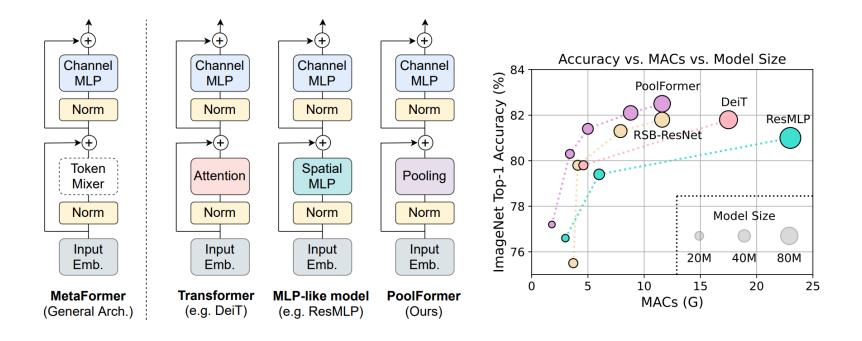


MLP-Mixer [Tolstikhin et al., 2021]

- Replacing the self-attention into MLP layers
- Removing position embedding & [class] token
- Mixing spatial & channel dimension separately
- MLP-Mixer shows competitive performances compared to Vision Transformers

| | ImNet top-1 | ReaL top-1 | Avg 5 top-1 | VTAB-1k 19 tasks | Throughput img/sec/core | TPUv3 core-days |
|-------------------|----------------|---------------|----------------|---------------------|----------------------------|--------------------|
| | Pre-tr | rained on | ImageNe | et-21k (public | ;) | |
| • HaloNet [51] | 85.8 | | | | 120 | 0.10k |
| • Mixer-L/16 | 84.15 | 87.86 | 93.91 | 74.95 | 105 | 0.41k |
| • ViT-L/16 [14] | 85.30 | 88.62 | 94.39 | 72.72 | 32 | 0.18k |
| • BiT-R152x4 [22] | 85.39 | | 94.04 | 70.64 | 26 | 0.94k |
| | Pre-tr | ained on | JFT-300N | M (proprietary | /) | |
| • NFNet-F4+ [7] | 89.2 | | | | 46 | 1.86k |
| • Mixer-H/14 | 87.94 | 90.18 | 95.71 | 75.33 | 40 | 1.01k |
| • BiT-R152x4 [22] | 87.54 | 90.54 | 95.33 | 76.29 | 26 | 9.90k |
| • ViT-H/14 [14] | 88.55 | 90.72 | 95.97 | 77.63 | 15 | 2.30k |

- MetaFormers [Yu et al, 2022] reveals that patch-based architecture with any tokenmixing method can work well
- For example, replacing self-attention with sophisticated average pooling (**PoolFormer**) allows light-weight model in terms of both computations and # parameters

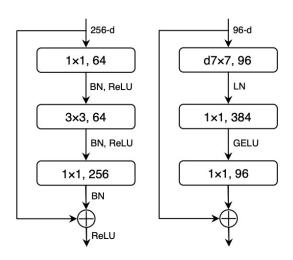


- MetaFormers [Yu et al, 2022] reveals that patch-based architecture with any tokenmixing method can work well
- For example, replacing self-attention with sophisticated average pooling (**PoolFormer**) allows light-weight model in terms of both computations and # parameters
 - Sophisticated design of **token-mixing is important** such as pooling sizes
 - Mixing different strategies (e.g., pooling + attention) is also effective

| Stage #Tokens Layer Specification | | | | Ро | olFor | mer | | | |
|-----------------------------------|---------------------------------------------|--------------|--------------|-------------------------|------------|--------|-------|------|--|
| Stage # TOKENS Layer | | Layer Sp | cemeation | S12 | S24 | S36 | M36 | M48 | |
| | | Patch | Patch Size | | $7 \times$ | 7, str | ide 4 | | |
| | | Embedding | Embed. Dim. | | 64 | | 9 | 6 | |
| 1 | $\frac{H}{4} \times \frac{W}{4}$ | PoolFormer | Pooling Size | | $3 \times$ | 3, str | ide 1 | | |
| | | Block | MLP Ratio | | | 4 | | | |
| | | BIOCK | # Block | 2 | 4 | 6 | 6 | 8 | |
| | | Patch | Patch Size | | $3 \times$ | 3, str | ide 2 | | |
| | | Embedding | Embed. Dim. | | 128 | | 19 | 92 | |
| 2 | $\frac{H}{8} \times \frac{W}{8}$ PoolFormer | PoolFormer | Pooling Size | | $3 \times$ | 3, str | ide 1 | | |
| | Block | MLP Ratio | 4 | | | | | | |
| | DIOCK | # Block | 2 | 4 | 6 | 6 | 8 | | |
| | | Patch | Patch Size | 3×3 , stride 2 | | | | | |
| | | Embedding | Embed. Dim. | 320 | | | 384 | | |
| 3 | $\frac{H}{16} \times \frac{W}{16}$ | PoolFormer | Pooling Size | 3×3 , stride 1 | | | | | |
| | | Block | MLP Ratio | 4 | | | | | |
| | | BIOCK | # Block | 6 | 12 | 18 | 18 | 24 | |
| | | Patch | Patch Size | | $3 \times$ | 3, str | ide 2 | | |
| | | Embedding | Embed. Dim. | | 512 | | 76 | 58 | |
| 4 | $\frac{H}{32} \times \frac{W}{32}$ | PoolFormer | Pooling Size | | $3 \times$ | 3, str | ide 1 | | |
| 02 02 | | Block | MLP Ratio | | | 4 | | | |
| | Block | | # Block | 2 | 4 | 6 | 6 | 8 | |
| | Pa | rameters (M) | | 11.9 | 21.4 | 30.8 | 56.1 | 73.4 | |
| | | MACs (G) | | 1.8 | 3.4 | 5.0 | 8.8 | 11.6 | |

| Ablation | Variant | Params (M) | MACs (G) | Top-1 (%) |
|------------------|---------------------------------------------------------------------------------------|------------|----------|-----------|
| Baseline | None (PoolFormer-S12) | 11.9 | 1.8 | 77.2 |
| | Pooling \rightarrow Identity mapping | 11.9 | 1.8 | 74.3 |
| | Pooling \rightarrow Global random matrix [*] (extra 21M frozen parameters) | 11.9 | 3.3 | 75.8 |
| Token mixers | Pooling \rightarrow Depthwise Convolution [9, 38] | 11.9 | 1.8 | 78.1 |
| Token mixers | Pooling size $3 \rightarrow 5$ | 11.9 | 1.8 | 77.2 |
| | Pooling size $3 \rightarrow 7$ | 11.9 | 1.8 | 77.1 |
| | Pooling size $3 \rightarrow 9$ | 11.9 | 1.8 | 76.8 |
| | Modified Layer Normalization \rightarrow Layer Normalization [1] | 11.9 | 1.8 | 76.5 |
| Normalization | Modified Layer Normalization [†] \rightarrow Batch Normalization [28] | 11.9 | 1.8 | 76.4 |
| | Modified Layer Normalization ^{\dagger} \rightarrow None | 11.9 | 1.8 | 46.1 |
| Activation | $GELU [25] \rightarrow ReLU [41]$ | 11.9 | 1.8 | 76.4 |
| Activation | $GELU \rightarrow SiLU [18]$ | 11.9 | 1.8 | 77.2 |
| Other components | Residual connection [25] \rightarrow None | 11.9 | 1.8 | 0.1 |
| Other components | Channel MLP \rightarrow None | 2.5 | 0.2 | 5.7 |
| | [Pool, Pool, Pool] \rightarrow [Pool, Pool, Pool, Attention] | 14.0 | 1.9 | 78.3 |
| Unbrid Stores | [Pool, Pool, Pool, Pool] \rightarrow [Pool, Pool, Attention, Attention] | 16.5 | 2.5 | 81.0 |
| Hybrid Stages | $[Pool, Pool, Pool, Pool] \rightarrow [Pool, Pool, Pool, SpatialFC]$ | 11.9 | 1.8 | 77.5 |
| | $[Pool, Pool, Pool, Pool] \rightarrow [Pool, Pool, SpatialFC, SpatialFC]$ | 12.2 | 1.9 | 77.9 |

- **ConvNext [Liu et al, 2022]** reveals that introducing X-former (e.g., transformers) architectural characteristic to CNNs is effective
- Patch-based input projection
 - In the input layer of ResNet, a 7×7 convolution is applied (overlapping patches)
 - In vision transformers, a more aggressive strategy is used:
 - A linear transform of patch as tokens (i.e., non-overlapping convolution)
- Wide feed-forward MLP
 - Note that FFN in ViT is effectively 1×1 convolution with $4 \times$ channel width as the input
 - Design principle is opposite to that of ResNet (i.e., the bottleneck block)



ResNet Block ConvNeXt Block

- **ConvNext [Liu et al, 2022]** reveals that introducing X-former (e.g., transformers) architectural characteristic to CNNs is effective
- There are various design transfers from X-former to CNN in ConvNext (refer to the paper for details)
- Simply transferring design principles from X-former to CNNs could make them outperfor m vision transformers

| model | image size | #param. | FLOPs | throughput (image / s) t | IN-1K top-1 acc. | | | | |
|--------------------------------|------------------|---------|--------|-----------------------------|---------------------|--|--|--|--|
| ImageNet-1K trained models | | | | | | | | | |
| • RegNetY-16G [54] | 224^{2} | 84M | 16.0G | 334.7 | 82.9 | | | | |
| • EffNet-B7 [71] | 600^{2} | 66M | 37.0G | 55.1 | 84.3 | | | | |
| • EffNetV2-L [72] | 480^{2} | 120M | 53.0G | 83.7 | 85.7 | | | | |
| • DeiT-S [73] | 224^{2} | 22M | 4.6G | 978.5 | 79.8 | | | | |
| • DeiT-B [73] | 224^{2} | 87M | 17.6G | 302.1 | 81.8 | | | | |
| • Swin-T | 224^{2} | 28M | 4.5G | 757.9 | 81.3 | | | | |
| ConvNeXt-T | 224^{2} | 29M | 4.5G | 774.7 | 82.1 | | | | |
| • Swin-S | 224^{2} | 50M | 8.7G | 436.7 | 83.0 | | | | |
| ConvNeXt-S | 224^{2} | 50M | 8.7G | 447.1 | 83.1 | | | | |
| • Swin-B | 224^{2} | 88M | 15.4G | 286.6 | 83.5 | | | | |
| ConvNeXt-B | 224^{2} | 89M | 15.4G | 292.1 | 83.8 | | | | |
| • Swin-B | 384^{2} | 88M | 47.1G | 85.1 | 84.5 | | | | |
| ConvNeXt-B | 384^{2} | 89M | 45.0G | 95.7 | 85.1 | | | | |
| ConvNeXt-L | 224^{2} | 198M | 34.4G | 146.8 | 84.3 | | | | |
| • ConvNeXt-L | 384 ² | 198M | 101.0G | 50.4 | 85.5 | | | | |

Table of Contents

Part 1. Basics

- Evolution of CNN architectures
- Batch normalization and ResNet
- Attention module in CNNs
- Vision transformers

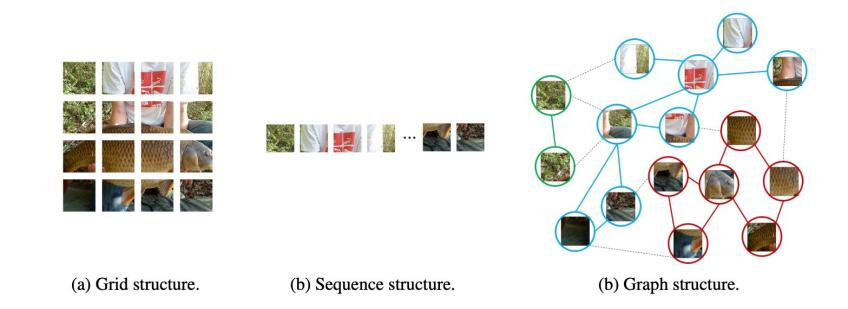
Part 2. Advanced Topics

- Toward automation of network design
- Flexible architectures
- Observational study on network architectures
- Deep spatial-temporal models

Part 3. Beyond CNNs and Vision Transformers

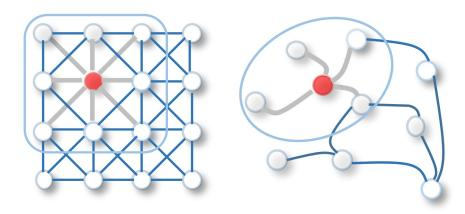
- Patch-based architectures for vision
- New design paradigms

- Grid (and sequence) of image patches can be views a s a special case of graph
- VisionGNN represents images as a graph (V, E) with image patch as nodes (V) and learnable edges (E)



Motivation: Can we go beyond **grid-based representation** of images?

- Grid (and sequence) of image patches can be views a s a special case of graph
- VisionGNN represents images as a graph (V, E) with image patch as nodes (V) and learnable edges (E)
- For modeling graph-based representation, a new graph model base-on Graph Convolution Networks is proposed
 - Graph Convolution Networks
 - Graph convolutional operation aggregates value of the node features of neighbors (Note that there is no ordering between nodes)



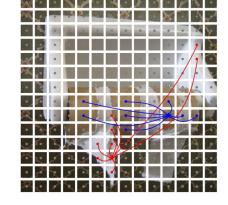
 $\begin{aligned} \mathcal{G}' &= F(\mathcal{G}, \mathcal{W}) \\ &= Update(Aggregate(\mathcal{G}, W_{agg}), W_{update}), \end{aligned}$

- Grid (and sequence) of image patches can be views a s a special case of graph
- VisionGNN represents images as a graph (V, E) with image patch as nodes (V) and learnable edges (E)
- VisionGNN can outperform vision transformers and CNNs

| Model | Resolution | Params (M) | FLOPs (B) | Top-1 | Top-5 |
|------------------------------|------------------|------------|-----------|-------|-------|
| ♠ ResMLP-S12 conv3x3 [50] | 224×224 | 16.7 | 3.2 | 77.0 | - |
| ConvMixer-768/32 [52] | 224×224 | 21.1 | 20.9 | 80.2 | - |
| ♠ ConvMixer-1536/20 [52] | 224×224 | 51.6 | 51.4 | 81.4 | - |
| ♦ ViT-B/16 [9] | 384×384 | 86.4 | 55.5 | 77.9 | - |
| 🔶 DeiT-Ti [51] | 224×224 | 5.7 | 1.3 | 72.2 | 91.1 |
| ♦ DeiT-S [51] | 224×224 | 22.1 | 4.6 | 79.8 | 95.0 |
| ♦ DeiT-B [51] | 224×224 | 86.4 | 17.6 | 81.8 | 95.7 |
| ResMLP-S24 [50] | 224×224 | 30 | 6.0 | 79.4 | 94.5 |
| ResMLP-B24 [50] | 224×224 | 116 | 23.0 | 81.0 | 95.0 |
| Mixer-B/16 [49] | 224×224 | 59 | 11.7 | 76.4 | - |
| ★ ViG-Ti (ours) | 224×224 | 7.1 | 1.3 | 73.9 | 92.0 |
| ★ ViG-S (ours) | 224×224 | 22.7 | 4.5 | 80.4 | 95.2 |
| ★ ViG-B (ours) | 224×224 | 86.8 | 17.7 | 82.3 | 95.9 |

- Grid (and sequence) of image patches can be views a s a special case of graph
- VisionGNN represents images as a graph (V, E) with image patch as nodes (V) and learnable edges (E)
- More importantly, the graph structure naturally provides interpretability in the hidden layers
 - Earlier blocks connects low-level features (e.g., colors) and local features
 - Later blocks connect semantically-related (e.g., same category) features





(c) Graph connection in the 12th block.

(a) Input image.

(b) Graph connection in the 1st block.

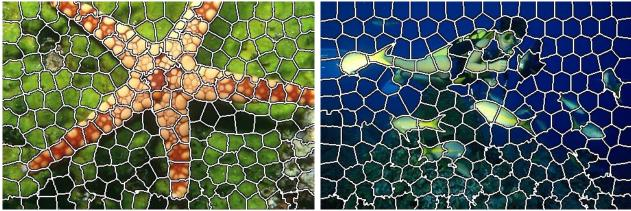
- Grid (and sequence) of image patches can be views a s a special case of graph
- VisionGNN represents images as a graph (V, E) with image patch as nodes (V) and learnable edges (E)
- More importantly, the graph structure naturally provides interpretability in the hidden layers
 - Earlier blocks connects low-level features (e.g., colors) and local features
 - Later blocks connect semantically-related (e.g., same category) features

- However, nodes are still regular-shaped in VisionGNN
 - Can we make more flexible model?
 - Treating each pixel as a node which will result in too many nodes (>10K)

Context Clusters (CoC) [Ma et al, 2023]

Motivation: Can we go beyond grid-based patches of images?

- Context Clusters view an image as a set of unorganized points and extract features via simplified clustering algorithm
- **n** points $P \in \mathbb{R}^{n \times d}$ are clustered using **SuperPixel** method
 - SuperPixel SLIC [Achanta et al., 2013]
 - For inputs, **n** is the number of all pixels, however, an initial 4×4 convolution projects them to feature space, reducing # points to $\frac{n}{16}$
 - For clustering *c* centers are evenly proposed, and each point is assigned to the nearest center (feature cosine similarity is used as the distance metric)
 - After clustering, each cluster can have variable number of points (even 0 is possible)



Algorithmic Intelligence Lab

Context Clusters (CoC) [Ma et al, 2023]

Motivation: Can we go beyond grid-based patches of images?

- Context Clusters view an image as a set of unorganized points and extract features via simplified clustering algorithm
- Assuming a cluster has *m* points, **aggregation** and **dispatching** are done **within the cluster**
- The cosine similarity $s \in \mathbb{R}^m$ between *m* points and the cluster center is used as weights:
 - Feature aggregation (g)
 - (note that v_i is **MLP projection** of each point p_i and α , β are **learnable scalars**)

$$g = \frac{1}{C} \left(v_c + \sum_{i=1}^m \operatorname{sig} \left(\alpha s_i + \beta \right) * v_i \right), \quad \text{s.t., } C = 1 + \sum_{i=1}^m \operatorname{sig} \left(\alpha s_i + \beta \right).$$

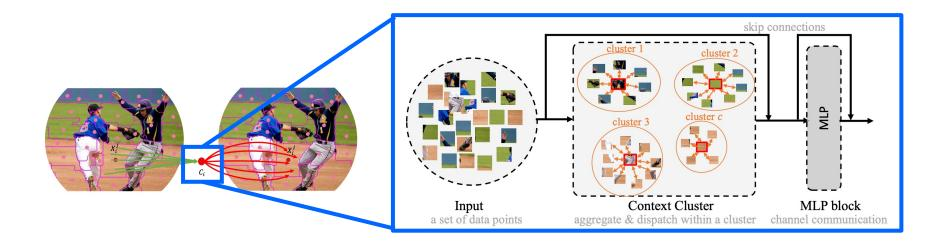
• Feature dispatching

$$p'_i = p_i + \operatorname{FC}(\operatorname{sig}(\alpha s_i + \beta) * g).$$

Context Clusters (CoC) [Ma et al, 2023]

Motivation: Can we go beyond grid-based patches of images?

- Context Clusters view an image as a set of unorganized points and extract features via simplified clustering algorithm
- Assuming a cluster has *m* points, **aggregation** and **dispatching** are done **within the cluster**
- Finally, additional MLP block is applied for channel-wise mixing in each point

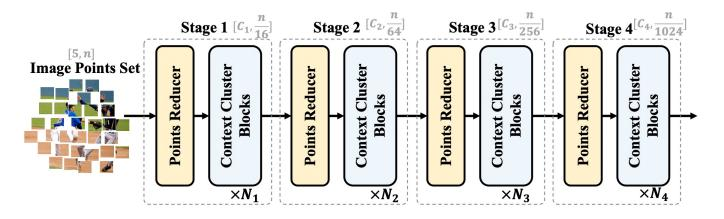


• Context Clusters (CoC) [Ma et al, 2023]

Motivation: Can we go beyond grid-based patches of images?

- Context Clusters view an image as a set of unorganized points and extract features via simplified clustering algorithm
- Assuming a cluster has *m* points, **aggregation** and **dispatching** are done **within the cluster**
- Finally, additional MLP block is applied for channel-wise mixing in each point

- To save the computation, some stages of **Points Reducer** is applied
 - Reducing is simply done by regular **convolution operations** (e.g., 4×4) over the spatial grid



• Context Clusters (CoC) [Ma et al, 2023]

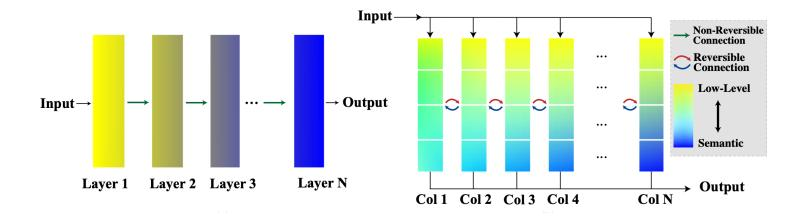
Motivation: Can we go beyond grid-based patches of images?

- Context Clusters view an image as a set of unorganized points and extract features via simplified clustering algorithm
- CoC can outperform CNNs and Transformers
 - More importantly, CoC shows clustering with the semantics in image

| | Method | Param. | GFLOPs | Top-1 | Throughputs (images/s) | | | | | | |
|------------|--------------------------------------------------------------|--------|--------|-------|------------------------|------------------------------|---------------|--------------------|------------------------------------------|--------------------------------------------------------------------------------------------------------------------------------------------------------------------------------------------------------------------------------------------------------------------------------------------------------------------------------------------------------------------------------------------------------------------------------------------------------------------------------------------------------------------------------------------------------------------------------------------------------------------------------------------------------------------------------------------------------------------------------------------------------------------------------------------------------------------------------------------------------------------------------------------------------------------------------------------------------------------------------------------------------------------------------------------------------------------------------------------------------------------------------------------------------------------------------------------------------------------------------------------------------------------------------------------------------------------------------------------------------------------------------------------------------------------------------------------------------------------------------------------------------------------------------------------------------------------------------------------------------------------------------------------------------------------------------------------------------------------------------------------------------------------------------------------------------------------------------------------------------------------------------------------------------------------------------------------------------------------------------------------------------------------------------------------------------------------------------------------------------------------------------|----|
| | ResMLP-12 (Touvron et al., 2021a) | 15.0 | 3.0 | 76.6 | 511.4 | | | | | | |
| Ч | ResMLP-24 (Touvron et al., 2021a) | 30.0 | 6.0 | 79.4 | 509.7 | | | | | | |
| | ResMLP-36 (Touvron et al., 2021a) | 45.0 | 8.9 | 79.7 | 452.9 | | - | The State | | | |
| N | MLP-Mixer-B/16 (Tolstikhin et al., 2021) | 59.0 | 12.7 | 76.4 | 400.8 | ap) | | SL IN | 1 | And a second | |
| 2 | MLP-Mixer-L/16 (Tolstikhin et al., 2021) | 207.0 | 44.8 | 71.8 | 125.2 | B/1 | | Property. | | | |
| | # gMLP-Ti (Liu et al., 2021a) | 6.0 | 1.4 | 72.3 | 511.6 | H if | | | | and all all and and | |
| | # gMLP-S (Liu et al., 2021a) | 20.0 | 4.5 | 79.6 | 509.4 | ViT-B/16 (attention map | A | provide a | | and the second s | |
| | ViT-B/16 (Dosovitskiy et al., 2020) | 86.0 | 55.5 | 77.9 | 292.0 | 0 | | St. PAGE | | | |
| - | ViT-L/16 (Dosovitskiy et al., 2020) | 307 | 190.7 | 76.5 | 92.8 | | | Charles and | | | 83 |
| | PVT-Tiny (Wang et al., 2021) | 13.2 | 1.9 | 75.1 | - | mag 20 | | P. | A start for the start | | |
| en | PVT-Small (Wang et al., 2021) | 24.5 | 3.8 | 79.8 | - | ResNet50 (class act. map) | | 1. 1 | C. T. S. C. S. | and the second second second | |
| Ē | ◆ T2T-ViT-7 (Yuan et al., 2021a) | 4.3 | 1.1 | 71.7 | - | est ss a | 1 ft | 1 Bar | 1 000 | and the second | |
| ~ | DeiT-Tiny/16 (Touvron et al., 2021b) | 5.7 | 1.3 | 72.2 | 523.8 | (cla | | Contraction of the | and and a second second | and while and | 1 |
| | DeiT-Small/16 (Touvron et al., 2021b) | 22.1 | 4.6 | 79.8 | 521.3 | | Sauce a salar | No. Cake | | | |
| a | • ResNet18 (He et al., 2016) | 12 | 1.8 | 69.8 | 584.9 | (d | | | | | |
| <u>[</u>] | ResNet50 (He et al., 2016) | 26 | 4.1 | 79.8 | 524.8 | Ina 🖌 | 2443.3 | 14 | | | |
| Ē | ConvMixer-512/16 (Trockman et al., 2022) | 5.4 | - | 73.8 | - | ling C | 43225 | | | | |
| | ConvMixer-1024/12 (Trockman et al., 2022) | 14.6 | - | 77.8 | - | ster | 147 | 100 | Concernance of the second | | |
| ō | ConvMixer-768/32 (Trockman et al., 2022) | 21.1 | - | 80.16 | 142.9 | (clu | | E | 100 - 24 - 24 - 24 - 24 - 24 - 24 - 24 - | | |
| <u> </u> | Context-Cluster-Ti (ours) | 5.3 | 1.0 | 71.8 | 518.4 | 14 | | | | | |
| ste | Context-Cluster-Ti‡ (ours) | 5.3 | 1.0 | 71.7 | 510.8 | | | | | | |
| n, | Context-Cluster-Small (ours) | 14.0 | 2.6 | 77.5 | 513.0 | | | | | | |
| | Context-Cluster-Medium (ours) | 27.9 | 5.5 | 81.0 | 325.2 | | | | | | |

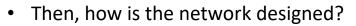
• RevCol: Reversible Column Networks [Cai et al, 2023]

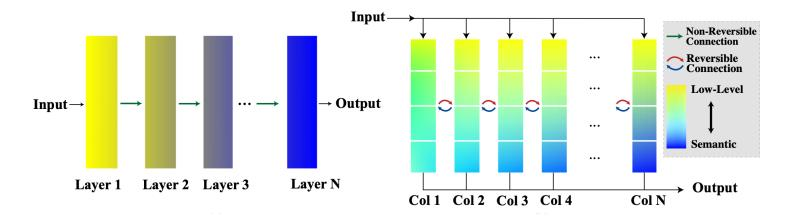
- Deep networks (left) are built on the Information Bottleneck
 - Layers close to the input contain more low-level information
 - Features close to the output are rich in semantics
- However, **downstream tasks may suffer** if the learned features are **over-compressed** e.g., Transfer learning for object detection



• RevCol: Reversible Column Networks [Cai et al, 2023]

- Deep networks (left) are built on the Information Bottleneck
 - Layers close to the input contain more low-level information
 - Features close to the output are rich in semantics
- Instead, RevCol suggests a design where information in the *earlier layer* could be (approximately) restored with information in the later layers



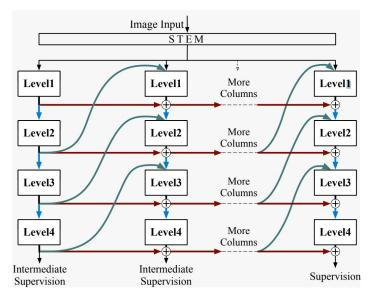


RevCol: Reversible Column Networks [Cai et al, 2023]

- Inspired by *invertible neural networks* in Normalizing Flow, reversible operations are defined:
 - t is the depth index, F_t is the layer at t, γ is a simple channel-wise scaling
- Specifically, the output x_t is the weighted sum of x_{t-m} and non-linear transform of intermediate states x_{t-1}, ..., x_{t-m+1}
 - Note that the operation is invertible
 - Any **deep networks** can implement **F**_t (e.g., ConvNext is employed)

Forward:
$$x_t = \mathbf{F}_t(x_{t-1}, x_{t-2}, ..., x_{t-m+1}) + \gamma x_{t-m}$$

Inverse: $x_{t-m} = \gamma^{-1}[x_t - \mathbf{F}_t(x_{t-1}, x_{t-2}, ..., x_{t-m+1})],$



• RevCol: Reversible Column Networks [Cai et al, 2023]

- Inspired by *invertible neural networks* in Normalizing Flow, reversible operations are defined:
 - t is the depth index, F_t is the layer at t, γ is a simple channel-wise scaling
- Despite the restrictive design, ConvNext with RevCol is comparable to the vanilla model
 - More importantly, transfer learning is improved in object detection

| | Image | ParamsFLOPs Top-1 | | | | |
|------------------------------------------|-----------|-------------------|-----------|--------|--|--|
| Model | Size | (M) | (G) | Acc. | | |
| ImageNet-22K pre-trained mo | dels (Im | ageNet | -1K fine- | tuned) | | |
| • Swin-B (Liu et al. | 224^{2} | 88 | 15.4 | 85.2 | | |
| Swin-B↑ (Liu et al. | 384^{2} | 88 | 47.0 | 86.4 | | |
| • ViT-B↑ (Dosovitskiy et al.) | 384^{2} | 86 | 55.4 | 84.0 | | |
| • RepLKNet-31B (Ding et al.) | 224^{2} | 79 | 15.3 | 85.2 | | |
| • RepLKNet-31B [↑] (Ding et al. | | 79 | 45.1 | 86.0 | | |
| • ConvNeXt-B (Liu et al.) | 224^{2} | 89 | 15.4 | 85.8 | | |
| • ConvNeXt-B↑ (Liu et al.) | 384^{2} | 89 | 45.1 | 86.8 | | |
| • RevCol-B | 224^{2} | 138 | 16.6 | 85.6 | | |
| • RevCol-B↑ | 384^{2} | 138 | 48.9 | 86.7 | | |
| • Swin-L (Liu et al.) | 224^{2} | 197 | 34.5 | 86.3 | | |
| Swin-L↑ (Liu et al.) | 384^{2} | 197 | 103.9 | 87.3 | | |
| • ViT-L↑ (Dosovitskiy et al.) | 384^{2} | 307 | 190.7 | 85.2 | | |
| • RepLKNet-31L (Ding et al.) | 384^{2} | 172 | 96.0 | 86.6 | | |
| • ConvNeXt-L (Liu et al.) | 224^{2} | 198 | 34.4 | 86.6 | | |
| • ConvNeXt-L↑ (Liu et al.) | 384^{2} | 198 | 101.0 | 87.5 | | |
| • RevCol-L | 224^{2} | 273 | 39.0 | 86.6 | | |
| • RevCol-L↑ | 384^{2} | 273 | 116.0 | 87.6 | | |

| Backbone | AP^{box} | AP_{50}^{box} | AP_{75}^{box} | AP^{mask} | AP_{50}^{mask} | ${ m AP}_{75}^{mask}$ | Params | FLOPs | | | |
|------------------------------|------------|-----------------|-----------------|-------------|------------------|-----------------------|--------|-------|--|--|--|
| ImageNet-22K pre-trained | | | | | | | | | | | |
| • Swin-B (Liu et al.) | 53.0 | 71.8 | 57.5 | 45.8 | 69.4 | 49.7 | 145M | 982G | | | |
| • ConvNeXt-B (Liu et al.) | 54.0 | 73.1 | 58.8 | 46.9 | 70.6 | 51.3 | 146M | 964G | | | |
| • RepLKNet-B (Ding et al.) | 53.0 | - | - | 46.3 | - | - | 137M | 965G | | | |
| • RevCol-B | 55.0 | 73.5 | 59.7 | 47.5 | 71.1 | 51.8 | 196M | 988G | | | |
| • Swin-L (Liu et al.) | 53.9 | 72.4 | 58.8 | 46.7 | 70.1 | 50.8 | 253M | 1382G | | | |
| • ConvNeXt-L (Liu et al.) | 54.8 | 73.8 | 59.8 | 47.6 | 71.3 | 51.7 | 255M | 1354G | | | |
| • RepLKNet-L (Ding et al.) | 53.9 | - | - | 46.5 | - | - | 229M | 1321G | | | |
| • RevCol-L | 55.9 | 74.1 | 60.7 | 48.4 | 71.8 | 52.8 | 330M | 1453G | | | |
| Extra data pre-trained | | | | | | | | | | | |
| • RevCol-H (HTC++) | 61.1 | 78.8 | 67.0 | 53.0 | 76.3 | 58.7 | 2.41G | 4417G | | | |
| • RevCol-H (Objects365+DINO) | 63.8 | 81.8 | 70.2 | - | - | - | 2.18G | 4012G | | | |

Summary

- The larger the network, the more difficult it is to design
 - 1. Optimization difficulty
 - 2. Generalization difficulty
 - **ResNet**: Optimization ⇒ Generalization
 - Many variants of ResNet have been emerged
 - Very recent trends towards network design and scaling
- Recently, various types of **patch-based architectures** are explored
 - Vision transformers, MLP-mixing models, etc.
- Many types of **architectures** are explored to capture good representation
 - Automated network designs and flexible model architectures
 - Many observational study supports the advantages of each architecture
 - Spatial-temporal models (e.g., 3D CNNs and video transformers)
- A new architectural paradigms are actively searched e.g., Graph-based architectures and Reversible networks

[Jónsson et al., 1998] Jónsson, H., Mills, G., & Jacobsen, K. W. (1998). Nudged elastic band method for finding minimum energy paths of transitions. In Classical and quantum dynamics in condensed phase simulations (pp. 385-404).

link : https://www.worldscientific.com/doi/abs/10.1142/9789812839664_0016

[LeCun et al., 1998] LeCun, Y., Bottou, L., Bengio, Y., & Haffner, P. (1998). Gradient-based learning applied to document recognition. Proceedings of the IEEE, 86(11), 2278-2324. link : <u>https://ieeexplore.ieee.org/abstract/document/726791/</u>

[Bergstra et al., 2012] Bergstra, J., & Bengio, Y. (2012). Random search for hyper-parameter optimization. Journal of Machine Learning Research, 13(Feb), 281-305. link : http://www.jmlr.org/papers/v13/bergstra12a.html

[Krizhevsky et al., 2012] Krizhevsky, A., Sutskever, I., & Hinton, G. E. (2012). Imagenet classification with deep convolutional neural networks. In *Advances in neural information processing systems* (pp. 1097-1105). link : <u>http://papers.nips.cc/paper/4824-imagenet-classification-with-deep-convolutional-neural-networks</u>

[Farabet et al., 2013] Farabet, C., Couprie, C., Najman, L., & LeCun, Y. (2013). Learning hierarchical features for scene labeling. IEEE transactions on pattern analysis and machine intelligence, 35(8), 1915-1929. link : <u>https://ieeexplore.ieee.org/abstract/document/6338939/</u>

[Eigen et al., 2014] Eigen, D., Rolfe, J., Fergus, R., & LeCun, Y. (2013). Understanding Deep Architectures using a Recursive Convolutional Network. ArXiv Preprint ArXiv:1312.1847, 1–9. link : <u>http://arxiv.org/abs/1312.1847</u>

[Simonyan et al., 2014] Simonyan, K., & Zisserman, A. (2014). Very deep convolutional networks for large-scale image recognition. arXiv preprint arXiv:1409.1556. link: <u>https://arxiv.org/abs/1409.1556</u> [Zeiler et al., 2014] Zeiler, M. D., & Fergus, R. (2014). Visualizing and understanding convolutional networks. In European conference on computer vision (pp. 818-833). Springer, Cham. link : <u>https://link.springer.com/chapter/10.1007/978-3-319-10590-1_53</u>

[Ioffe et al., 2015] Ioffe, S. & Szegedy, C.. (2015). Batch Normalization: Accelerating Deep Network Training by Reducing Internal Covariate Shift. Proceedings of the 32nd International Conference on Machine Learning, in PMLR 37:448-456

link : <u>http://proceedings.mlr.press/v37/ioffe15.html</u>

[Ren et al., 2015] Ren, S., He, K., Girshick, R., & Sun, J. (2015). Faster R-CNN: Towards real-time object detection with region proposal networks. In *Advances in neural information processing systems*(pp. 91-99). link : <u>http://papers.nips.cc/paper/5638-faster-r-cnn-towards-real-time-object-detection-with-region-proposal-networks</u>

[Russakovsky et al., 2015] Russakovsky, O. et al. (2015). Imagenet large scale visual recognition challenge. International Journal of Computer Vision, 115(3), 211-252. link : <u>https://link.springer.com/article/10.1007/s11263-015-0816-y</u>

[Szegedy et al., 2015] Szegedy, C., Liu, W., Jia, Y., Sermanet, P., Reed, S., Anguelov, D., ... & Rabinovich, A. (2015). Going deeper with convolutions. In Proceedings of the IEEE conference on computer vision and pattern recognition (pp. 1-9).

link : <u>https://www.cv-foundation.org/openaccess/content_cvpr_2015/html/Szegedy_Going_Deeper_With_2015_</u> <u>CVPR_paper.html</u>

[Han et al., 2016] Han, D., Kim, J., & Kim, J. (2017, July). Deep pyramidal residual networks. In Computer Vision and Pattern Recognition (CVPR), 2017 IEEE Conference on (pp. 6307-6315). IEEE. link : <u>https://ieeexplore.ieee.org/document/8100151/</u>

[Yu et al., 2016] Yu, F., & Koltun, V. (2016) Multi-Scale Context Aggregation by Dilated Convolutions. In International Conference on Learning Representations. link : https://arxiv.org/abs/1511.07122

References

[He et al., 2016a] He, K., Zhang, X., Ren, S., & Sun, J. (2016). Deep residual learning for image recognition. In Proceedings of the IEEE conference on computer vision and pattern recognition (pp. 770-778). link : <u>https://ieeexplore.ieee.org/document/7780459/</u>

[He et al., 2016b] He, K., Zhang, X., Ren, S., & Sun, J. (2016). Identity mappings in deep residual networks. In European conference on computer vision (pp. 630-645). Springer, Cham. link : <u>https://link.springer.com/chapter/10.1007/978-3-319-46493-0_38</u>

[Huang et al., 2016] Huang, G., Sun, Y., Liu, Z., Sedra, D., & Weinberger, K. Q. (2016). Deep networks with stochastic depth. In European Conference on Computer Vision (pp. 646-661). link : <u>https://link.springer.com/chapter/10.1007/978-3-319-46493-0_39</u>

[Kolsbjerg et al., 2016] Kolsbjerg, E. L., Groves, M. N., & Hammer, B. (2016). An automated nudged elastic band method. The Journal of chemical physics, 145(9), 094107. link : <u>https://aip.scitation.org/doi/abs/10.1063/1.4961868</u>

[Targ et al., 2016] Targ, S., Almeida, D., & Lyman, K. (2016). Resnet in Resnet: generalizing residual architectures. arXiv preprint arXiv:1603.08029.

link : <u>https://arxiv.org/abs/1603.08029</u>

[Veit et al., 2016] Veit, A., Wilber, M. J., & Belongie, S. (2016). Residual networks behave like ensembles of relatively shallow networks. In Advances in Neural Information Processing Systems (pp. 550-558). link : <u>http://papers.nips.cc/paper/6556-residual-networks-behave-like-ensembles-of-relatively-shallow-networks</u>

[Xie et al., 2016] Xie, S., Girshick, R., Dollár, P., Tu, Z., & He, K. (2017, July). Aggregated residual transformations for deep neural networks. In Computer Vision and Pattern Recognition (CVPR), 2017 IEEE Conference on (pp. 5987-5995). IEEE.

link : <u>http://openaccess.thecvf.com/content_cvpr_2017/papers/Xie_Aggregated_Residual_Transformations_</u> <u>CVPR_2017_paper.pdf</u> [Zagoruyko et al., 2016] Zagoruyko, S. and Komodakis, N. (2016). Wide Residual Networks. In Proceedings of the British Machine Vision Conference (pp. 87.1-87.12).

link : http://www.bmva.org/bmvc/2016/papers/paper087/index.html

[Zoph et al., 2016] Zoph, B., & Le, Q. V. (2016). Neural architecture search with reinforcement learning. arXiv preprint arXiv:1611.01578.

link : https://arxiv.org/abs/1611.01578

[Chen et al., 2017] Chen, Y., Li, J., Xiao, H., Jin, X., Yan, S., & Feng, J. (2017). Dual path networks. In Advances in Neural Information Processing Systems (pp. 4467-4475).

link : <u>https://papers.nips.cc/paper/7033-dual-path-networks</u>

[Huang et al., 2017] Huang, G., Liu, Z., Van Der Maaten, L., & Weinberger, K. Q. (2017, July). Densely Connected Convolutional Networks. In CVPR (Vol. 1, No. 2, p. 3). link : <u>http://openaccess.thecvf.com/content_cvpr_2017/papers/Huang_Densely_Connected_Convolutional_</u> <u>CVPR_2017_paper.pdf</u>

[Szegedy et al., 2017] Szegedy, C., loffe, S., Vanhoucke, V., & Alemi, A. A. (2017, February). Inception-v4, inception-resnet and the impact of residual connections on learning. In AAAI (Vol. 4, p. 12). link : <u>https://www.aaai.org/ocs/index.php/AAAI/AAAI17/paper/download/14806/14311</u>

[Dai et al., 2017] Dai, J., Qi, H., Xiong, Y., Li, Y., Zhang, G., Hu, H., & Wei, Y. (2017). Deformable convolutional networks. In *Proceedings of the IEEE international conference on computer vision* (pp. 764-773). link : <u>https://arxiv.org/abs/1703.06211v3</u>

[Chen et al., 2017] Chen, L. C., Papandreou, G., Schroff, F., & Adam, H. (2017). Rethinking atrous convolution for semantic image segmentation. *arXiv preprint arXiv:1706.05587*. link : <u>https://arxiv.org/abs/1706.05587</u>

[Howard et al., 2017] Howard, A. G., Zhu, M., Chen, B., Kalenichenko, D., Wang, W., Weyand, T., ... & Adam, H. (2017). Mobilenets: Efficient convolutional neural networks for mobile vision applications. *arXiv preprint arXiv:1704.04861*. link: <u>https://arxiv.org/abs/1704.04861</u> [Draxler et al., 2018] Draxler, F., Veschgini, K., Salmhofer, M. & Hamprecht, F. (2018). Essentially No Barriers in Neural Network Energy Landscape. Proceedings of the 35th International Conference on Machine Learning, in PMLR 80:1309-1318.

link : <u>http://proceedings.mlr.press/v80/draxler18a.html</u>

[Luo et al., 2018] Luo, R., Tian, F., Qin, T., Chen, E. & Liu, T. (2018) Neural Architecture Optimization. arXiv preprint arXiv:1808.07233.

link : <u>https://arxiv.org/abs/1808.07233</u>

[Li et al., 2018] Li, H., Xu, Z., Taylor, G., & Goldstein, T. (2017). Visualizing the loss landscape of neural nets. arXiv preprint arXiv:1712.09913. link : https://arxiv.org/abs/1712.09913

[Pham et al., 2018] Pham, H., Guan, M., Zoph, B., Le, Q. & Dean, J.. (2018). Efficient Neural Architecture Search via Parameters Sharing. Proceedings of the 35th International Conference on Machine Learning, in PMLR 80:4095-4104 link : <u>http://proceedings.mlr.press/v80/pham18a.html</u>

[Real et al., 2018] Real, E., Aggarwal, A., Huang, Y., & Le, Q. V. (2018). Regularized evolution for image classifier architecture search. arXiv preprint arXiv:1802.01548. link : https://arxiv.org/abs/1802.01548

[Zoph et al., 2018] Zoph, B., Vasudevan, V., Shlens, J., & Le, Q. V. (2017). Learning transferable architectures for scalable image recognition. arXiv preprint arXiv:1707.07012, 2(6).

link : <u>http://openaccess.thecvf.com/content_cvpr_2018/papers/Zoph_Learning_Transferable_Architectures_</u> <u>CVPR_2018_paper.pdf</u>

[Brock et al., 2018] Brock, A., Lim, T., Ritchie, J. M., & Weston, N. (2018). SMASH: one-shot model architecture search through hypernetworks. In International Conference on Learning Representations. link : <u>https://openreview.net/forum?id=rydeCEhs-</u>

References

[Hu et al., 2018] Hu, J., Shen, L., & Sun, G. (2018). Squeeze-and-excitation networks. In Proceedings of the IEEE conference on computer vision and pattern recognition (pp. 7132-7141). link : <u>https://arxiv.org/abs/1709.01507</u>

[Woo et al., 2018] Woo, S., Park, J., Lee, J. Y., & Kweon, I. S. (2018). Cbam: Convolutional block attention module. In *Proceedings of the European conference on computer vision (ECCV)* (pp. 3-19). link : <u>https://arxiv.org/abs/1807.06521v2</u>

[Tan et al., 2019] Tan, M., Chen, B., Pang, R., Vasudevan, V., Sandler, M., Howard, A., & Le, Q. V. (2019). Mnasnet: Platform-aware neural architecture search for mobile. In *Proceedings of the IEEE/CVF Conference on Computer Vision and Pattern Recognition* (pp. 2820-2828). link : https://arxiv.org/abs/1807.11626

link : <u>https://arxiv.org/abs/1807.11626</u>

[Dosovitskiy et al., 2021] Dosovitskiy, A., Beyer, L., Kolesnikov, A., Weissenborn, D., Zhai, X., Unterthiner, T., ... & Houlsby, N. (2020). An image is worth 16x16 words: Transformers for image recognition at scale. *arXiv preprint arXiv:2010.11929*.

link : https://arxiv.org/abs/2010.11929

[Liu et al., 2021] Liu, Z., Lin, Y., Cao, Y., Hu, H., Wei, Y., Zhang, Z., ... & Guo, B. (2021). Swin transformer: Hierarchical vision transformer using shifted windows. In *Proceedings of the IEEE/CVF International Conference on Computer Vision* (pp. 10012-10022).

link :

https://openaccess.thecvf.com/content/ICCV2021/html/Liu_Swin_Transformer_Hierarchical_Vision_Transformer_Using_Shifted_Windows_ICCV_2021_paper.html

[Tolstikhin et al., 2021] Tolstikhin, I. O., Houlsby, N., Kolesnikov, A., Beyer, L., Zhai, X., Unterthiner, T., ... & Dosovitskiy, A. (2021). Mlp-mixer: An all-mlp architecture for vision. *Advances in Neural Information Processing Systems*, *34*. link : <u>https://proceedings.neurips.cc/paper/2021/hash/cba0a4ee5ccd02fda0fe3f9a3e7b89fe-Abstract.html</u>

References

[Heo et al., 2021] Heo, B., Yun, S., Han, D., Chun, S., Choe, J., & Oh, S. J. (2021). Rethinking spatial dimensions of vision transformers. In Proceedings of the IEEE/CVF International Conference on Computer Vision (pp. 11936-11945). link : <u>https://arxiv.org/abs/2103.16302</u>

[Li et al., 2021] Yuan, L., Chen, Y., Wang, T., Yu, W., Shi, Y., Jiang, Z. H., ... & Yan, S. (2021). Tokens-to-token vit: Training vision transformers from scratch on imagenet. In Proceedings of the IEEE/CVF International Conference on Computer Vision (pp. 558-567).

link : https://arxiv.org/abs/2101.11986

[Raghu et al., 2021] Raghu, M., Unterthiner, T., Kornblith, S., Zhang, C. and Dosovitskiy, A., 2021. Do vision transformers see like convolutional neural networks?. Advances in Neural Information Processing Systems, 34, pp.12116-12128.

link: https://arxiv.org/abs/2108.08810

[Park et al., 2022] Park, Namuk, and Songkuk Kim. "How Do Vision Transformers Work?." In *International Conference* on Learning Representations. link: <u>https://arxiv.org/abs/2202.06709</u>

[Raghu et al., 2021] Park, Namuk, and Songkuk Kim. "How Do Vision Transformers Work?." In International Conference on Learning Representations.

link: https://arxiv.org/abs/2202.06709

[Karpathy et al., 2014] Karpathy, A., Toderici, G., Shetty, S., Leung, T., Sukthankar, R., & Fei-Fei, L. (2014). Large-scale video classification with convolutional neural networks. In Proceedings of the IEEE conference on Computer Vision and Pattern Recognition (pp. 1725-1732).

link : <u>https://ieeexplore.ieee.org/document/6909619</u>

[Wang et al., 2016] Wang, L., Xiong, Y., Wang, Z., Qiao, Y., Lin, D., Tang, X., & Gool, L. V. (2016, October). Temporal segment networks: Towards good practices for deep action recognition. In European conference on computer vision (pp. 20-36).

link : https://arxiv.org/abs/1608.00859

[Carreira and Zisserman, 2017] Carreira, J., & Zisserman, A. (2017). Quo vadis, action recognition? a new model and the kinetics dataset. In proceedings of the IEEE Conference on Computer Vision and Pattern Recognition (pp. 6299-6308).

link : https://arxiv.org/abs/1705.07750

[Tran et al., 2017] Tran, D., Wang, H., Torresani, L., Ray, J., LeCun, Y., & Paluri, M. (2018). A closer look at spatiotemporal convolutions for action recognition. In Proceedings of the IEEE conference on Computer Vision and Pattern Recognition (pp. 6450-6459).

link : https://arxiv.org/abs/1711.11248

[Qiu et al., 2018] Qiu, Z., Yao, T., & Mei, T. (2017). Learning spatio-temporal representation with pseudo-3d residual networks. In proceedings of the IEEE International Conference on Computer Vision (pp. 5533-5541). link : <u>https://arxiv.org/abs/1711.10305</u>

[Tran et al., 2019] Tran, D., Wang, H., Torresani, L., & Feiszli, M. (2019). Video classification with channel-separated convolutional networks. In Proceedings of the IEEE/CVF International Conference on Computer Vision (pp. 5552-5561).

link : https://arxiv.org/abs/1904.02811

[Arnab et al., 2021] Arnab, A., Dehghani, M., Heigold, G., Sun, C., Lučić, M., & Schmid, C. (2021). Vivit: A video vision transformer. In Proceedings of the IEEE/CVF International Conference on Computer Vision (pp. 6836-6846). link : <u>https://arxiv.org/abs/2103.15691</u>

[Bertasius et al., 2021] Bertasius, G., Wang, H., & Torresani, L. (2021). Is space-time attention all you need for video understanding. arXiv preprint arXiv:2102.05095, 2(3), 4. link : <u>https://arxiv.org/abs/2102.05095</u>

[Liu et al., 2021] Liu, Z., Ning, J., Cao, Y., Wei, Y., Zhang, Z., Lin, S., & Hu, H. (2021). Video swin transformer. arXiv preprint arXiv:2106.13230. link : <u>https://arxiv.org/abs/2106.13230</u>

[Bulat et al., 2021] Bulat, A., Perez Rua, J. M., Sudhakaran, S., Martinez, B., & Tzimiropoulos, G. (2021). Space-time mixing attention for video transformer. Advances in Neural Information Processing Systems, 34. link : <u>https://proceedings.neurips.cc/paper/2021/hash/a34bacf839b923770b2c360eefa26748-Abstract.html</u>

[Li et al., 2022] Li, K., Wang, Y., Gao, P., Song, G., Liu, Y., Li, H., & Qiao, Y. (2022). Uniformer: Unified Transformer for Efficient Spatiotemporal Representation Learning. arXiv preprint arXiv:2201.04676. link : <u>https://arxiv.org/abs/2201.04676</u>

[Touveron et al., 2022] Touvron, Hugo, Matthieu Cord, and Hervé Jégou. "Deit iii: Revenge of the vit." In Computer Vision–ECCV 2022: 17th European Conference, Tel Aviv, Israel, October 23–27, 2022, Proceedings, Part XXIV, pp. 516-533. Cham: Springer Nature Switzerland, 2022.

link: https://arxiv.org/abs/2204.07118

[Jiahui et al., 2020] Yu, Jiahui, Pengchong Jin, Hanxiao Liu, Gabriel Bender, Pieter-Jan Kindermans, Mingxing Tan, Thomas Huang, Xiaodan Song, Ruoming Pang, and Quoc Le. "Bignas: Scaling up neural architecture search with big single-stage models." In Computer Vision–ECCV 2020: 16th European Conference, Glasgow, UK, August 23–28, 2020, Proceedings, Part VII 16, pp. 702-717. Springer International Publishing, 2020. link: <u>https://arxiv.org/abs/2003.11142</u>

[Gong et al., 2021] Gong, Chengyue, Dilin Wang, Meng Li, Xinlei Chen, Zhicheng Yan, Yuandong Tian, and Vikas Chandra. "Nasvit: Neural architecture search for efficient vision transformers with gradient conflict aware supernet training." In International Conference on Learning Representations. 2021. link: <u>https://openreview.net/forum?id=Qaw16njk6L</u>

[Zhu et al., 2021] Zhu, Xizhou, Weijie Su, Lewei Lu, Bin Li, Xiaogang Wang, and Jifeng Dai. "Deformable DETR: Deformable Transformers for End-to-End Object Detection." In International Conference on Learning Representations. link: <u>https://arxiv.org/abs/2010.04159</u>

[Liang et al., 2022] Liang, Youwei, G. E. Chongjian, Zhan Tong, Yibing Song, Jue Wang, and Pengtao Xie. "EViT: Expediting Vision Transformers via Token Reorganizations." In International Conference on Learning Representations. link: <u>https://arxiv.org/abs/2202.07800</u>

[Fayyaz et al., 2022] Fayyaz, Mohsen, Soroush Abbasi Koohpayegani, Farnoush Rezaei Jafari, Sunando Sengupta, Hamid Reza Vaezi Joze, Eric Sommerlade, Hamed Pirsiavash, and Jürgen Gall. "Adaptive token sampling for efficient vision transformers." In Computer Vision–ECCV 2022: 17th European Conference, Tel Aviv, Israel, October 23–27, 2022, Proceedings, Part XI, pp. 396-414. Cham: Springer Nature Switzerland, 2022. link: <u>https://arxiv.org/abs/2111.15667</u>

References

[Kai et al 2022] Han, Kai, Yunhe Wang, Jianyuan Guo, Yehui Tang, and Enhua Wu. "Vision GNN: An Image is Worth Gra ph of Nodes." In *Advances in Neural Information Processing Systems*. link: https://arxiv.org/abs/2206.00272

[Yu et al., 2022] Yu, Weihao, Mi Luo, Pan Zhou, Chenyang Si, Yichen Zhou, Xinchao Wang, Jiashi Feng, and Shuicheng Yan. "Metaformer is actually what you need for vision." In *Proceedings of the IEEE/CVF conference on computer vision and pattern recognition*, pp. 10819-10829. 2022. link: https://arxiv.org/abs/2111.11418

[Liu et al., 2022] Liu, Zhuang, Hanzi Mao, Chao-Yuan Wu, Christoph Feichtenhofer, Trevor Darrell, and Saining Xie. "A convnet for the 2020s." In *Proceedings of the IEEE/CVF Conference on Computer Vision and Pattern Recognition*, pp. 11976-11986. 2022.

link: https://arxiv.org/abs/2201.03545

[Ma et al., 2023] Xu Ma and Yuqian Zhou and Huan Wang and Can Qin and Bin Sun and Chang Liu and Yun Fu. "Imag e as Set of Points" in International Conference on Learning Representations 2023 link: <u>https://openreview.net/forum?id=awnvqZja69</u>

[Cai et al., 2023] Cai, Yuxuan, Yizhuang Zhou, Qi Han, Jianjian Sun, Xiangwen Kong, Jun Li, and Xiangyu Zhang. "Revers ible Column Networks" in International Conference on Learning Representations 2023 link: <u>https://arxiv.org/abs/2212.11696</u>